INVESTIGATION ON THERMAL BEHAVIOR OF NITINOL BASED ACTUATING ELEMENTS FOR BIOMEDICAL APPLICATIONS

H. S. L. PERERA

(148483 G)

MEng/PG Diploma in Manufacturing Systems Engineering
Department of Mechanical Engineering
University of Moratuwa

Sri Lanka

February 2020

INVESTIGATION ON THERMAL BEHAVIOR OF NITINOL BASED ACTUATING ELEMENTS FOR BIOMEDICAL APPLICATIONS

Hettige Suranja Lakmal Perera

(148483 G)

Thesis/ Dissertation submitted in partial fulfillment of the requirements for the degree
Master of Engineering

Department of Mechanical Engineering

University of Moratuwa
Sri Lanka

February 2020

DECLARATION

I declare that this is my own work and this thesis/dissertation does not incorporate without acknowledgement any material previously submitted for a Degree or Diploma in any other University or institute of higher learning and to the best of my knowledge and belief it does not contain any material previously published or written by another person except where the acknowledgement is made in the text.

Also, I hereby grant to University of Moratuwa the non-exclusive right to reproduce and distribute my thesis/dissertation, in whole or in part in print, electronic or other medium. I retain the right to use this content in whole or part in future works (such as articles or books).

Signature   :   Date   :

Name of Student   : H S Lakmal Perera
Registration No   : 148483G

The above candidate has carried out research for the Masters thesis/dissertation under my supervision.

Signature   :   Date   :

Name of Supervisor : Dr. Y.W.R. Amarasinghe

Abstract

In modern material world, important consideration is given to the group of fascinating materials called shape memory materials (SMMs) which respond quickly to a definite change of heat, light and chemical. The shape memory materials that have been established to date are shape memory alloys (SMA), shape memory polymers (SMPs) and shape memory hybrids (SMH). SMA play a significant role in various applications such as sensors, actuators, clamping devices, etc. Nickel – titanium (NiTiNOL) alloys are heavily used in SMA due to their strain recovery, excellent thermal characteristics, reliability and commercial availability, in addition to being used in macro and micro electro mechanical systems based biomedical applications (BMA) due to high biocompatibility, resistance to corrosion and high fatigue limit.

Previous researches have focused on developing integration between thermal stability and SMA microstructure. But they don't have enough thermal behavior data with different heat treatment temperatures. Although phase transformation temperatures and microstructure patterns with different heat treatment temperatures are unique characteristics of NiTiNOL. The aim of this study is to investigate NiTiNOL characteristics and thermal behavior of SMA based actuating elements for biomedical applications. The overall objective of this research study is to investigate the phase transformation temperatures for NiTiNOL alloy during different heat treatment temperatures and to propose the appropriate geometric shape of the actuating element in BMAs.

Therefore, a number of experiments were done at the laboratory level to characterize the thermal related behavior of the NiTiNOL alloy. Differential scanning calorimetry test measurements are used in this study to analyze the dissimilarities in phase transformation temperatures and properties of NiTiNOL (Ni-54 and Ti-46, weight percentages) alloy due to the variation of heat treatment temperature ranging from 400 °C to 600 °C. Further, microstructure and Energy – dispersive X-ray are determined using Scanning Electron Microscopy. It is found that most critical phase transformations are taken place between heat treatment temperatures of 550 °C and 600 °C and extraordinary unique behavior of phase transformations are exhibited by the respective specimens subjected to these temperatures. Further it is found that thermal behavior of actuator elements is dominated by the changes incurred in the microstructure of the NiTiNOL alloy during heat treatment.

Keywords: NiTi materials, Mechanical behavior, Transformation temperature

Acknowledgements

I would like to thank my project Supervisor Dr. Y.W.R. Amarasinghe, Senior Lecturer from Department of Mechanical Engineering, University of Moratuwa and his aspiring guidance, invaluably constructive criticism and friendly advice during the project work. I am sincerely grateful to him for sharing their truthful and illuminating views on a number of issues related to the project.

Again I am thankful Prof. R.A.R.C. Gopura, Head of the Department of Mechanical Engineering, University of Moratuwa and Dr. Manoj Ranaweera the course coordinator of this programme, they always encouraged us to continue this course module with past experiences.

I thank Mr. T.A.U. Roshan (Research Student, Department of Mechanical Engineering, and University of Moratuwa) for being very supportive, and for all the encouragements he has provided to me in these days.

Lastly, I would like to acknowledge all the people who provided me with the facilities being required and conductive conditions for my MEng research project

Content

List of Figures

List of Tables

List of Abbreviations

M_f : Martensite start

M_s : Martensite finish

A_s : Austenite starts

A_f : Austenite finish

R_s : R – Phase start

R_f : R – Phase finish

B2   : Austenite (cubic)

B2'   : R – Phase (rhomohedral)

B19   : Orthorhombic

B19'   : Martensite (monoclinic)

HTT   : Heat Treatment Temperature

TT   : Transition Temperature

DSC   : Differential Scanning Calorimetry

OM   : Optical Microscopy

SEM   : Scanning Electron Microscopy

EDX/EDS   : Energy – dispersive X-ray

BMA   : Biomedical Applications

MIS   : Minimally Invasive Surgery

Chapter 01

1 Introduction

1.1. Motivation

For centuries, metals have played an important role as structural materials of various elements. Researches ability to understand material behavior such as mechanical, thermal, electrical, etc. from microstructure, and to engineer different material properties for a variety of applications has enabled the development of new alloys and composites.

Right now, there is vital thought from the inquiries about for a gathering of materials called Stimulus Responsive Materials (SRMs), which can react to a specific boost, for example, substance, light or warmth. As indicated by many work done by researcher, this class of materials can be partitioned into two gatherings, for example, Shape Change Material (SCM) and shape memory materials (SMMs). Shape memory materials that have been grown so far are Shape Memory Polymers (SMPs), Shape Memory Hybrid (SMH), and Shape Memory Alloy (SMA).

SMAs are known primarily for one fundamental and unique property that is the ability to remember and recover from large strains without permanent deformation. Due to their ability to recover large deformations/strains upon mechanical unloading or heating, SMAs are suitable for innovative application in almost all engineering fields including civil, mechanical, aerospace and bio-medical engineering.

Shape memory alloys are a unique class of shape memory materials with the ability to recover their shape when the temperature is increased. In addition, under specific conditions, when subjected to apply mechanical/thermal cyclic loading, SMAs can absorb and dissipate mechanical /thermal energies by undergoing a reversible hysteretic shape change. These unique characteristics of SMAs have made them popular for their use for sensing elements and actuating elements in biomedical devices, impact absorption and vibration damping applications.

Shape memory alloys have fascinated a lot of attention, and have motivated a variety of constitutive models to facilitate their efficient utilization in advanced engineering applications. Within last two decades, researchers presented many constitutive models to describe the critical behavior presented by SMAs. Two approaches given bellow;

i) Micromechanical - granular microstructure of SMA

ii) Phenomenological - isolating different energies associated with phase transformation through internal state variables.

Researchers and engineers have been mainly focusing on the mathematical developments and physical relevancy of SMA material models to capture various experimentally observed phenomena. Very limited studies are conducted on implementation and practical utilization of the developed models in the available large scale FE codes such as COMSOL, ABAQUS, and ANSYS. In year 2018, COMSOL introduce SMA 1D simulation model according to Lagoudas 1D model, was presented in 2008 [33].

Furthermore, SMA used to a major revolution into biomedical context after its introduction in bioengineering applications. These products are developed and introduced into the market after the approval of the Mitek surgical product (i.e. Mitek Anchor) for orthopaedic surgery by US Food and Drug Administration (FDA) in September 1989. According to unique characteristics of shape memory alloys, it used in many biomedical applications such as minimally invasive surgery (MIS) [1-3].

1.2. Scope of Study

First, the shape memory alloy (NITiNOL) thermal behavior studied and found the SMA - based grippers used for MIS. Then, using DSC and SEM, experimentally characterized the thermal behavior of NiTiNOL and determined the transformation temperatures of the selected NiTiNOL alloy. Again given the microstructure changes of NiTiNOL material by varying heat treatment temperatures according to SEM figures. Finally, select the appropriate transformation temperatures and NiTiNOL alloy for actuating element. In this study the appropriate actuating element use to operate MIS gripper.

1.3. Aim and Organization of Thesis

1.3.1. Aim

The main aim of this present study is the investigation of material characteristics of SMA (NiTiNOL) based actuating elements for the biomedical applications.

1.3.2. Objectives

The main aim can be subdivided into three main objectives:

1. To study of the shape memory alloys (SMA) behaviour (thermal and mechanical), properties, programming techniques (heat treatment procedures) and SMA constitutive model.

2. To investigate the thermal characteristics and phase transformation of selected NiTiNOL wire for actuating elements in BMAs.

3. To proposed the thermal phase transformation temperatures and geometrical shape of NiTINOL based actuator elements used in BMAs

1.3.3. Chapter Organization

The first chapter is followed by an introduction, history and overview to the study. Complete review of the literature is given in chapter two. Development and manufacture of the actuating element are discussed in chapter 03 and chapter 04, respectively. Also, chapter 03 of the available critical study of form memory alloy based grippers and their applications of biomedical engineering and little description of constitutive models of form memory materials.

Chapter 05 gives the experimental procedure based on this study. The material characterization and thermal behavior will be discussed in Chapter 06 and the collection of all data presented by DSC, OM and SEM. In the final chapter, further discussion of results, conclusions and direction on the future aspect of research are available.

Chapter 02

2 Literature Review

2.1. Shape Memory Alloy

2.1.1. A brief history of SMA

In 1932, a Swedish physicist, Ölander discovered that gold - cadmium (Au - Cd) alloys could be plastically deformed when cool, and when heated returned to its original configuration, discovered the solid phase transformation in shape memory alloy (SMA). Greninger and Mooradian first observed the shape memory effect (SME) for copper-zinc (Cu-Zn) alloys and copper-tin (Cu-Sn) alloys in 1938. A decade later, Kurdjumov and Khandros reported on the fundamental memory effect phenomenon governed by the martensite phase thermoelastic behavior as well as Chang and Read in 1951. Similar effects were also observed in the 1950s in other alloys such as In-Tl and Cu-Al-Ni. These findings captured the interest of many researchers and inventors, but due to their high material costs, complexity of manufacturing and unattractive mechanical properties, practical and industrial applications could not be realized [4-5].

Although William Buehler discovered the NiTi alloy in 1959 [5], the potential for commercialization of SMA applications was available only after William Buehler and Frederick Wang disclosed the SME in NiTi alloy in 1962. Nitinol alloys are cheaper to produce, easier to handle and safer and have better mechanical properties than other existing SMAs at the time. The principal business accomplishment of the SMA application was the CryoFitTM "contract - to - fit" pipe coupler from the Raychem Corporation for the F-14 jet fighter developed by the Aerospace Corporation in Grumman at 1969, trailed by George B. Andreasen's orthodontic extension wires in 1971. Since the 1980s, the business utilization of NiTiNOL alloy has created in numerous zones because of the expanded interest for less weight and progressively smaller actuators, specifically in the biomedical business. Table 2.1 demonstrates the amalgams in which these combinations are made and financially accessible.

Table 2:1: Shape memory alloy and composition [6, 9]

	SMA Alloy	Composition (%)	Commercially Available	Transformations range Austenite start (°C)
1	Ag-Cd	44-49 Cd, at	No	-190 to 50
2	Au-Cd	46.5-48.0 Cd, 49-50 Cd, at	No	30 to 100
3	Cu-Zn	38.5-41.5 Zn, wt	No	-180 to 200
4	Cu-Zn-(X) (X=Si, Sn, Al, Ga)	A few at%, wt	Yes	-180 to 200
5	Cu-Al-Ni	28-29 Al, 3.0-4.5 Ni, wt	Yes	-140 to 100
6	Ni-Al	36-38 Al, at	No	-180 to 100
7	**Ti-Ni (NITINOL)**	**49-51 Ni**	**Yes**	**-50 to 110**
8	Ti-Ni-X	5-50 Ni + X, at 5- 50 X, at	No	-200 to 700
9	Ti-Ni-Cu	0 – 15 Cu at	No	-150 to 100
10	Ti-Ni-Nb	0 – 15 Nb at	No	-200 to 50
11	Ti-Ni-Au	50 Ni + Au, at	No	20 to 610
12	Ti-Pd-X	50 Pd + X, at	No	0 to 600
13	In-Ti	18-23 Ti, at	No	60 to 100
14	Mn-Cu	5-35 Cu, at	No	-250 to 180
15	Fe-Pt	0 - 25 Pt, at	No	-130
16	Fe-Mn-Si	62 Fe, 32 Mn, 6 Si, wt	No	-200 to 150
17	Fe-Pd	0 - 30 Pd, at	No	50

*Ti-Pd-Ni alloy with high Pd content do not exhibit good shape memory effect.

Even though some non-alloy material displaying the shape memory effect, such as polymers, ceramics, biomaterials which is shown in Table 2.2.

Table 2:2: Material systems with shape memory properties [7]

Material System	Material type
Metallic SMA	NiTi-based alloys: NiTi, NiTiCu, NiTiPd, NiTiFe, ... Cu-based alloys: CuZn, CuZnAI, CuAINiMn, ... Fe-based alloys: FePt, FeMnSi, FeNiC, ...
Polymer	PTFE (polytetrafluoroethylene)
Ceramic	ZrO_2
Biological systems:	bacteriophages

However, because of their larger memory effect and better pseudoelasticity, NiTi alloys dominate the commercial market. They have superior ductility, fatigue, corrosion resistance, biocompatibility, and recoverable strain properties. Fe - Mn alloys are by far the cheapest that can increase their market interest. Other shape memory alloy with higher phase transformation temperatures will supplement existing alloys, extending the temperature range for SMA application.

2.1.2. The Phase of Shape Memory Alloy

A Nitinol (Ni-Ti) shape memory alloy can exist in different temperatures which depend on the crystal structures or phases in the practical applications. These exhibit structures are martensite and austenite. And also stress-induced martensite structure is more complex than austenite structure.

At room temperature (or low lemperature), the alloy is in the martensite phase. This phase is weaker, soft and can be easily stretched. Once heated up to the high temperature (over the transformation point), the alloy contracts and reverts to the austenite phase. This phase becomes stronger and more rigid [09]. Its transformation and reverse transformation are lattice transformations involving a deformation which results from atomic movements.

Typically mechanical properties of austenitic Ni–Ti are different to the same properties in NiTi. For this reason, SMA in austenite and in martensite can be consider as two different materials.

2.1.2.1.   Martensite Phase

Crystalline Structure

The martensite phase (low temperature) of Ni-Ti has a monoclinic structure which is shown in Figure 2.1 with a = 0.2889 nm, b = 0.4120 nm, c = 0.4622 nm and β = 96.8° (Nenno, 1982; Funakubo,1987).
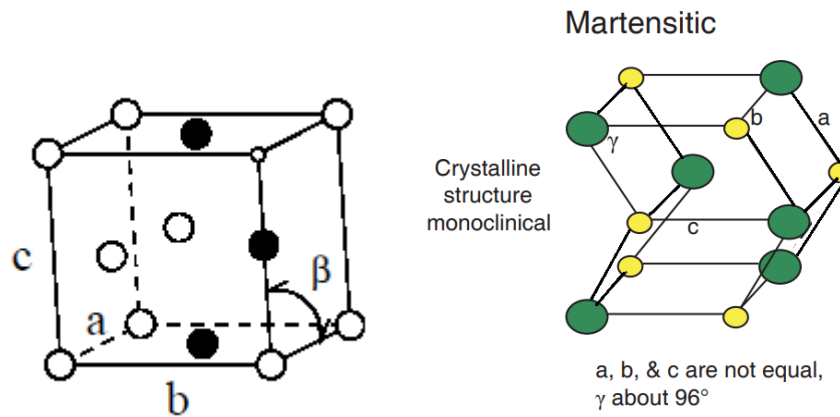
Figure 2.1: Crystal structure of martensite phase [9]

The crystal structure of the martensite phase is aligned. The alloy can be bent or formed easily. The required deformation pressure is 65 to 140 MPa. Bending twists, the crystalline structure of the alloy creating inside stress [11].
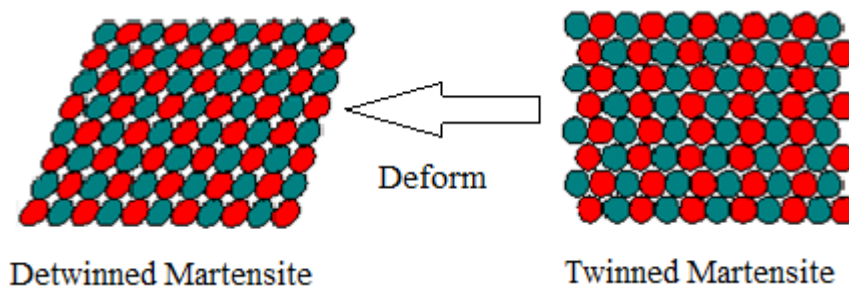
Figure 2.2: Crystalline structure of martensite phase [9]

As we can see, there are two martensite variants between martensite phase transformations which are called martensite re-orientation. This procedure is constantly related by pressure and is related with the change between variations.

As the stress expands, one gathering of changes happens until the example comprises of just a single variation until an extensive perceptible strain is delivered. This procedure is called detwinning.Corresponding to this concept, the initial martensite phase is called twinned martensite (TM, right). It is called detwinned martensite (DM, left) after this process which is shown as Figure 2.2.

Stress-Strain Curve of Martensite Phase

Generally, stress-strain curves are unique for each material. These curves are found by recording the amount of deformation (strain) at distinct intervals of tensile or compressive loading (stress). The relationship between the stress and strain that a particular material displays is known as that material's Stress-Strain curve.

Strain is defined as "deformation of a solid due to stress" and can be expressed as

$$\varepsilon = \frac{\Delta L(mm)}{L(mm)} \tag{2.1}$$

where Δ L is the difference of length and L is initial length.

Stress is the ratio of applied force F and cross section A, defined as "force per area", and can be expressed as

$$\sigma(N/m^2) = \frac{F(N)}{A(m^2)} \tag{2.2}$$

where F is normal component force and A is area.

Young's Modulus (E) = stress / strain

The stress-strain curves of martensite phase, are depicted in Figure 2.3 [12].
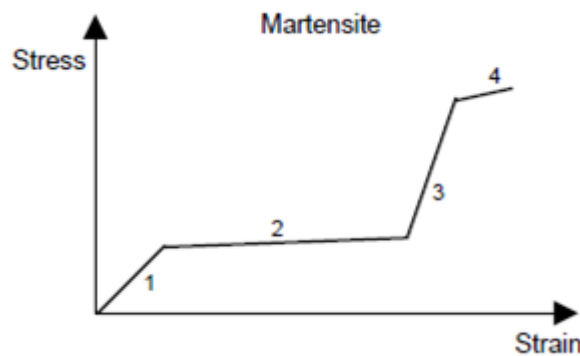
Figure 2.3: The stress and strain curve of martensite phase [12]

When an external stress is applied to the alloy that is fully martensitic, the alloy deforms elastically (Figure 2.3, stage 1). If the stress exceeds the martensite yield strength, a large non-elastic deformation will occur, which allows a large strain in the material with a small increase in external stress. The martensite is strain recoverable up until this stage 2. However, further increase in stress causes the material to again behave elastically up to the point where the external stress begins to break the atomic bonds between the martensite layers in stage 3 and 4 shown in the Figure 2.3 [12].

The strain at which this permanent deformation occurs in Ni-Ti material is 8%. Most applications will restrict strains to 4% or lower [2, 12].

2.1.2.2. Austenite Phase

Crystalline Structure

The austenite phase of Ni-Ti alloy shows body-centered cubic lattice with $a_0=0.3015nm$, shown in Figure 2.4.
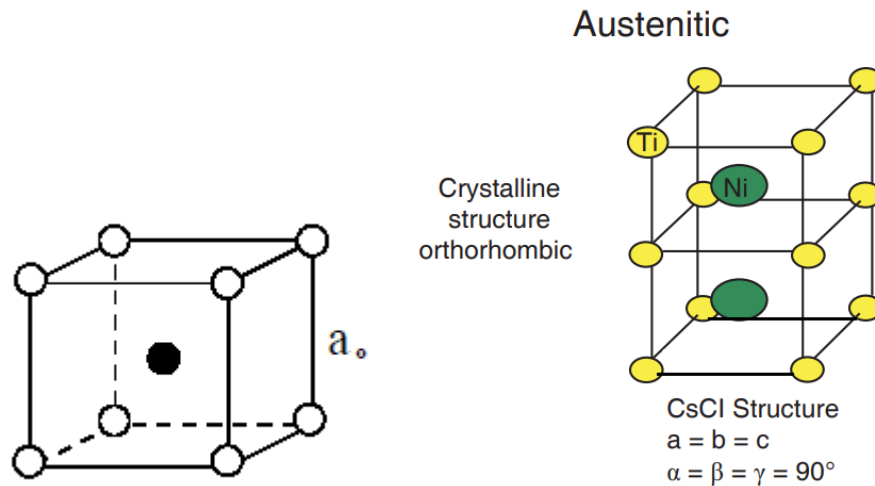
Figure 2.4: The crystal structure of austenite phase (Nenno, 1982; Funakubo, 1987).

The development is created in this stage when the temperature is above progress temperature. The careful progress temperature differs relying on the arrangement of the shape memory alloy which is appeared Table 2.1. The yield quality with which the material endeavors to come back to its unique shape is 240 to 485 MPa which is a lot higher than the martensite stage which is appeared in Figure 2.5.
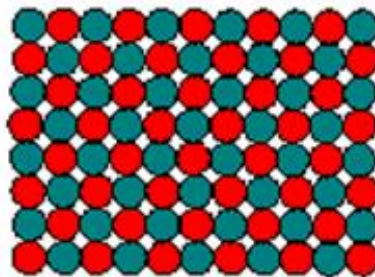
Figure 2.5: Crystalline structure of austenite phase [4].

Stress vs Strain Curve of Austenite Phase
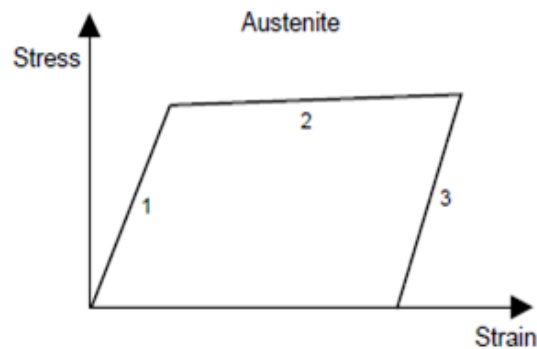
Figure 2.6: The stress and strain curve [7]

The austenite phase has a higher yield strength compared to martensite phase. Initially, the alloy will behave elastically which is shown in the stage 1 in Figure 2.6 until the stress exceeds its yield strength. From this point, plastic deformation will ensue causing unrecoverable stretching upon unloading shown in stage 2 and 3 of Figure 2.6 [6, 7].

2.1.2.3.   Annealing Phase

The high temperature phase in an annealing phase. The alloy will reorient its crystalline structure to remember its present (original) shape. The annealing phase for the Nitinol wire we are working with is approximately 540°C.

2.1.2.4.   Martensite Transformation

The shape memory mechanism is based on a reversible, solid-state phase transformation between martensite phase (low temperature or present phase) and austenite phase (high temperature) on atomic scale. This transformation is called martensite transformation. If the Ni-Ti alloys haven't been deformed or stressed in the martensite phase, the crystalline structure changes still occur from martensite transformation, but do not result in any movement.
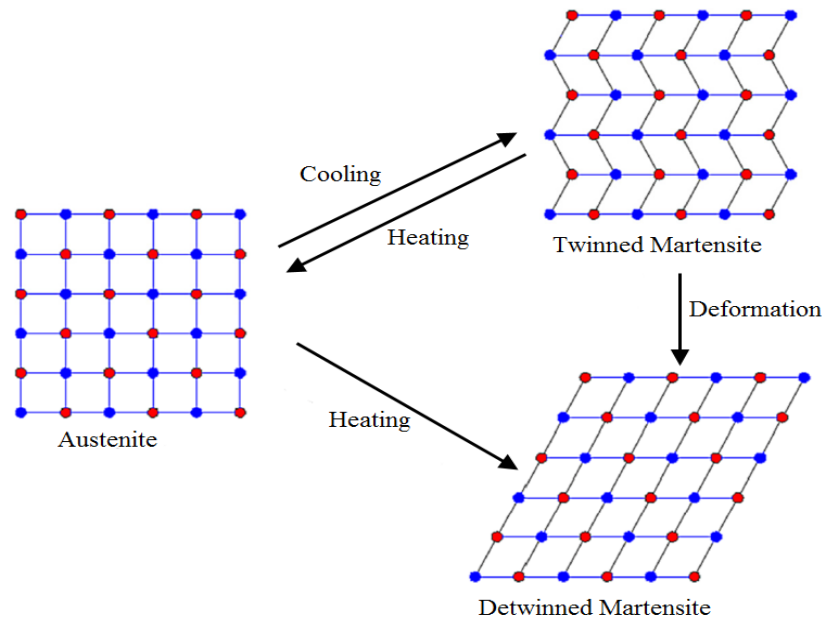
Figure 2.7: Microscopy view of phase transformation [7]

Shape memory effect shown microscopically in figure 2.7. Heating state will return the original austenitic structure and shape. Once austenite is cooled, it becomes martensite [11]. If the external stress causes Ms, the martensite start temperature to increase beyond the current temperature, martensite will form. This makes the alloy malleable under small increase in stress. Once the stress is removed, the transition temperatures decreases and the alloy returns to the austenite phase.

There are also other transformations associated with shape memory, such as rhombohedral (R-) and bainitic transformations [7]. In this research is focusing on martensite transformation between martensite and austenite phase.

Thermomechanical behavior of NiTi

Figure 2.8 illustrates the mechanical behaviour of a NiTi alloy as a function of temperature. In order to relate the mechanical behaviour of the alloy which occurs on the macro level with the phase transformations that occur on the micro level, the microstructure of the alloy is shown in the Figure 2.9 at the various strain/temperature levels [15].
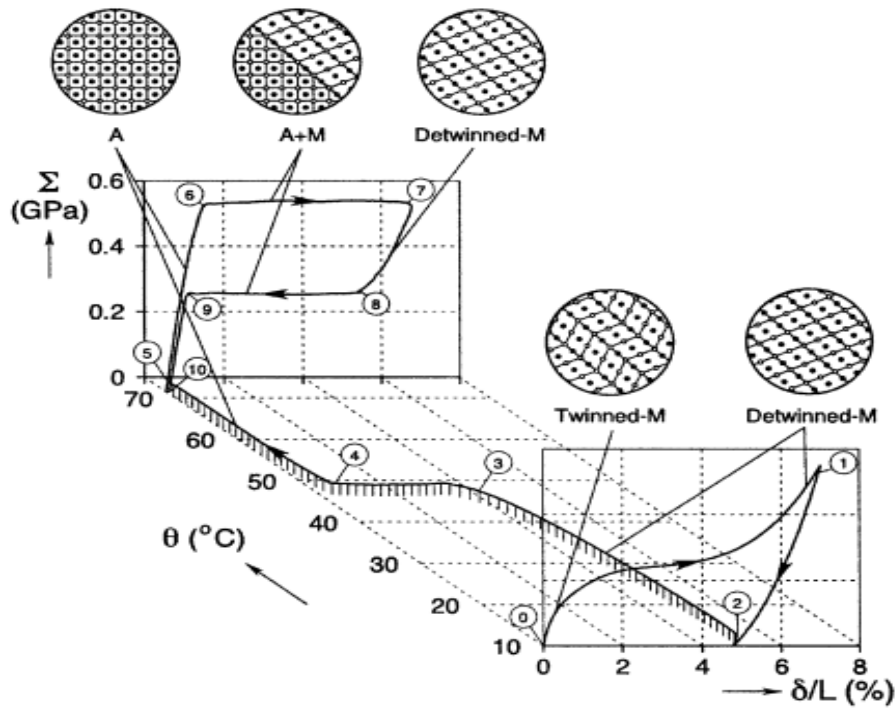
Shape memory effect (01 to 04), Pseudoelastic loop (04 to 10)

Figure 2.8: Thermomechanical behavior of NiTi wire [15]

Stress-Strain Figure Vs Austenite and Twinned, Detwinned Martensite
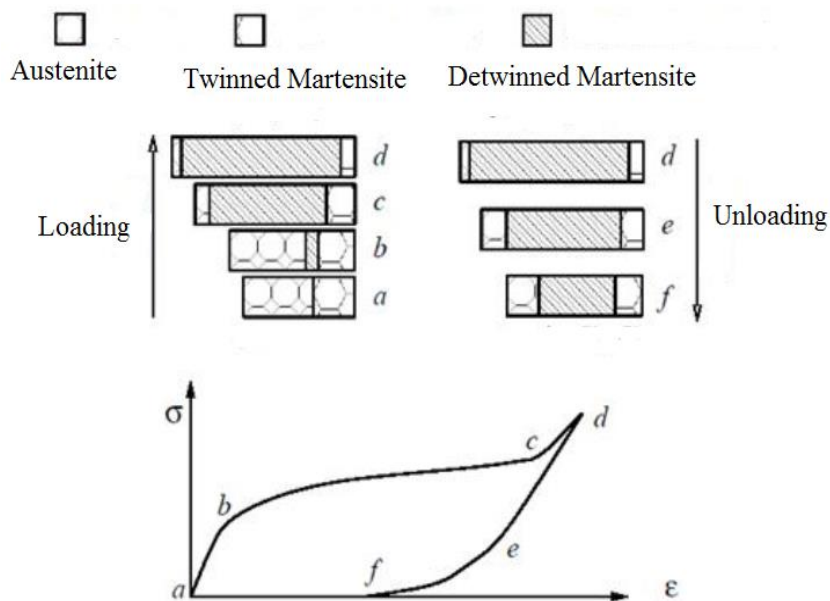
Figure 2.9: Stress/ strain figure Vs austenite and martensite (twinned, detwenned) [3].

This is the simplest type of loading of one dimensional uniform tensile test. A graph from this test is shown in Figure 2.9. In this SMA wire containing a mixture of austenite and twinned martensite. Put this wire into a standard tension testing machine and carry out a tension test [3].

The behavior is mostly elastic when loading from stage ' a ' to stage ' b, ' even though many transformations may occur, as designated by a small quantity of nonlinearity in the Figure 2.9.

If the stress goes beyond a specific basic stress, the extent of which depends on the example temperature, a vast change of incited strain happens all of a sudden from stage ' b ' to arrange ' c. ' The changes in this procedure are martensite change and re - introduction of martensite. After the martensite change is almost over, from stage ' c ' to stage ' d, ' the martensite reorganizes (detwinning) commands [3].

During the load removing, after a period of full elastic recovery, a small segment of the detwinned martensite may change back to twinned martensite with some turn around martensite change, which appears from stage 'd ' to organize ' e'. If the example's temperature is not excessively high, further emptying will prompt to increasingly turn around change (from stage e to arrange f). The main method for fully recovering the first shape is to warm the wire under zero stress over a specific temperature value.

2.1.2.5. Hysteresis

The temperature ranges for the martensite-to-austenite change that happens after warming is higher than that for the turnaround change after cooling (Figure 2.7). The contrast between the change temperatures after warming and cooling is called hysteresis. Hysteresis is commonly characterized as the distinction between the temperatures at which the alloy is in half changed to austenite after warming and in half changed to martensite after cooling. This distinction can be up to 20– 30°C [7].
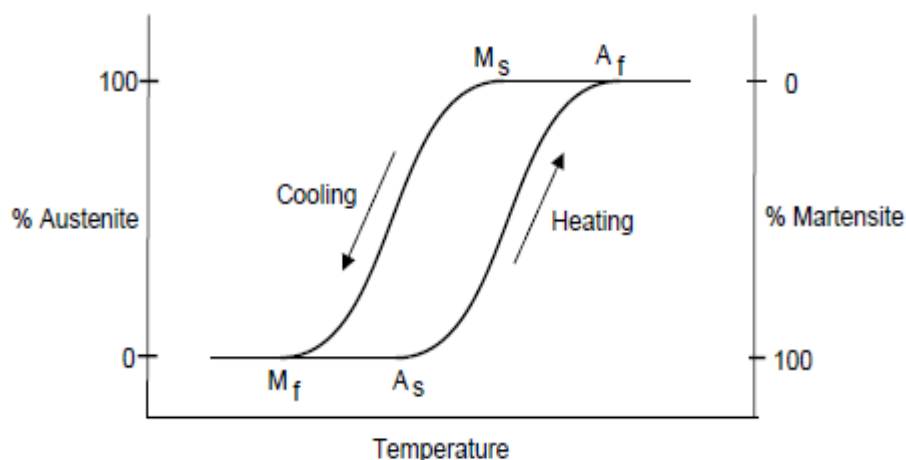
Figure 2.10: The curve of martensite-to-austenite transformation [7].

The phase transformation temperature of NiTiNOL alloy is divided into four phase transformation temperatures.

As - temperature of austenite start

A_f - temperature of austenite finish

Ms - temperature of martensite start

M_f - temperature of martensite finish

The shape memory alloy comprises just of the martensite stage when the temperature is not as much as M_f, which is from left of the bend appeared in Figure 2.10. As the temperature is expanded over As, austenite stage frames in the alloy and while the temperature surpasses A_f, the SMA alloy is completely in the austenite stage. As the composite shape memory chills off, the martensite stage strat to frame while the temperature drops below Ms, and when the temperature reaches Mf, the compound is again in the martensite stage. Austenite start shown in Figure 2.10, a wide warm hysteresis circle can shape this progress between the austenite and martensite stages. The hysteresis fluctuates as indicated by the amalgam framework. The temperature hysteresis is between 30-50°C for NiTiNOL alloys [7].

During the martensite phase transformation, in the range where both martensite and austenite co-exist, the stress-train response of shape memory alloys are nonlinear and prominently hysteretic [7, 8]. They are influenced by material composition, processing, temperature and the number and sequence of activated thermo-mechanical loading cycles. During phase transitions between martensite and austenite, most of the properties of shape memory vary. These include Young's Modulus, electrical resistance and thermal conductivity and so on. Parts of them are shown in the following tables.

Table 2:3: Properties of NiTi under different phase [16, 17]

Properties	Unit	Austenite	Martensite
Young's Modulus	GPa	70 – 98	26 – 28
Yield Strength	MPa	100 - 800	50 – 300
Ultimate Tensile Strength	MPa	800 – 1500	700 - 2000
Shear Module	GPa	11.5	14.5
Elongation at Failure	%	15 – 20	20 – 60
Recovery Strain	%	8	

Max. Recovery Stress	MPa	600 – 900	
Specific Damping Capacity	%	15 – 20	
Fatigue Strength (N = 10^6)	MPa	350	
Poisson's Ratio	-	0.33	
Shape Memory Transformation temperature	°C	-210 – 110	
Hysteresis	°C	30 - 50	
Thermal Conductivity	Wcm^{-1}°C	0.18	0.086
Density	Kg/m^3	6400 – 6500	
Resistivity	10^6 Ωm	0.5	1.1
Magnetic Permeability	H/m	<1.002	
Magnetic Susceptibility	emu g^{-1}	3.0 x 10^6	

2.1.3. Principles of Shape Memory Effect

The principle of SME is the capacity to remember a programmed form or profile even after a few misshapenness fit as some fiddle memory materials. Notwithstanding normal shape change impacts, for example, flexible and plastic distortions, just as warm development and withdrawal, shape memory combinations additionally show three key impacts relying upon the temperature variety that are essentially ascribed to martensite stage change, which are given below.

1) Shape Memory Effect – One Way

After removing external load, the material exhibits permanent deformation. On heating, material can retain its original shape. The successive cooling will not change the shape unless it is stressed again.

2) Shape Memory Effect – Two Way

Furthermore, to the two way SME, shape change occurs when cooling and without applying external load or stress

3) Superelastisity or Pseudoelasticity

Mechanical loading at temperatures beyond Af stretches the alloy and upon removing load, it returns to its initial shape. Thermal operations are not involved.
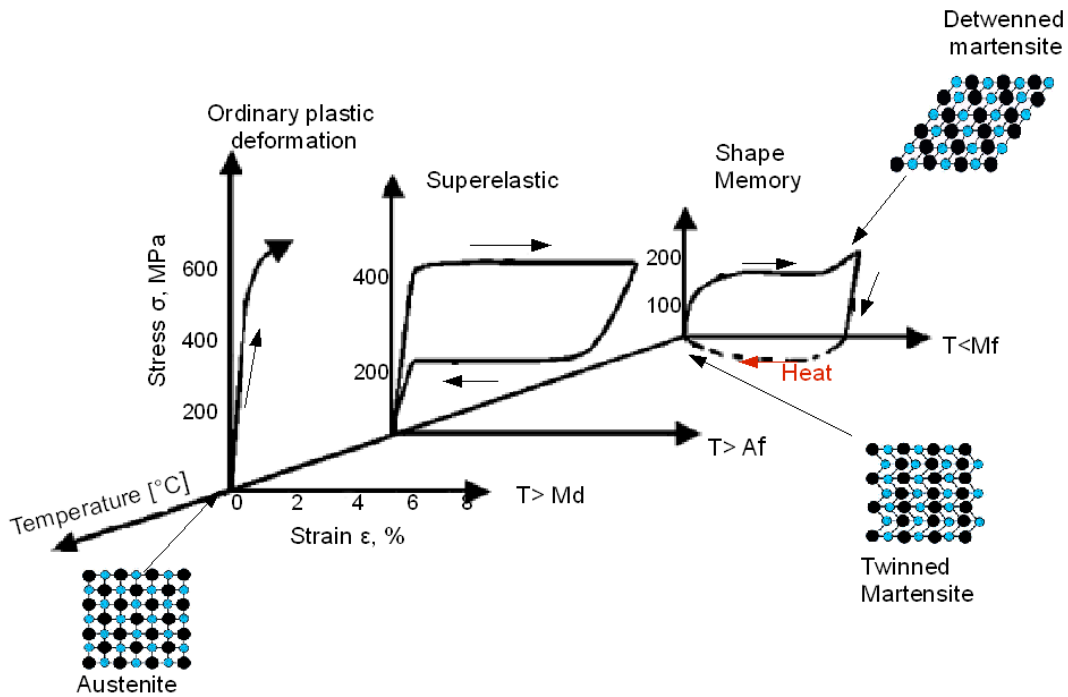
Figure 2.11: Stress/Strain Vs Temperature for SMA materials [13]

Md is the transition temperature between the pseudoelastic phases and that austenitic that is usually above the Af temperature for the NiTi alloy.

The qualities related with these three practices are exhibited beneath, and the different strain instruments behind these impacts are shown utilizing streamlined two dimensional crystal structure models and stress-strain-temperature diagrams.

2.1.3.1.   Shape Memory Effect - One Way

The OWSME is the premise type of SME. The shape recuperation and the high powers are empowering in the stage change, which is appeared in Figure 2.10.
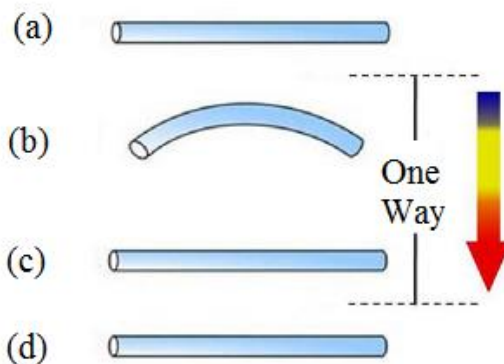
(a) Martensite, (b) Loaded and deformed in martensite phase, (c) Heated above As,

(d) Cooling up to martensite

Figure 2.10: One Way Shape Memory Effect: [11].

The One Way Shape Memory Effect of shape memory alloy is depicted in Figure 2.11 and Figure 2.12.
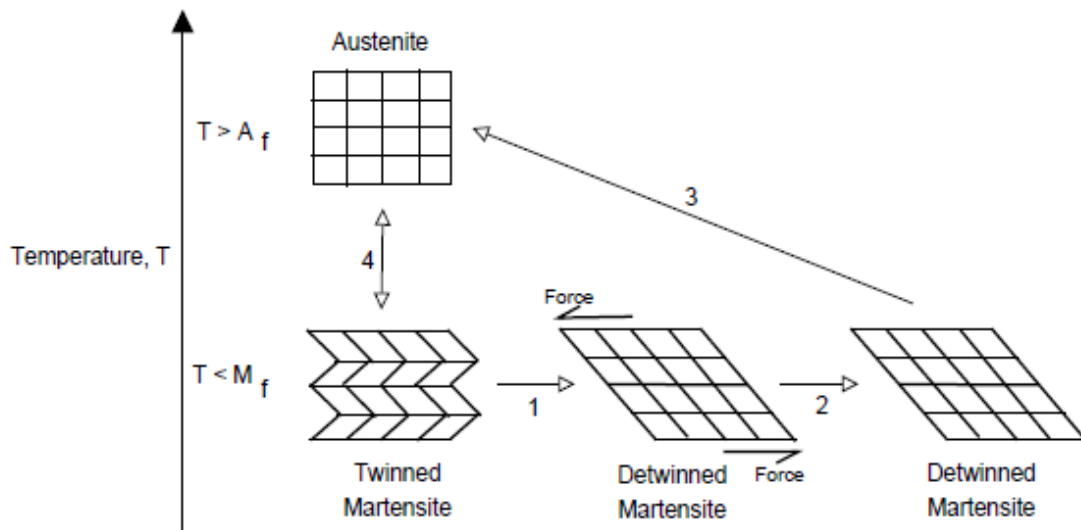
Figure 2.11: The phase changes in OWSME [7]
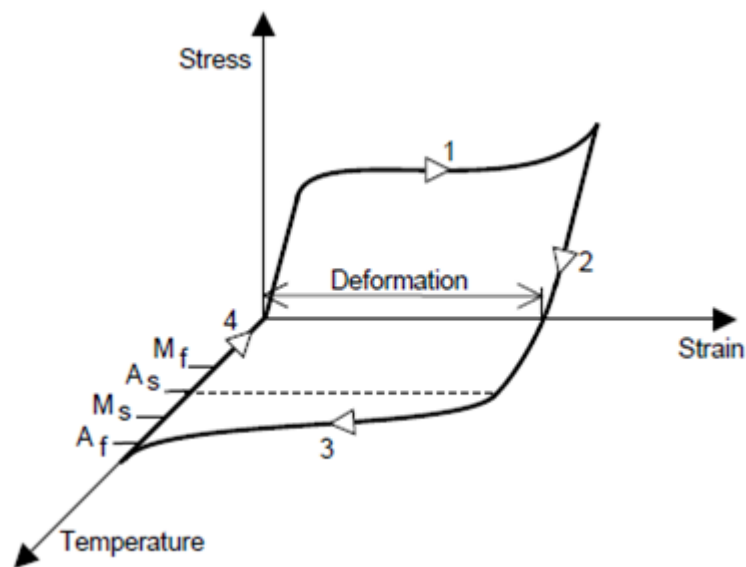
Figure 2.12: The curve of stress, strain and temperature in [7]

In Figure 2.12 shown in the 2D model, it tends to be realized that as austenite temperature reduce, martensite strat to develop. During cooling process, there are no shape change happen (additionally portrayed as stage 4 in both Figure 2.10 and Figure 2.11). The martensite structure is said to be ' twined ' with each layer isolated by a twinning limit [4]. The application of external forces to the martensite will be observed in stage 1 in both Figure 2.10 and Figure 2.11. Martensite is called to be ' detwinned ' in this state.

In this state, martensite is exceptionally pliant and has a low versatile containment point to simply change the shape. 7]

After applying more stress to the SMA specimen, it becomes a failure due to unrecoverable strain. The relaxation in the recoverable strain that controls the deformed shape of the specimen was shown in Figure 2.11 and Figure 2.12 in stage 2.

The beginning of austenite start to austenite finish under heating is shown in Figure 2.12, stage 3. Beyond heating Af, material again achieves full form recovery and alloy forms a complete austenite phase. Recovery only occurred in one direction in this shape. The effect is named the one way shape memory effect (OWSME). The OWSME, many cycles occur in repeatable and shown in Figure 2.12. Then, as shown in the temperature vs phase transformation graph, this phenomenon gives a large hysteresis loop.

2.1.3.2.   Shape Memory Effect - Two Way

The austenite phase is remembering its parent shape according to the shape memory effect. Even though, under certain conditions it is possible to remember the shape of the martensite. Again, the effect is a general behavior of shape memory materials and is called a two - way shape memory effect (TWSME). This effect is clearly shown in Figure 2.13 [12].
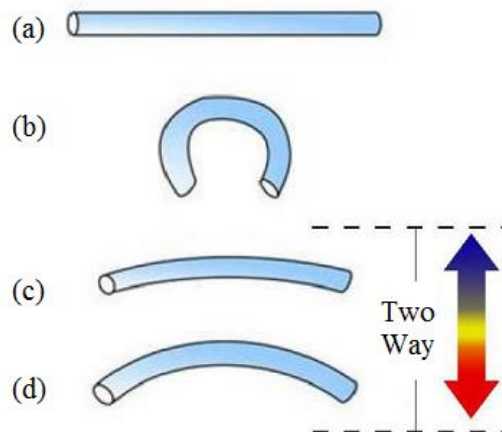
(a) Martensite

(b) Several deformations

(c) Heated

(d) Cooled

Figure 2.13: Two Way Shape Memory Effect [11]

Two Way Shape Memory Effect isn't characteristic features (as the OWSME) to shape memory combination, yet it very well may be displayed after explicitly thermo-mechanical medicines known as preparing, so it is additionally called reversible shape change [7].

The TWSME indicates to the changeable shape modification of materials with heat cycling both heating and cooling without requiring any outside load. A schematic portrayal of the naturally visible watched conduct is accounted for in Figure 2.13 and Figure 2.14 [29].
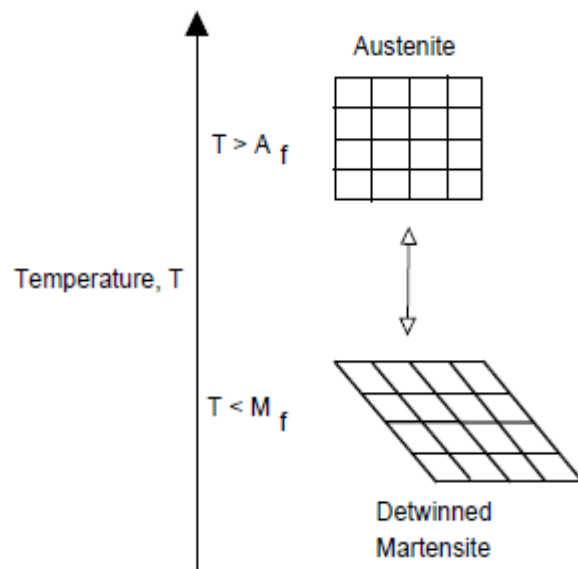
Figure 2.14: The phase changes in TWSME [7]
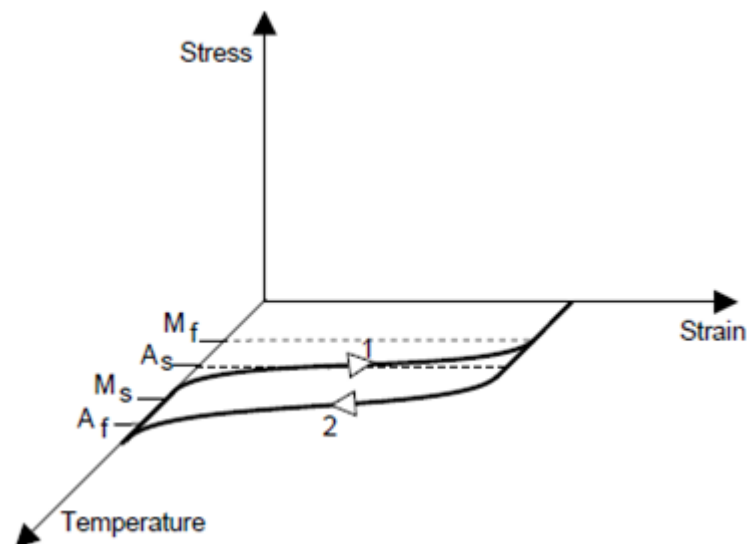
Figure 2.15: The curve of stress, strain and temperature in TWSME [7]

The TWSME is less particular than the single direction impact and as a rule requires preparing. This outcome in the immediate changes among the austenite and martensite (detwinned) is in Figure 2.14. It can likewise be portrayed utilizing the bends found just in the strain temperature level, as appeared in Figure 2.14. Hysteresis is additionally conspicuous in the TWSME appeared in Figure 2.15. Shape memory compounds can be prepared to display the TWSME utilizing two techniques, which are unconstrained and outside burden helped enlistment [10]. In any case, the shape change got is by and by not as much as one way effect.

2.1.3.3. Pseudoelasticity or Superelasticity

At the point when a shut circle begins from a pressure incited change after stacking and the turnaround change after emptying, it is called super-versatility. With a difference, it is called elastic like characteristics or behavior on the off chance that it happens on the reversible development of twin limits in the martensitic state [15].

Stress makes martensite structure if the combination is in the austenite stage and an outside pressure is connected. In the event that the pressure is evacuated, the material returns into austenite. This impact is known as pseudoelasticity (SE) [7].

Figure 2.16 and Figure 2.17 grants the 2D show bend of and the pressure strain vs temperature fit as a shape memory alloys.
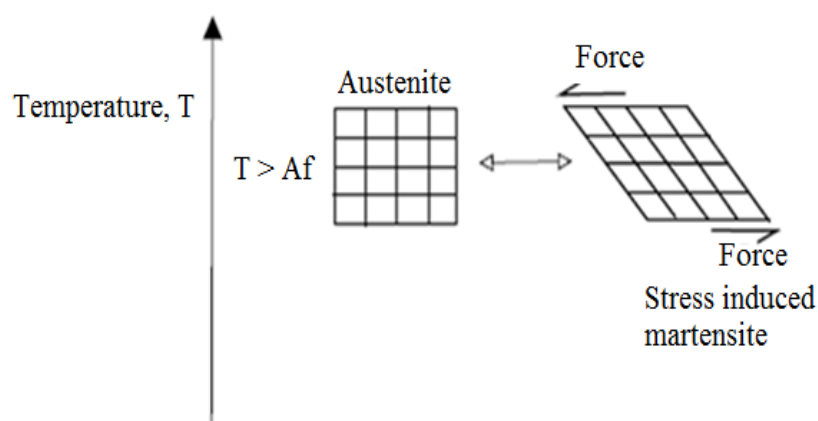
Figure 2.16: The phase changes in pseudoelasticity [7]
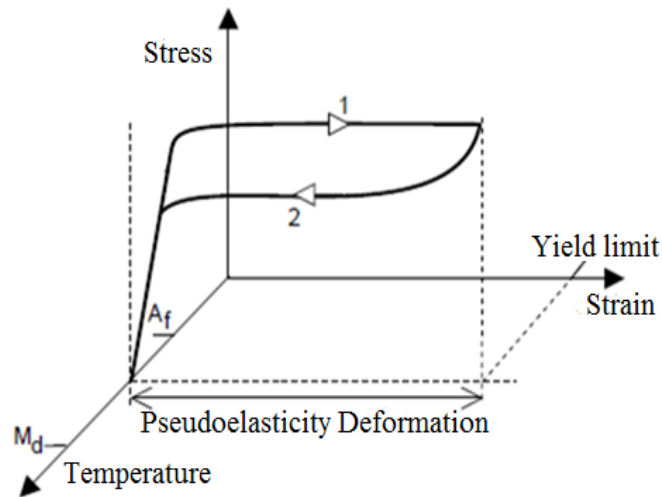
Figure 2.17: The curve of stress, strain and temperature in pseudoelasticity [7]

There was no temperature modification need for pseudoelastic behavior. The stress and strain plane shown in Figure 2.17 explained the characteristics of normal strain. By applying outside over the Af, the austenite at first carries on in a flexible way pursued by a level in which exceedingly nonlinear twisting happens up to a virtual yield limit. After emptying, the bend returns by means of the lower hysteresis circle for full strain recuperation.

2.1.4. Summarization of shape memory effect

From the portrayal over, the normal for shape memory impact is appearing in the Table 2.4. It is anything but difficult to change the shape fit as a fiddle memory impact and two-way shape memory impact while it is extremely inflexible in the pesudoelasticity. Furthermore, there is no shape change from warming explanation to cooling proclamation in the OWSME and pseudoelasticity.

Table 2:4: Summary of SME in the different situations.

SME	Original	Loading	Unloading	Heating	Cooling
One way	——	⌃	⌃	——	——
Two way	——	⌃	⌃	——	⌃
Pseudoelesticity	——	⌃	——	——	——

2.1.5. Stress and Temperature

The stress and the temperature are linear in the shape memory alloy both in martensite phase and austenite phase which is shown in Figure 2.18.
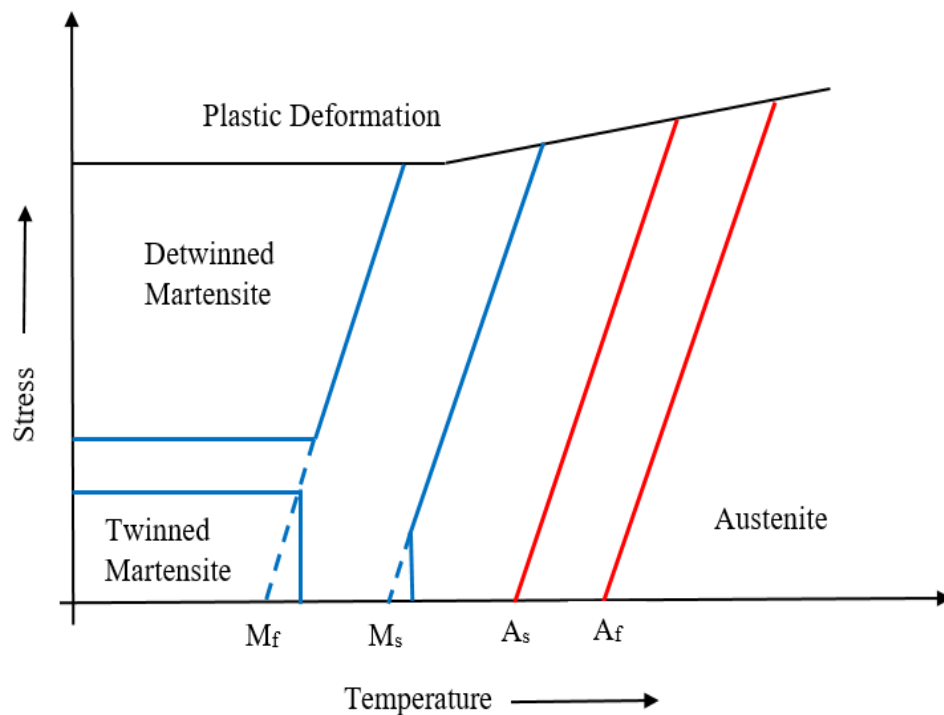
Figure 2.18: Shape memory alloy stress-temperature phase diagram [13]

The plateau region is an aftereffect of the arrangement of stress actuated martensite from austenite. Outside weight on the alloy builds the stage change temperatures [13]. The relationship of alloy is genuinely direct, as can be found in Figure 2.18, despite the fact that As and Af carry on nonlinearly at low stress levels.

This stress reliance of the four change temperatures can be around spoken to as:

$$\frac{d\sigma}{dT} = \frac{1}{c_m} \qquad (2.3)$$

$$T(\sigma) = c_m\,\sigma + T_0 \qquad (2.4)$$

Where; 1/Cm - Stress rate

$T(\sigma)$ - The transformation temperature at stress dependent

T_0 - The transformation temperature at zero stress

Stress-Temperature Schematic Diagram in SME and Pseudoelasticity
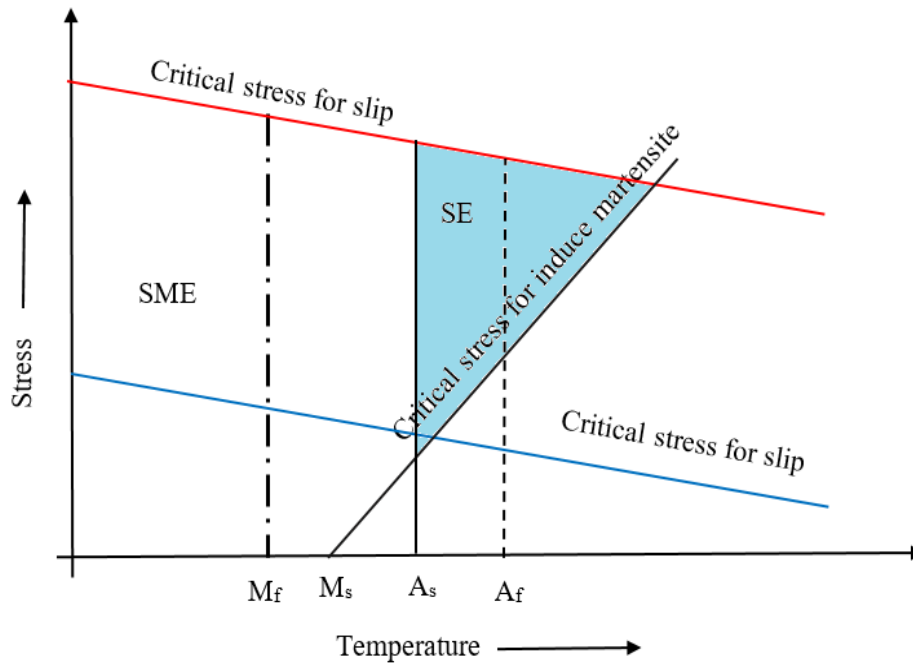
Figure 2.19: Indicating of SE and SME in stress Vs temperature [13]

In Figure 2.19 shown in low critical stress (blue line) and high critical stress (red line) [13].

2.2. Transformation Temperatures measuring techniques

2.2.1. Thermal Analysis

Thermal Analysis (TA) implies the investigation of an adjustment in a workpiece property, which is identified with a forced temperature change. Calorimetry implies the estimation of warmth. A gathering of systems in which a property of the workpiece is observed by changing time or temperature. However, it can change the temperature of the workpiece, in a predetermined atmosphere, simultaneously [21].

2.2.2. Types of thermo analytical methods

Here give meanings of the most vital canteen diagnostic strategies. Reference is made to essentially unique examples or estimating standards of the instruments concerned. In the event that fundamental, bearings are given as respects the introduction of the deliberate curve.

1. Cooling and heating curve examination

A system in that the difference in the temperature parameter of an example is examined simultaneously being exposed to a modified temperature either cooled or heated.

2. Differential thermal analysis (DTA)

A procedure where difference in distinction with respect to temperature between an example and reference test is broken down simultaneously being exposed to an adjusted temperature. For this purpose, two designs are available namely the block measuring system and the free-standing crucible measuring system.

3. Differential Scanning Calorimeter

This happens to be a technique for deciding change in temperature at zero pressure, yet one requiring a costly tool, is to utilize a DSC. The contrast among this method and DTA method described above is task of a warmth stream rate distinction (by alignment) to an initially estimated temperature contrast. To enable task be completed, instruments' plan is to be with the end goal being fit for adjustment.

For this purpose, two designs are available that namely the Power compensating DSC and Heat flux DSC with two modifications.

i.   Heat flux DSC

Considering warmth transition DSC, distinction with respect to temperature among test & reference test is taken into account as an immediate proportion of distinction in warmth stream degrees to the example and reference test. The warmth stream rate contrast is doled out by calorimetric adjustment.

Instruments are accessible for this purpose are

- Disk type (Figure 2.20)
- Cylinder type (Figure 2.21)

Plate type DSC dictates the cauldrons consisted of examples to be situated on a circle which are constructed of metal, pottery etc.). Temperature contrast ΔTSR between examples is estimated by temperature sensors incorporated in plate or reaching the circle surface.
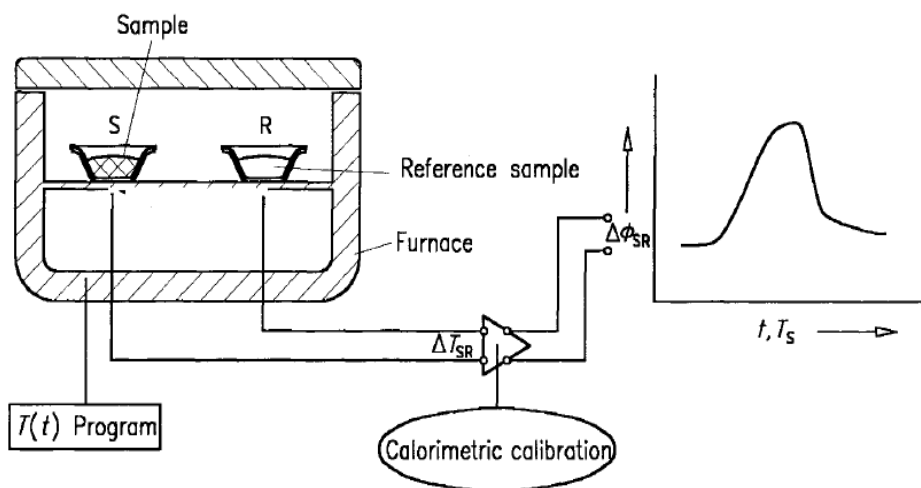
Figure 2.20: Disk-type DSC [20]

In a chamber type DSC, the (square sort) heater is furnished with (at least two) round and hollow holes. It starts empty chambers where bottoms are shut which holds examples specifically and if not inside reasonable cauldrons. Thermopiles are organized between empty chambers and heater that take measures of temperature distinction between empty barrel and heater (necessary estimation). A point to note is possible usage of thermoelectrical semi-leading sensors instead of thermopiles. An association of thermopiles outfits temperature contrast of the empty barrels that is enlisted as temperature distinction ΔTSR among test and reference test. Variations of the structure: The two empty barrels are orchestrated one next to the other in said heater. They are straightforwardly associated via a thermopile which can however, as well be a few. Other DSC designs are available whose architecture fall between plate & barrel types.
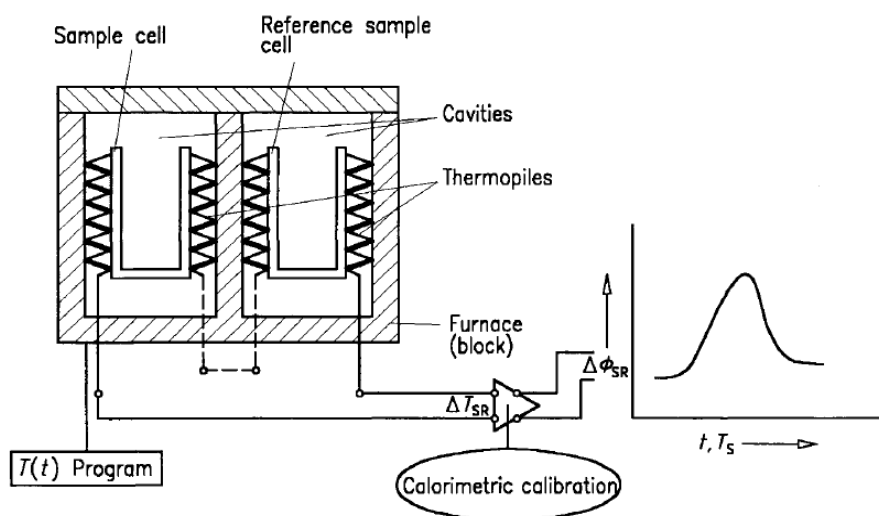
Figure 2.21: Cylinder-type DSC [20]

i. **Power compensating DSC**

The power remunerating differential scanning calorimeter, the examples have to be organized inside a couple of distinctive little heaters every one of which is given a temperature sensor along with heating system (Figure 2.23). Amid estimation, contrast in temperature between heaters has to be kept up via guidance by control circle which properly adjusts warming forces P. Due to above reason utilization of a corresponding controller is carried out leading to remaining of a dependable temperature contrast between examples (balance). At the point in the presence of warm symmetry exhibited considering the estimating framework, remaining temperature contrast corresponds along distinction between heating forces nourished to test & reference test. In the event that the subsequent temperature distinction is because of contrasts in the warmth limit among test & reference test, or enthalpy instead of "exothermic/endothermic" changes in the example, it's a necessity for warming force to have temperature distinction to the minimum that could be expected under the circumstances (which would achieve indistinguishable incentive with the heat flux differential scanning calorimeter provided no pay warming takes place) is relative to distinction A q~sR between heat stream rates provided to test and reference test ($\Delta\emptyset SR = \Delta CP * \beta$), or corresponding to the warmth stream rate of progress $\Delta\emptyset trs$.
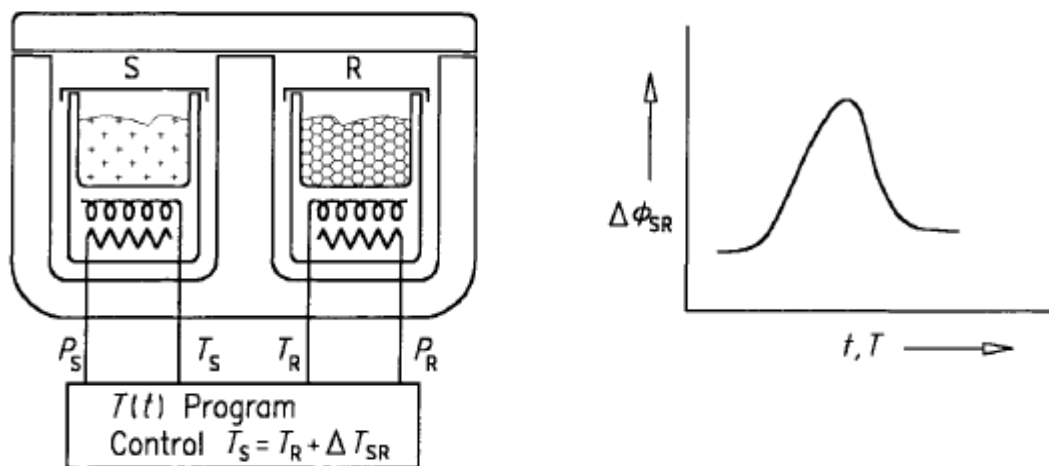
Figure 2.22: Power compensating DSC [20].

4. Thermogravimetric analysis (TGA) and thermogravimetry (TG)

This happens to be a system used to analyze alteration in mass in a sample while undergoing temperature change.

5. Thermomechanical analysis (TMA)

Procedures employed to dissect alteration in mechanical aspects of a sample while exposed to temperature change.

- Static force thermomechanical analysis (sf-TMA)
- Thermodilatometry
- Dynamic force thermomechanical analysis (df-TMA)
- Modulated force thermomechanical analysis (mf-TMA)

4. Thermomanometric analysis

This method is employed to analyze alteration in exerted pressure incurred while sample undergoes temperature change

5. Thermoelectrical analysis

This method is employed to analyze alteration in electrical property incurred while sample undergoes temperature change.

- Thermally stimulated current analysis
- Alternating current thermoelectrical analysis
- Dielectric thermal analysis (DETA)

6. Thermomagnetic analysis

This method is employed to analyze alteration in magnetic property incurred while sample undergoes temperature change.

7. Thermooptical analysis (TOA)

This method is employed to analyze change of optical property incurred while sample undergoes temperature change.

- Thermoluminescence analysis
- Thermophotometric analysis
- Thermospectrometric analysis
- Thermorefractometric analysis
- Thermomicroscopic analysis

8. Thermoacoustic analysis (TAA)

This method is used to analyze the change incurred in acoustic waves followed by being led through the sample in context carried out while the said sample undergoes temperature changes.

- Thermally stimulated sound analysis

11. Thermally stimulated exchanged gas analysis (EGA)

This method is used to examine the replaced gas while having the sample undergo change in temperature.

- Thermally stimulated exchanged gas detection
- Thermally stimulated exchanged gas determination

12. Thermodiffractometric analysis (TDA)

This particular method diffraction methodology is employed while having the sample undergo change in temperature in order to analyze the alteration in structure.

2.3.   Measuring Transformation Temperatures in NiTi Alloys

There are various methods for deciding TTRs, yet there are in like manner use for NiTi combinations to give supportive information to item fashioners, three critical ways:

i.   Constant Load Test

ii.   Differential Scanning Calorimeter Test

iii.   Active A_f

i.   Constant Load Test

It is technique to apply a heap to the combination and screen its distortion and shape recuperation at the same time the temperature of the material is cooled and heated over the change extend. The Figure 2.21 is demonstrated the prolongation and withdrawal of a SMA wire under ductile stacking as the temperature is brought down and therefore increased. In this temperature focuses distinguished are ones much of the time used to portray the conduct of a specific alloy.
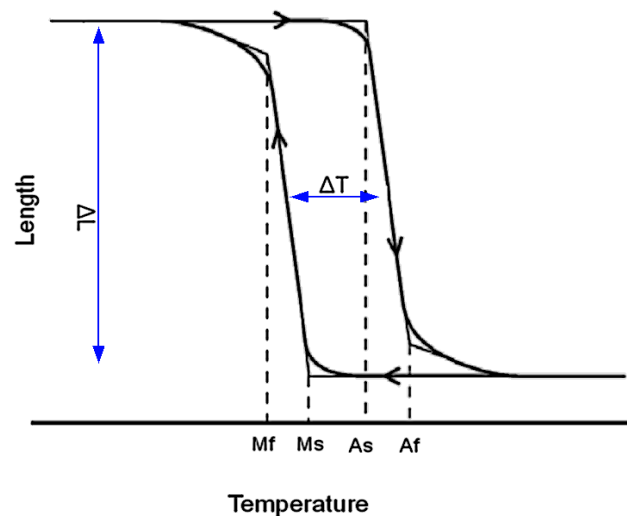
Figure 2.23: Sample Length Vs Temperature (constant load) [13]

ii. Differential Scanning Calorimeters

DSC is a thermal investigation method to determine the required amount of heat flow of a sample or specimen and reference sample with increasing or decreasing temperature. Both the example and reference are kept up at almost a similar temperature all through the test. Figure 2.24 shown in the DSC thermogram and its measured amount of absorption and release energy due to the cooling or heating of the specimen through its phase transformation.The main disadvantage of the DSC test is that it is only used in cold workpieces. In DSC testing, this means poor and uncertain results for superelastic specimens.

This equivalent disadvantage likewise may use to tests which have experienced a heat treatment next cold strengthening. DSC is a control strategy for deciding the transformation temperature rates, yet in addition, it permits see whether the examples display the R-Phase change or not. Thusly, it grants to attempt remark on the creation and manufacture techniques for the materials.
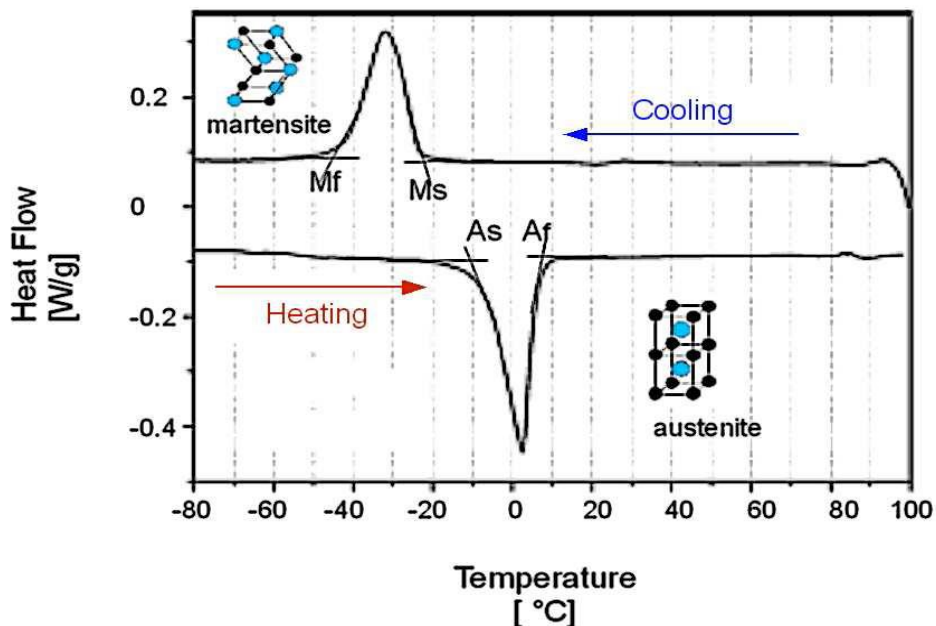
Figure 2.24: DSC experimental thermogram for common NiTi alloy [13]

iii. Active A_f Test

Usually to be specific likewise the Active Af experiment. This experiment is directed by simply twisting an example of the compound, while it is beneath Ms and after that observing the shape recuperation while it is warmed. In the event that an example is delicately twisted into a clasp shape by finger weight, at that point warmed gradually in a

blended fluid shower while observing shower temperature, one can without much of a stretch measure the held twist edge at explicit temperatures (drawing diagrams is appeared in Figure 2.25). This strategy, while not refined, will yield shockingly precise, repeatable outcomes whenever performed cautiously, and it requires next to no test mechanical assembly. The testing of superelastic materials by this technique need to beginning at negative temperature - 50°C. In this experiment may be suitable for combinations of higher temperatures, it is used to account for the Af of pseudoelastic (superelastic) materials
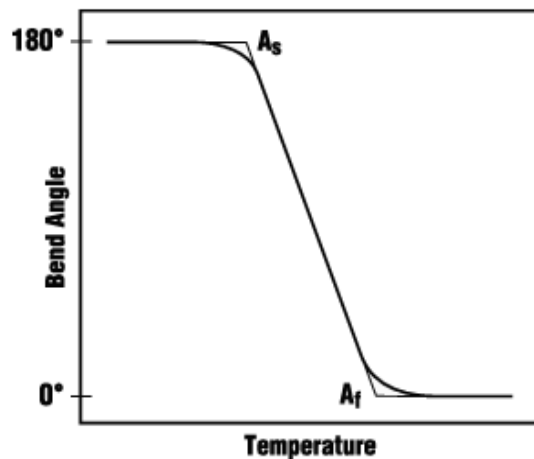
Figure 2.25: Curve of Active Af for common NiTi alloy [13]

2.4.   Mechanical Characteristics of NiTi Alloy

Many researches are very interested to find the two phases formed of NiTiNOL under mechanical characteristics. A couple of test considers have been coordinated to demonstrate the mechanical highlights of SMAs and the exploratory research developed a range for the mechanical properties that would be typical from NiTi in its austenite and martensite arranges as saw above in Table. 2.3. Then the SMA stress/strain relationship depends upon temperature, the Young's modulus moreover depends upon temperature. Youthful's modulus is the extent of the associated stress to the resulting strain. Thusly, the mechanical direct of a NiTi blend as a component of temperature. At low temperature, so that in martensitic arrange, the mechanical direct of the material is portrayed by significant inelastic distortion ensuing to exhausting it could be recovered by warming the compound (Shape Memory Effect, SME). As the multivariate martensitic

organize is mutilated, a detwinning system occurs, similarly as advancement of legitimately produced martensitic varieties to the next various varieties.

The external force in the martensitic stage initiates rearrangement of the variations and results in an extensive plastic strain, that isn't recouped after emptying. Toward the finish of the disfigurement, and subsequent to emptying, it is conceivable that just a single martensitic variation remains if the finish of the pressure level is achieved; something else, if the distortion is ended halfway, the material will contain a few distinctive correspondence variations.

During load removing, the detwinned martensite changes in austenite because of material is not stable at temperature over austenite finish, at a minor stress level, identified with the turnaround change, shows up in the stress/ strain vs temperature curve (SE), by and large, without inelastic strain.

2.5.   Thermodynamic Modeling of Shape Memory Alloy

From 1980 until today, constitutive modeling of SMAs have been an energetic subject of research. The resulting models can generally be divided into three main categories:

Macro level models

This phenomenological models depend on phenomenological thermodynamics just as explicitly twist fitting test data. Many rely upon the typical stage layout of SMA change where the advancement territories of martensite to basic stage or basic stage to martensite change are settled examined and drafted in stress and temperature diagram. The martensite volume fraction is used for explain the smooth transition between inside factors and different mathematical functions.

These sorts of models are commonly increasingly reasonable for designing applications because of their straightforwardness and quick calculations, however they can just portray the worldwide mechanical reaction while all the infinitesimal subtleties are disregarded; in light of the fact that the stage graph is based on test information, the models are additionally very exact. In view of continuum thermodynamics with inner factors, a few three-dimensional plainly visible phenomenological models already proposed, in the writing, with progress. In this exploration, we will utilize the naturally visible or phenomenological method and will introduce more subtleties in the following segments.

Micro level models

Micro scale models center on the portrayal of miniaturized scale highlights, for example, nucleation, interface movement, twin development, and so on. They are incredibly useful to Microscopic thermodynamics models (smaller scale models): Micro-models center around the depiction of miniaturized scale highlights, for example, nucleation, interface movement, twin development, and so forth. They are incredibly useful to comprehend the principal marvels, however are regularly hard to apply for building applications. They don't consider stage volume parts as from the earlier inward factors, yet as a result of interface developments [21-25].

Macro micro level models

The spirit of the miniaturized scale mechanics based models is in the demonstrating of a solitary grain and further averaging the outcomes over a delegate volume component to acquire a polycrystalline reaction of the SMA. Some models have been introduced in the writing by various analysts. For instance, Patoor et al. (1996) have demonstrated the conduct of a polycrystalline SMA by using the model for single precious stones and utilizing the self-predictable averaging strategy to represent the communications between the grains. A small scale mechanical model for SMAs which can catch diverse impacts of SMA conduct, for example, superelasticity and shape memory impact [21-25].

2.5.1. Small deformation (strain) models of SMA elements

The designing strain is the most well-known meaning connected to materials utilized in mechanical and basic building, that are exposed to exceptionally little disfigurements. Then again, for certain materials, for example elastomers and polymers, exposed to extensive misshapenings, the designing meaning of strain isn't pertinent, and along these lines other progressively complex meanings of strain are required. In this part we survey many 3D SMA constitutive models inside the minute hypothesis structure. Concentrating just on essential impacts, researches are recast all models in a basic structure, called fundamental model. A while later, researches build up a type of constitutive models and demonstrate that it incorporates a few models accessible in the writing. Researches emphasis around a particular individual from the planned type and contrasting and the accessible models, in hypothetical plan and numerical outcomes, researches demonstrate

its capacities in catching SMAs conduct under multiaxial non-corresponding loadings [21-25].

2.5.2. Models available in the literature

i. Basis of Souza Model

The model introduced by Souza and his team, is created inside the hypothesis of irreversible thermodynamics in the domain of a little disfigurement routine. As needs be, at every moment the thermodynamical condition of a homogenized volume component is depicted by a lot of (manageable) outside and inside factors. Additionally, introduce legitimate possibilities and following traditional contentions, it is conceivable to process the amounts thermodynamically conjugate to both the outside and the inward factors.

Table Basic Souza model

$$External\ variables: \varepsilon, T$$

$$Internal\ variables: e^{in}$$

$$Stress\ quantites$$

$$s = 2G\ (e - e^{in}) \tag{2.3}$$

$$x = \left[\tau_M\ (T) + h\ \|e^{in}\| + \gamma\right] \frac{e^{in}}{\|e^{in}\|} \tag{2.4}$$

$$e^{in} = s - x$$

with

$$\begin{cases} \gamma \geq 0 & \text{if } \|e^{in}\| = \epsilon_L \\ \gamma = 0 & \text{otherwise} \end{cases}$$

ii. Panico and Brinson Model (2007)

This model introduced by Panico and Brinson and it for the small strain constitutive model. The stress proposed martensite fraction, Z_σ is related to the plastic strain as given below:

Stress quantites

$$\begin{cases} \sigma = \mathbb{L}:(\varepsilon - \varepsilon^{in}) \\[2mm] \bar{x} = \dfrac{\rho}{\sqrt{\frac{3}{2}}\,\gamma_0} \, |[\langle T\Delta_{n0} - \Delta_{u0}\rangle + H_{\sigma z\sigma}] \dfrac{\epsilon^{in}}{\|\epsilon^{in}\|} \\[4mm] x^{tr} = s - \bar{x} \\[2mm] x^{re} = s \\[2mm] x^{T} = -\rho\,(T\Delta_{n0} - \Delta_{u0}) \end{cases}$$

iii. A basic extracted Panico-Brinson model

External variables: ε, T

Internal variables: e^{in}

Stress quantites

$$s = 2G\,(e - e^{in}) \tag{2.6}$$

$$\bar{x} = [\tau_M\,(T) + h\|\,e^{in}\|]\dfrac{\varepsilon^{in}}{\|\varepsilon^{in}\|} \tag{2.7}$$

$$x^{tr} = s - \bar{x} \tag{2.8}$$

$$x^{re} = \hat{\mathbb{I}}:s \tag{2.9}$$

iv. A Panico and Brinson model with modifications (2007)

The first study, they have utilized a logarithmic capacity to authorize the plastic strain standard limitation (2.4). Besides, they utilize diverse capacities in forward and turn around stage changes. In any case, in the Souza show, rather than utilizing a logarithmic capacity, they utilize the pointer work which is all the more intriguing from a numerical

perspective*External variables: ε, T*

Internal variables: e^{in}

Stress quantites

$$s = 2G\,(e - e^{in}) \tag{2.10}$$

$$x = \left[\tau_M\left(T\right) + h\|e^{in}\| + \gamma\right]\frac{\varepsilon^{in}}{\|\varepsilon^{in}\|} \tag{2.11}$$

$$x^{tr} = s - \bar{x} \tag{2.12}$$

$$x^{re} = \hat{\Pi}{:}s \tag{2.12}$$

with

$$\begin{cases} \gamma \geq 0 & \text{if } \|e^{in}\| = \epsilon_L \\ \gamma = 0 & \text{otherwise} \end{cases}$$

v. Lagoudas Model (2008)

Lagoudas and his associates have utilized a SMA demonstrate in a few studies. This research team have accepted of the forward stage change from austenite phase to martensite phase ($z\_ > 0$) the change strain will frame toward the deviatoric stress. Amid the turnaround change from martensite stage to the austenitic at parent stage ($z\_ < 0$), the change strain will be recuperated relatively to the current change resist the inversion point (et-r) from forward to the switch change. Summarization of Lagoudas demonstrate as in Table 2.4.

External variables: ε, T

Internal variables: z

Stress quantites

$$s = 2G\left(e - e^{in}\right) \tag{2.13}$$

$$\bar{x} = \tau_M\left(T\right) + h\varepsilon_L z_\sigma \tag{2.14}$$

$$x^{tr} = s : n - \bar{x} \tag{2.15}$$

with

$$e^{in} = (\varepsilon_L z)n \tag{2.16}$$

and

$$n = \begin{cases} \dfrac{s}{\|s\|} & \text{if } \dot{z}_\sigma > 0 \\[4mm] \dfrac{e^{t-r}}{\|e^{t-r}\|} & \text{if } \dot{z}_\sigma < 0 \end{cases}$$

Table 2.4: Summary of Lagoudas Constitutive Models of SMAs [21-25]

Contributors	Description of Model
1996 Boyd and Lagoudas 1996a Boyd and Lagoudas 1996b	3D phenomenological model, using martensite volume fraction, accounting for pseudoelasticity and responses under non-proportional loading. The model is generalization of earlier study of Tanaka (1986), and Liang and Rogers (1990).
1999 Bo and Lagoudas 1999a, 1999b & 1999c Lagoudas and Bo 1999	3D phenomenological model accounting for pseudoelasticity, TWSME, and major and minor loops. This model is extension of Boyd and Lagoudas (1996). Transformation induced plasticity is accounted for by introducing transformation strain
2000 Qidwai and Lagoudas 2000b	Extension of Boyd and Lagoudas (1996) to account for ATC. Three different transformation functions (based on J_2, $J_2 - I_1$, and $J_2 - J_3 - I_1$ transformation functions) and their effect on ATC was presented.
2004 Entchev and Lagoudas 2004; Lagoudas and Entchev 2004	Extension of 3-D the model by Bo and Lagoudas (1999) to account for the simultaneous development of transformation and plastic strains during stress-induced phase transformation. The model is able to reproduce pseudoelasticity, ATC, and major and minor loops.

2.6.   SMA for Biomedical Applications

As featured in various examinations, shape memory composites (SMAs) can be promptly gotten in business amounts from various specific organizations around the globe, either as semi-completed item in different shapes and structures, for example, wires, bars, cylinders and strips or as completed items, for example, helical springs and wire actuators, at truly sensible costs. Albeit a huge number of licenses have been distributed on SMA applications, under 1% of these are industrially fruitful. This constrained business achievement is to some extent because of an absence of formal rules and related structure apparatuses to help in the compelling plan of NiTi uses. These requirements may have prompted the requirement for further research towards enhancement and development of NiTI actuators. [14]

Late 1980s has been developed in many intrusive medical procedure or minimally invasive surgery. MIS has been viewed as a standout amongst the most essential

accomplishments in current prescription. Laparoscopic cholecystectomy was the primary negligibly obtrusive strategy to be created and generally acknowledged [03]. From that point forward, numerous negligibly intrusive systems have been created and increased far reaching applications, they are currently settled in medical procedure and routinely working on, including cholecystectomy, Nissen fundoplication for gastro-oesophageal reflux ailment, appendicectomy, adrenalectomy, splenectomy and numerous other propelled methods.

Negligibly obtrusive medical procedure offers extraordinary advantages to patients over regular open medical procedure, the significant advantages incorporate decreased careful injury, diminished injury complexities, shorter clinic remain, and quickened recuperation. Be that as it may, BMA is in fact additionally requesting as contrasted and ordinary medical procedure, in light of the fact that the careful mediation is executed remotely by means of 2D imaging of the employable field, with loss of material input, confined mobility, and less effective control of significant draining [3].

The achievement of BMA was empowered by numerous innovative leaps forward, for example, cool light source, adaptable optical strands and small camcorder, especially the Hopkins pole focal point endoscope. BMA is progressed in term of innovation but on the other hand is innovation subordinate. The necessities of negligible obtrusiveness have exhibited extraordinary specialized difficulties to specialists and medicinal gadgets designs too [3]. Many designing advancements have been carried to take care of the issues related with BMA, the utilization of SMAs in medical procedure is a magnificent case of each one of those fruitful stories. The exceptional materials properties of SMAs, for example shape memory impact and superelasticity, have given ideal responses to the strict structure prerequisites in BMA, novel careful gadgets have been created dependent on SMAs, and they have turned out to be fundamental devices for some insignificantly intrusive methodology. The uses of NiTiNOL impelling components for drug incorporate orthodontic supports, Harrington pole for scoliosis treatment, and the Simon channel in 1977 [20]. In any case, it was not until the 1990s that NiTiNOL has begun to have genuine effect on drug with innovation leaps forward in the plan, demonstrating and fabricating. From that point forward, numerous restorative gadgets were created and made incredible progress, for example, stent for cardiovascular intercessions, careful gadgets for endoscopic and laparoscopic medical procedure, and orthopedic implants.

2.7.   Historical development of biomedical actuators

Types shape memory materials have been exposed over the past century, containing metals, ceramics and polymers. The NiTi SMA is the only one used for implants and bio medical devices among them.

Table 2:5: Historical Development of NiTiNOL elements for biomedical actuators [3]

Year	Biomedical Device/ Element	Actuating Elements
1971	Orthodontic braces	Wire
1976	Harrington rod for scoliosis	Rod
1977	Simon vena cava filter	Wired Mesh
1981	Orthopaedic Staple	Wire
1983	Prosthetic joint	Wire
1983	Nitinol stent	Wired Mesh
1990	Thin film SMA Thin film microdevices	SMA thin film
1991	Variable curvature spatula	Wire
1993	Laparoscopic hernia repair mesh	Wired Mesh
1995	Laparoscopic clamp Laparoscopic retractor	Wire
1995	Thin film microgripper	SMA thin film
1996	RF ablation device Hernia repair retractor	Wire
1998	Atrial septal occlude	Cable
1999	Thin film SMA microvalve Laparoscopic suturing clip	Tin film Wire
2000	Vascular ligation clip Multipoint injector	Wire and rod
2001	Drug-eluting stent and Thin film microstents Thin film microwrapper	Wired mesh
2004	Laparoscopic anastomosis ring	Wire ring
2005	Thin film heart valve	Thin film
2007	Endoscopic bleeding control device	Cable
2008	Thin film microtube and stent	Wired mesh
2009	Reinforced Annuloplasty Band	Wire
2010	Embedded endoscopic clamp	Wire
2011	Staples (Niti Clips)	Clip
2012	Bullet-shaped Microgripper	Wire
2013	Grasper actuated wire	Wire
2014	Minimally invasive cage (elliptical shaped Hinges)	Wire
2015	Spring for tendon–sheath mechanism	Wire
2016	4-DOF Origami Grasper	Rod and wire
2017	Modular soft robotic manipulator Spring actuators with real-time cooling	Helical spring
2018	Jaws of 5 DOFs robotic Variable-stiffness flexible manipulator	Wires Wires and cables

2.8. Characterization of SMA for Biomedical Applications

2.8.1. SMA-Based Actuators

Shape memory actuators are used where a large force or large stroke is required and thermodynamic efficiency is not essential. The reason for using shape-memory alloys as actuators is that a large amount of work can be obtained from a small volume of material. Repeated cycling at approximately 5 percent strain and more than 200 MPa stress produces more than a Joule of work output per cycle, among the highest work densities (the amount of work output per unit weight of the actuating element) known and details shown in Figure 2.27.
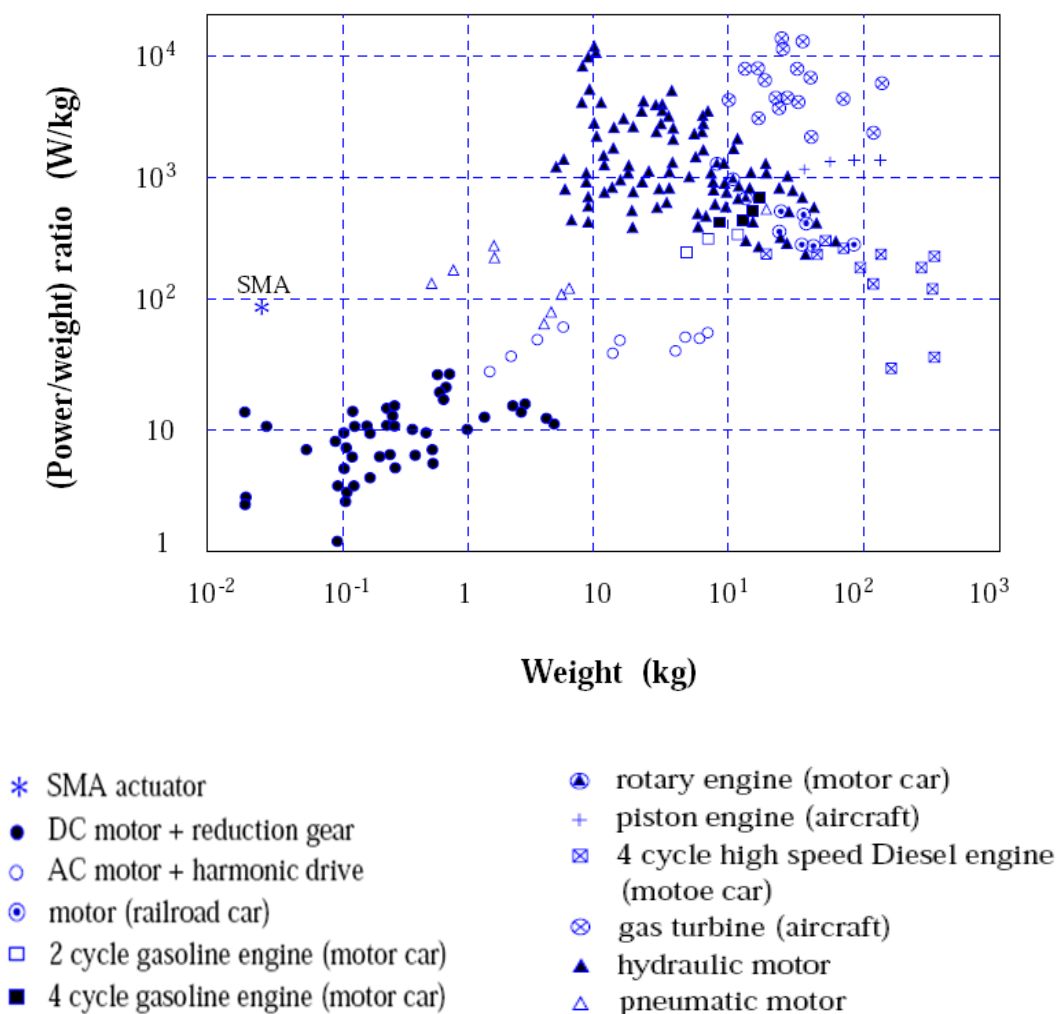

Figure 2.26: Power to weight ratio vs. weight diagram of different actuators [18]

2.9.   SMA-Based Actuator Elements

SMA components can either be prepared to recollect just high temperature austenite shape, single direction SMA; or both low and high temperature shapes, two-way SMA. The stage change strain of two-way SMAs is fundamentally less and their steadiness and repeatability are dubious [15].

Both single direction and two-way SMA components might be utilized for actuator applications. Though two way SMA can execute in two ways, anyway its change strain is typically just 50% of that in single direction SMA and the incitation cycle may not generally be precisely rehashed. Rather than two-way shape memory amalgams, two single direction shape memory composite components are orchestrated to work in predisposition to get a similar activation. As of late, the utilization of SMAs has been planned as an option in contrast to electrical engines.

2.9.1.   Importance of NiTi Elements

1) Mass and volume savings

   Scientists have thought about the power to weight proportion versus weight of a specific type of NiTi actuator with numerous other traditional engines in Figure 2.26. It recommends that NiTi actuators have the potential ability to accomplish a yield to weight proportion and conventional actuators not act as.

2) Overcome of End of deployment vibrating forces

   These are constantly connected with spring and sent structures. In this manner, no further requirement for dampers, and thus in general framework unpredictability can be decreased.

3) Noiseless activity that evacuates the shock unsettling influences to different payloads that are regularly connected with motor driven arrangement.

4) Sensing capability.

   Actuating and sensing capacities can be joined according to estimating variations in electrical opposition related with the stage change.

5) Reliability is high

   Sending is activated by a stage change and the speed of arrangement is identified with the temperature of the NiTi alloy, which is itself controlled by the heating input and warmth exchange.

6) Higher recoverable strains

Amazingly long strokes and the use of extensive powers when disfigurement is controlled.

7) High electrical resistivity

The shape change can be enacted by transitory an electrical flow through a NiTi, in this way maintaining a strategic distance from the requirement for independent heating method.

8) Plan adaptability.

Shape memory compound actuators can be direct, turning, or a blend of the two, as required, and can frame a fundamental piece of a segment.

2.10. Controlling of Actuator elements

Actuators utilizing single direction SMA components ought to be reset utilizing a biasing instrument or a resetting power to finish the work cycle. Distinctive power/relocation attributes might be acquired by changing the sort of the biasing component utilized in the actuator. Three essential sorts of SMA actuators utilizing just a single way SMA components are given in the accompanying passages.
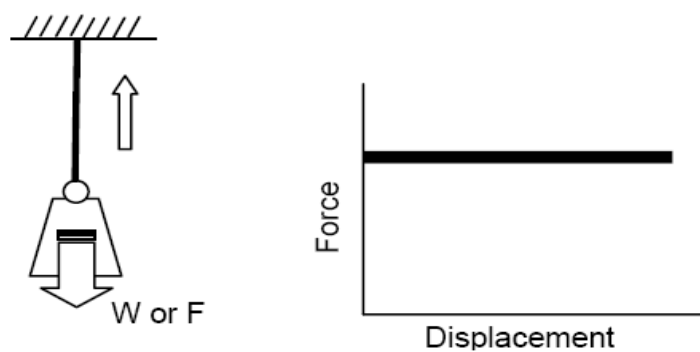
Figure 2.27: Constant force for opposite direction

In the main sort, the dead weight of a heap or some other outside power causes the SMA wire to prolong in martensitic stage, after warming, the heap is raised by the consistent power which is its weight or the restricting power (Figure 2.28). After cooling, the weight or the power makes the wire extend back. Actuators utilizing gravity or a consistent response as a resetting power give a flat power/dislodging trademark

The second sort of biasing component is the spring, fit as a fiddle memory amalgam neutralizes a spring, when the SMA component is warmed the spring is extended, putting away vitality after cooling the vitality put away in the helical spring is discharged and the shape memory alloy misshapes back, to the first diversion consequently finishing the cycle (Figure 2.29). The incline in the power relocation line essentially speaks to the spring rate. In any case, this application isn't suggested as far as life of the SMA since the restricting power increments as the SMA experiences change.
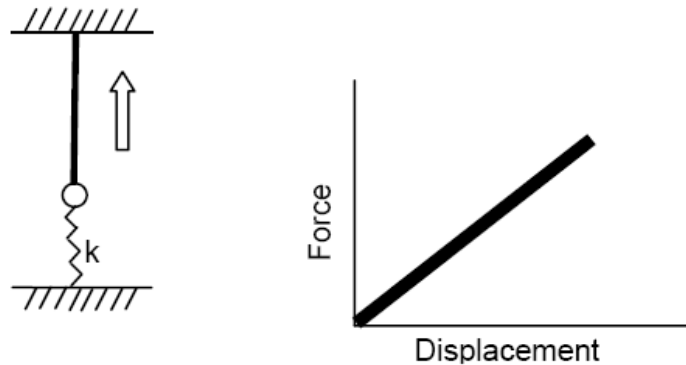

Figure 2.28: Spring to opposite direction

As portrayed over, two single direction SMA components can be orchestrated to neutralize each other as the third strategy. While one of the wires is warmed, therefore contracted doing work, the other one is stretched (Figure 2.30). After warming the following wire, the movement is turned around, along these lines the work cycle is finished.
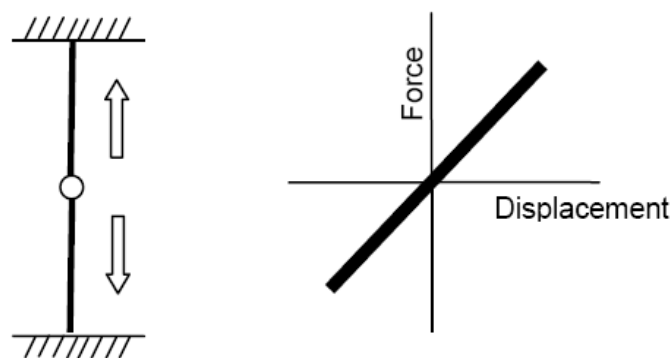

Figure 2.29: SMA in two one-way direction

Another order of SMA actuators can be made by their warming strategies. Shape memory based actuators can either be driven by warm changes or by electrical methods. The two activation types are especially not quite the same as configuration perspective, so a short writing review on the two sorts will be exhibited in the accompanying segments.

2.10.1. Thermal operated actuator elements

Heating a SMA component by warm changes can be accomplished by transitory an electrical flow through a high obstruction tape or wire folded over the SMA component as a functioning warm technique or by uncovering the SMA segment to warm radiation, which is a uninvolved strategy. In the last strategy no extra warming framework is required; in any case, this technique is unyielding, and it could be extremely hard to impel the gadget.

2.10.2. Electrical operated actuator elements

In this strategy, SMA components are incited by passing an electrical flow through them. This strategy is just relevant where a little breadth SMA spring or wire is utilized; generally the electrical obstruction is too little to even think about producing enough warming. The fundamental favorable position is straightforwardness, while the huge disservice is that the SMA component should be electrically protected.

Table 2:6: Types of conventional macroscopic SMA actuator elements [07]

SME	Functional mechanism	Application
OWSME	Thermal actuation constrained recovery	Couplings Joining rings Electrical connection units
	Thermal actuation Passive biasing mechanism	Anti-scald safety valves Air conditioners Circuit breakers Temperature switches
	Electrical actuation Passive biasing mechanism	Light controls Grippers

2.11. SMA based Macro level Biomedical Applications

Shape memory alloy has unique properties in biomedical applications such as non-magnetic, high biocompatibility and good corrosion resistance. Then it is more suitable for the development of many elements in the human body as shown in Figure 2.31. Another very important feature of NiTiNOL is its change of shape or form in the any condition of the human body temperature.
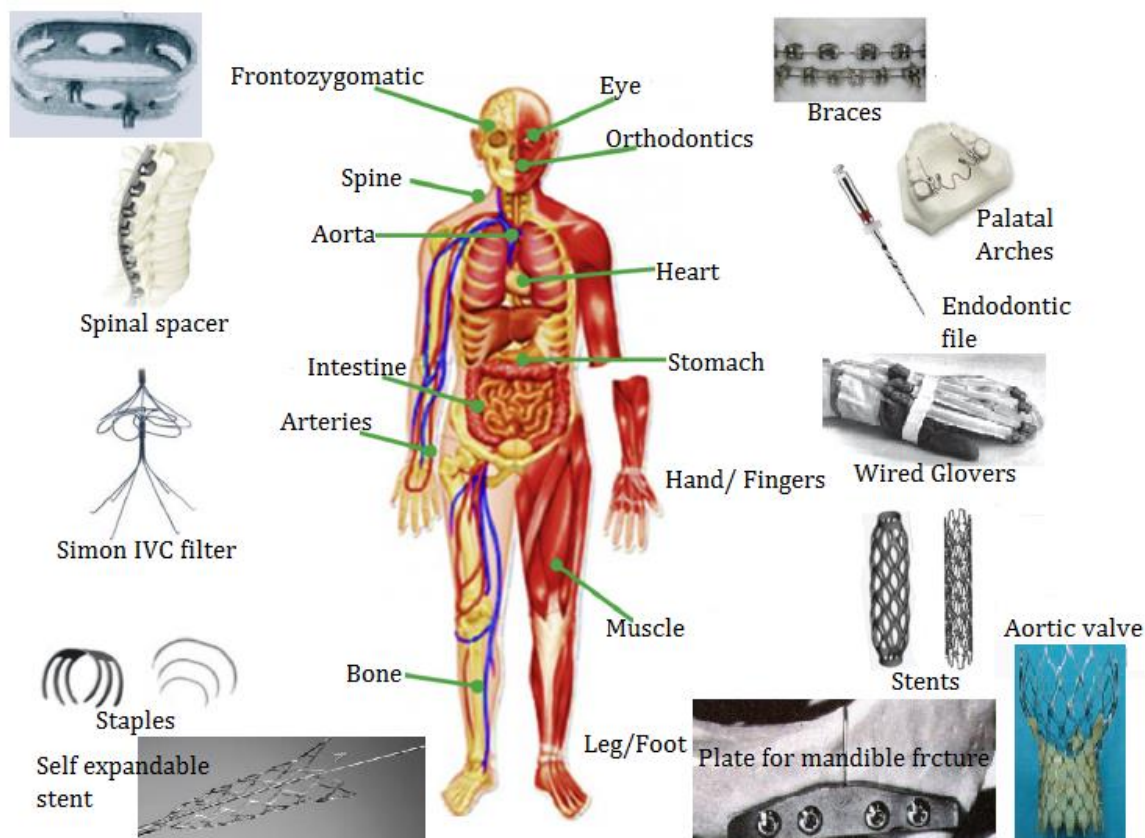
Figure 2.30 Biomedical applications of SMA [33]

Generally, any biomedical instrument requires accurate functioning and correct positioning for complex surgical processes and serious medical treatments. Then, during surgical treatment processes, SMA can achieve these advantages. Some of SMA's biomedical products are used in various fields in many biomedical devices and equipment. Table 2.7 shows important biomedical applications.

Table 2:7: Listed NiTiNOL based biomedical applications [33]

Fields				
Orthodontic	Orthopaedic	Vascular	Surgical Instruments	Miscellaneous
Braces/ brackets Palatal arches Files	Head Spine Bone Muscles Hand/fingers Legs	Aorta Arteries Vena cava filter Ventricular Septal Defects Vessels Valves	Catheters/ snares Scopes Suture	Cardiology Hepatology Urology Otorhinolaryngology Gastroenterology Ophthalmology

2.12. SMA based Micro (MEMS) Actuator for Biomedical Applications

As of late, much noteworthy research has underlined the advancement of MEMS (Small scale Electro-Mechanical-Frameworks) in light of its immense capacities in scaling down to play out an assortment of undertakings. The greater part of this examination has attempted to concentrate on SMAs slender movies because of its SME and PE characteristics that create it a dependable application on the miniaturized scale. Despite the fact that, numerous examinations have been led to think about the practicability of SMA based MEMS actuator for negligibly intrusive medical procedure applications. What's more, there the majority of utilizations are under trying condition and a few applications are specifically use as biomedical applications, for example, stents.

NiTi flimsy film is connected as the principle innovation for activation in numerous MEMS microdevices, due to its specific capacities, for example, huge power/stroke, occasional task and working limit in exceptional situations (space, radioactive, destructive and organic). Table 2.8 analyzes the properties of some regular small scale activation instruments [28].

Table 2:8: Variation of microactuators capabilities [27]

Microactuator	Max. Energy (Ws/m^3)	Max. Frequency (Hz)	Voltage (V)	Efficiency
NiTiNOL	2.5×10^7	<100	2 – 5	0.01
Electrostatic	1.8×10^5	<10000	5 – 500	0.5
Electromagnetic	4.0×10^5	<1000	~ 20	<0.01
Piezoelectric	1.2×10^5	<5000	5 – 100	0.3
Bimetallic	4.0×10^5	<100	~ 5	10^{-4}
Thermopneumatic	5.0×10^5	<100	~ 10	0.1
Conductive polymer	3.4×10^6	<1000	~ 5	0.6

At present, expanding consideration has likewise been paid to utilize TiNi thin film into insignificantly intrusive medical procedure, microstents and biomedical applications (bio MEMS). The small scale actuators produced using TiNiNOL shows might be utilized to mix medicates, or set in vital areas in the human body to help in various way. Most of natural applications used glass, silicon and polymers to develop the human body parts. Be that as it may, high affidavit or toughening temperatures for arrangement of TiNi thin films and the poor bond on these substrates represent the potential issues.

Superelasticity of TiNiNOL, a non-straight and its strain value 7– 10%, that officially discovered numerous uses for mass materials, however couple of investigations are done in MEMS applications so far utilizing slight movies. For some pleasant components in MEMS products, TiNiNOL thin film material under superelastic condition is encouraging.

Then TiNi movies can give extensive powers to activation and expansive relocation, along these lines, most utilizations of TiNi films in MEMS are centered around smaller scale actuators, for example, microvalves, micropumps springs, microspacers, microgrippers, micropositioners and microrappers, and so on.

2.12.1. MEMS applications of Biomedical Applications

1) Microvalues

   These microvalves are used for many uses such as analytical tools, chemical analysis, implantable drug delivery, etc.

2) Micropumps

   The application of NiTi thin films in micropumps is prevalent in some instruments and chemical analysis such as sealing or switching of liquids, implantable drug delivery, gasses or vacuums.
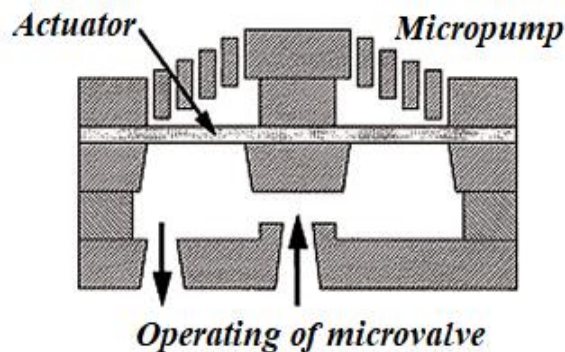

Figure 2.31: Shemetic view micrvalve and pump [27]

3) Microwrappers/ microcage

   These are very useful to operate micro - organisms to eliminate anomalies such as tumors in minimally invasive surgery as shown in Figure 2.32.
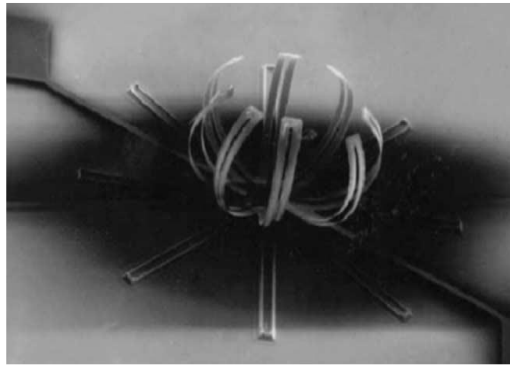
Figure 2.32: The micro-wrapper made of TiNi films [28]

4) Microclippers

Figure 3.8 shown in a novel microelectrode with a TiNi clipping structure that can be used for minimally invasive microelectrodes to clip a nerve cord or other living organisms. When a current is applied to the electrode, the TiNi film is actuated. The electrode's clipping force to the nerve is enhanced by a hook structure and two C-shaped probes
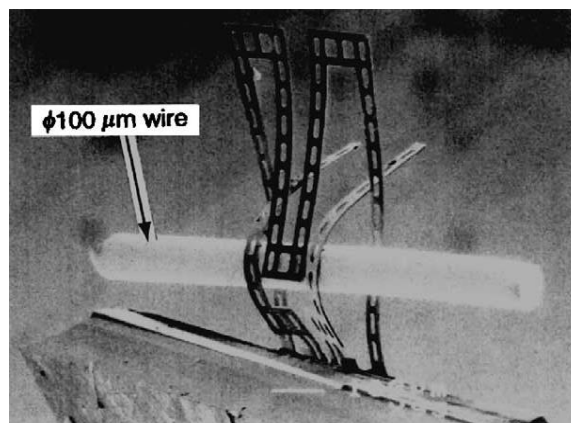

Figure 2.33: The 100μm wire for microelectrode clipping [28]

5) Microgripper

   i.   For grasping applications

For various requirmrnts such as gathering in microsystems, micromanipulators for cells, and endoscope for microsurgery (MIS), microgrippers are used to grip micro objects with high accuracy. Generally speaking, NiTi microgrippers have some main characteristics such as large gripping force and appropriate opening distance compared to other materials for some peculiar assembly operations.
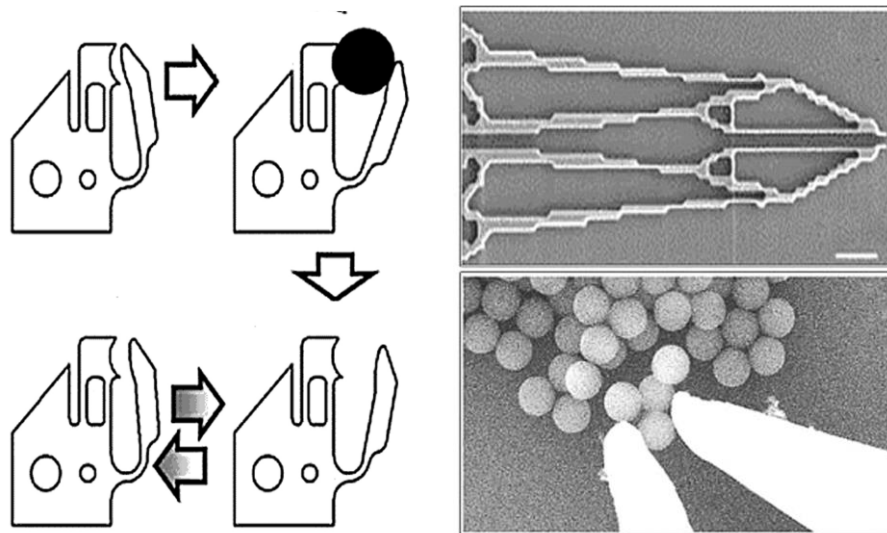
Figure 2.34: Types of microgrippers and grasping mechanisms [27]

Existing MI based robotic surgical microgrippers are operated using a motor pack located on the outside of the human body. The end - effector actuated by using mechanisms driven by sliding links or tendons. This microgripper has fewer degrees of freedom due to the power transmission method.

ii.   Mechanical properties measuring of cells and tiny biological tissues
       Applications: Test mechanical properties of cells

                       Testing pulse in micro vessels
       Materials: Piezo-Electric

                       NiTi alloy

        The creators are exploring another class of mechanical small scale instruments whose extreme objective is to expand the execution of the specialist amid MIS. Chiefly talked about the principle highlights and the execution of a model smaller than expected automated instrument comprising of a miniaturized scale created microgripper, instrumented with semiconductor strain-measures as power sensor. The microprobe chose as the end effector of the apparatus mechanical assembly is a LIGA-manufactured microgripper made out of electroplated nickel covered with a slender gold layer. The geometry of the microgripper (working length - 17 mm, large width - 7.5 mm and thickness - 0.4 mm) is appeared in Figure 2.36.
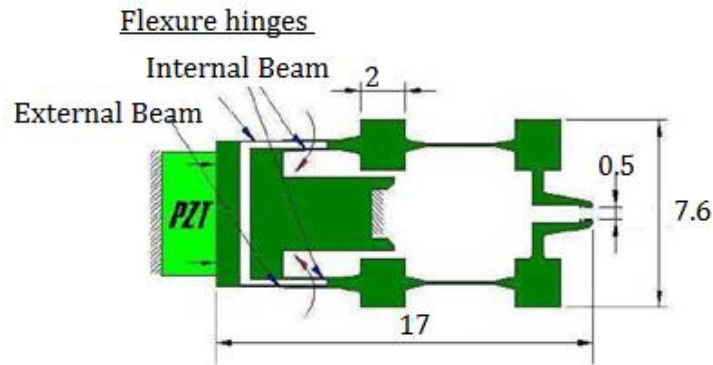
Figure 2.35: Geometry of the microgripper [29]

Likewise built up another variant of microgripper, manufactured in superelastic combination (Ni-50.8%, Ti-49.2%) by wire small scale Electro Release Machining (EDM) [30]. The gripper is as appeared in the Figure 2.37.
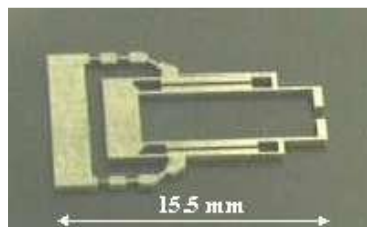

Figure 2.36: New microgripper (fabricated in superelastic alloy) [29]

   iii.   SMA thin-film-based microgrippers.

Application: Handle microscopic objects

Material: NiTi alloy

             Silicon

As illustrated in Figure 2.38, this thin film microgrippers are developed by connecting two NiTi-Si cantilever beams together with a silicon wafer in between. It is manufacturing by properly recognized clean room methods. These are photolithography, etching, fine alignment, eutectic bonding, and NiTi thin film sputtering.
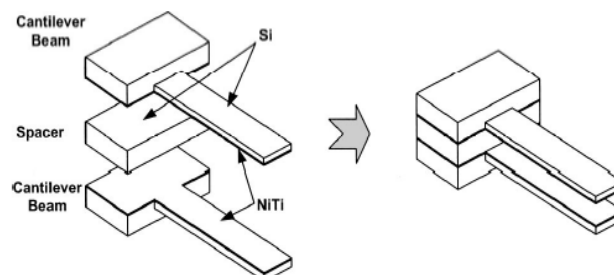

Figure 2.37: Microgripper with two NiTi-Si cantilever beams bonded together [30]

Following Figure 2.39 shows working method of the above microgripper and a SMA based cantilever system microgripper. Position (a) show the open at the room temperature. Position (b) shows closed on heating.
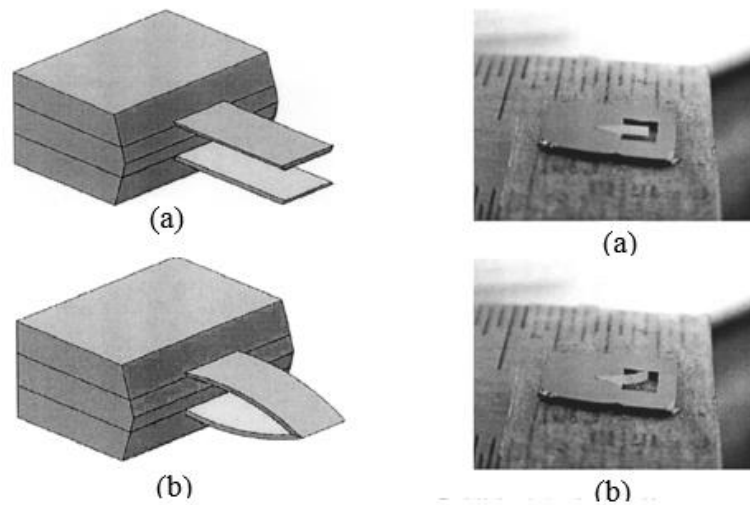

Figure 2.38: Working method of the above microgripper (left) and a SMA based cantilever system microgripper (Right) [31]

iv.   SMA microgripper with integrated antagonism

Application: For micro objects handling

Material: NiTi alloy

This is a microgripper created with NiTi and consisting of two integrated actuation parts with opposite moving directions. This allows separate antagonistic control of the opening and closing motion of integrated gripping jaws. Figure 2.40 shows an open and closed condition SMA microgripper schemeThe gripper consists mainly of two mechanical actuator units with bond pads.
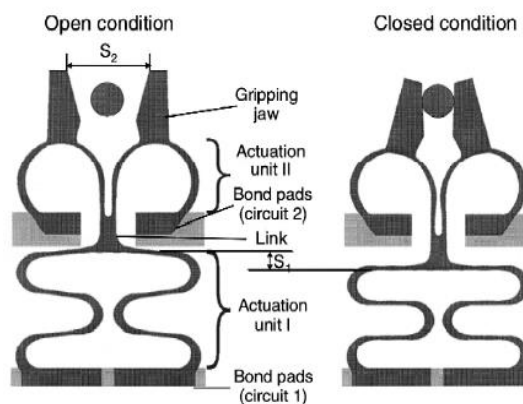

Figure 2.39: The SMA microgripper in open (left) and closed (right) state [31]

v.   SMA Microgripper for MIS

Application: Biomedical

Material: NiTi alloy

In recent years, the application of robotic instruments in MIS has been developing. The urge to implement biocompatible and less invasive devices found a way to use materials such as shape memory alloys. Following Figure 2.41 shows the 3D view and the drawing of the design.
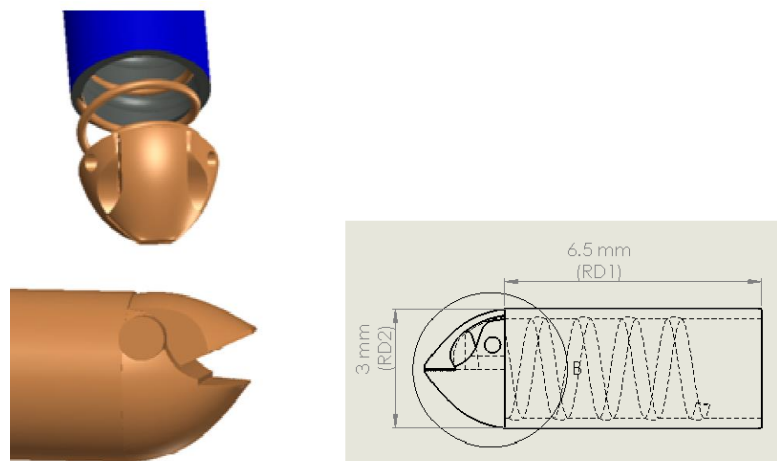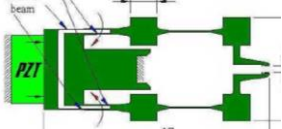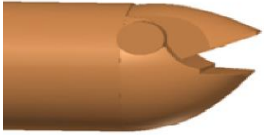

Figure 2.40: 3D view (left) and the drawing (right) of the design [31]

2.12.2. Dimensions of Biomedical (BM) microgrippers

Minimally inverse surgical procedures are carried out using small tubes, these tubes insert to small incision, and it is between 5 to 10mm in diameter [31]. Following Table 2.9 shows the some existing microgripper jaw dimensions in BMAs.

Table 2:9: Geometrical dimensions of exiting macro and micro grippers [31]

Biomedical Macro/ Micro gripper	Dimensions of the gripper
G1. For determine the mechanical properties of cells and tiny biological tissues	Length - 17 mm Width - 7.5 mm Thickness - 0.4 mm
G2. Design of SMA Micro-Gripper for Minimally Invasive Surgery	Major diameter 3mm, Length 6mm

G3. Grippers for MIS heart surgery	Diameter 5mm, Length 10mm
G4. Structure forceps	Diameter 2.8mm, Length 8mm
G5. Rongeurs forceps	Diameter 3mm, Length 11mm
G6. Needle holder	Diameter 0.35mm, Length 2mm
G7. RESANO toothing forceps	Diameter 3mm, Length 16mm

In this project was focused to investigate the thermomechanical characteristics or behavior of an actuator element for MIS microgripper which is helical spring with two diameters by using selected SMA. The fabrication of helical spring and their thermomechanical characteristics or behavior will have discussed in next chapters with more details.

Chapter 03

3 Investigation of Thermal and Topological Characteristics

3.1. Specifications of experimental apparatus

3.1.1. Electric Muffle Furnace

Electrical muffle furnaces are appropriate for heat changing processes up to 1500 °C, containing material testing, thermocouple calibration and physical analysis. Heating elements are prepared on a ceramic covered tube. The heating elements are located inside the chamber and the temperature profile is even. (Figure 3.1).

The dimension of muffle furnace:

- Depth = 450mm
- Width = 200mm
- Height = 150mm

Figure 3.1: Electric Muffle furnace

3.1.2. Differential Scanning Calorimetry (DSC)

DSC is mainly used to determine the substances, mixtures and materials and to characterize them. In accordance with DIN 51007, ASTM D3418 and ISO L409, this technique is internationally standardized. The operating principle is to measure the heat flow between the specimen and the reference material. The process is done over a distinct area where the heat moves. As the temperature changes, the heat flux is measured. For many applications, the results are very important and provide valuable information for material characterization. The DSC System is accomplished with hardware and software setups. DSC include temperature programming, atmosphere control, timed cycling to setup the parameters.

Figure 3.2: DSC analyzer placement of specimen

The DSC analysis measures the amount of energy absorbed or released by the sample when heated or cooled, providing quantitative and qualitative data on endothermic processes (heat absorption) and exothermic processes (heat evolution).

3.1.3. Scanning Electron Microscope (SEM)

SCM is a type of electron microscope that images the surface of the sample by scanning it in a raster scan pattern with a high energy beam of electrons. SEM with BSE detector and microanalysis of energy dispersion (SEM / EPMA). Gold and carbon sputtering facility. Areas ranging from approximately 1 cm to 5 microns in width can be imaged in a scanning mode using conventional SEM techniques, magnification ranging from 20X to approximately 30,000X and 50 to 100 nm spatial resolution.
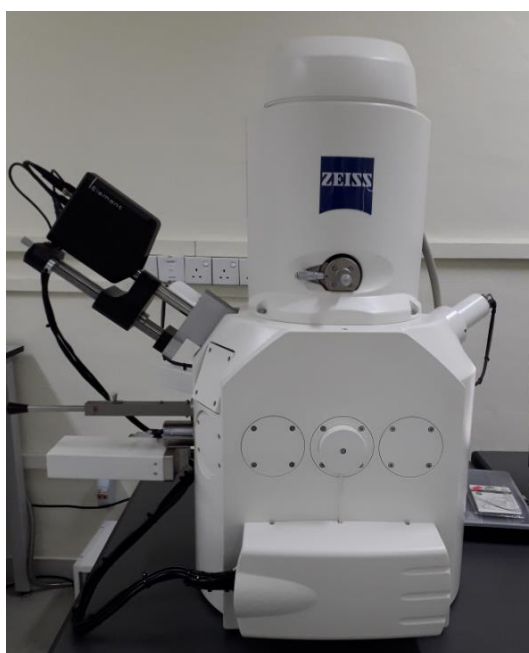

Figure 3.3: Scanning Electron Microscope (SEM)

3.2. Examine the thermal properties with DSC

In order to examine the properties of the produced SMAs, several material characterization tests were performed. The most convenient test is the calorimeter analysis for differential scanning (DSC).

Table 3:1: Labeling of heat treated of specimens.

Specimen No	Heat treatment Temperature (°C)	Heating Time (min)
Specimen – 01	400	30
Specimen – 02	450	30
Specimen – 03	500	30
Specimen – 04	550	30
Specimen – 05	600	30

DSC is an instrumental technique used in solid and liquid samples in different atmospheres to study thermal stability, temperature and heat associated with the transformation of state and chemical reactions. This method is established on the recognition and quantification of a sample's under exothermic and endothermic principles. Two resistors and two crevices form the instrument used: The samples to be examined are inserted into one, the riferiment is positioned in the other (normally empty). These two crucibles are connected to the thermocouples, as shown in Figure 3.4, the components are connected to the computer.
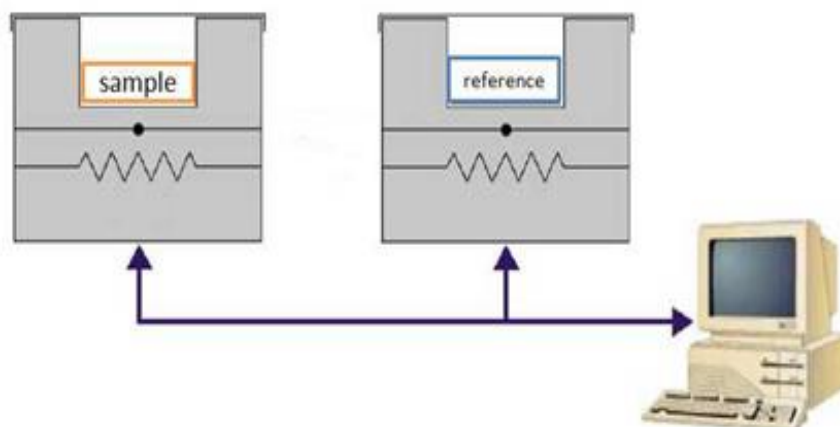

Figure 3.4: Schematization of DSC analysis machine

3.2.1. Sample preparation for DSC

In this project, sample prepared by according to given specification of manufacture of DSC machine.

SMA Manufacturer: Shaanxi Yunzhong Industry Development Co. LTD (Appendix – A)

Sample A - 2mm diameter wire

- Material – Shape Memory Alloy – NitiNOL (NiTi alloy)

- Activation temperature: 60°C

- Weight: 10 – 15mg

- Length: 0.50mm – 0.75mm

Sample B - 1mm diameter wire

- Material – Shape Memory Alloy – NitiNOL (NiTi alloy)

- Activation temperature: 30°C

- Weight: 10 – 15mg

- Length: 2.00mm – 3.00mm

3.2.2. Sample preparation for OM &b SEM

Selected NiTiNOL alloy wire diameter is 2 mm and section 3.2.1 is already mentioned. Then these specimens are hard to handle in the bare hand. The specimen holder (plastic) was used to mount the NiTiNOL specimen for sample preparation for the SEM experiment.
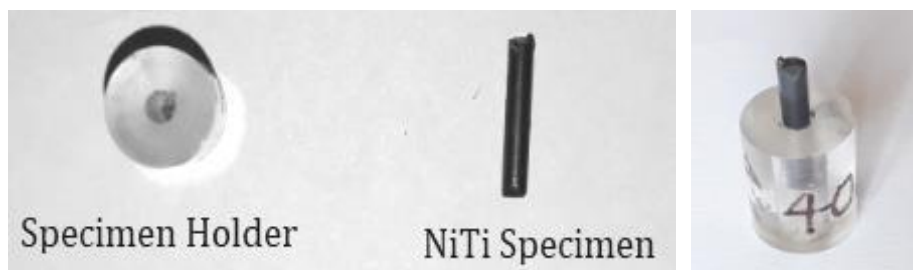
Figure 3.5: NiTINOL specimen and holder

Figure 4.6 shown for each six specimens in prepared separate specimen holder units, which are in raw material and other five heat treated specimens.

Specimen preparation for Optical Microscopy (OM) and Scanning Electron Microscope (SEM)

Specimen No.	Specimen 01	Specimen 02	Specimen 03
Specimen Figure			
Heat treatment Temperature (°C)	400	450	500
Specimen No.	Specimen 04	Specimen 05	Specimen 06
Specimen Figure			
Heat treatment Temperature (°C)	550	600	Raw Material

Figure 3.6 All specimens for OM and SEM

Chapter 04

4 Verification of Thermal Behavior and Topological Characteristics

4.1. Analysis of thermal behavior of NiTiNOL material

Differential Scanning Calorimetry is an experimental method used to investigate the heat flow (W/g), energy absorption or release (enthalpy–J/ g) and transformation temperatures of phases (martensite, R - phase and austenite) of NiTiNOL alloy specimens under different conditions. DSC testing is also responsible for determining and quantifying the exothermic and endothermic principles of a NiTiNOL specimen. The quantities of a specimen required for investigation are usually a few milligrams, and the velocity of the heating and cooling rate depends on the ability to use the operating apparatus. The DSC determines the difference between the NiTiNOL specimen heat flows and the reference. This temperature is controlled using the same program.

The basis of DSC thermogram, the correct finish temperatures of each and every phase transformation were measured by the intersections of the tangents to a peak temperature values and a base line. The common recognized notation of transformation temperatures is used in this project work given below.

M_s, M_f, As, A_f, Rs, R_f, - Martensitic and austenite, R phase, starting and finishing temperatures.

- Rp, Mp and Ap – The peak temperatures for the transformation.
- ΔH (with the proper subscripts) – Transformation heats (absorbed and released) This heats are given by the area bounded on the Bell shaped area under peak and base line of the DSC curve.

The exothermic phase transformations to martensitic and R phase on cooling are given in upper curve (positive) and also the endothermic phase transformations to austenite on heating are given in lower curve (negative). During the heating, a one transformation stage is observed namely, from the martensite (B19') to the parent shape austenite (B2). Again during cooling, two transformation stages observed namely, from Austenite to R phase (B2') and R phase to martensite (B19').
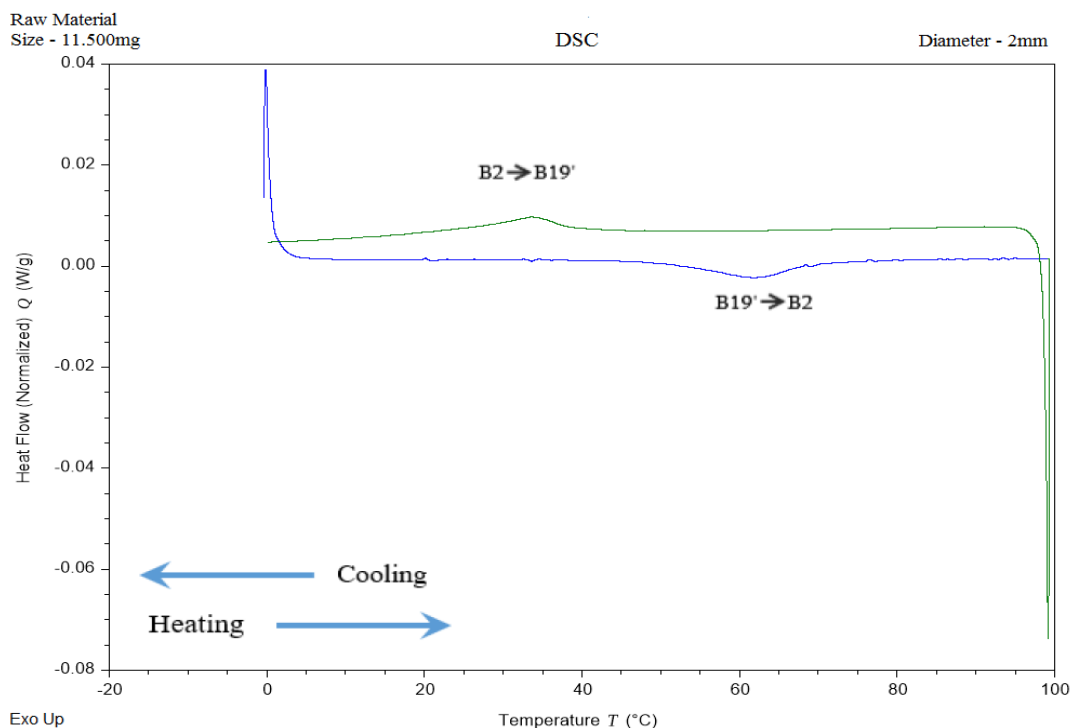
Figure 4.1: DSC Thermogram for Raw material

Figure 4.1 shown in the DSC thermogram of raw material and cannot correctly identify temperature transformation phases. Therefore, it is not suitable for practical applications. The DSC thermogram features represented on the NiTiNOL raw specimen without heat treatment and on the other specimens that were heat treated at selected temperatures (400, 450, 500, 550 and 600°C) for 30 minutes are reported. The results given the thermal properties of the selected NiTiNOL, such as phase reactions involving different heat treatments during cooling and heating at the stress free condition and latent heats of phase transformations. The arrows on all thermograms indicate the cooling and heating direction. The temperature range between 0 and + 100 ° C is given in this NiTiNOL raw material curve based DSC thermogram. This curve reported one endothermic and one exothermic peaks in cooling and heating.

During the forward direction transformation from austenite to martensite, the product of the first exothermic peak at higher temperatures corresponded to the reaction from austenite (A) to Rphase (R), whereas the product of the nextendothermic peak at lower temperatures corresponded to the reaction from R-phase (R) to martensite (M). Therefore, the raw material specimen for heating and cooling not clearly shown this two-transformation sequence of A to R to M, whereas the A to R peak and the R to M peak are narrow and strongly flattened.
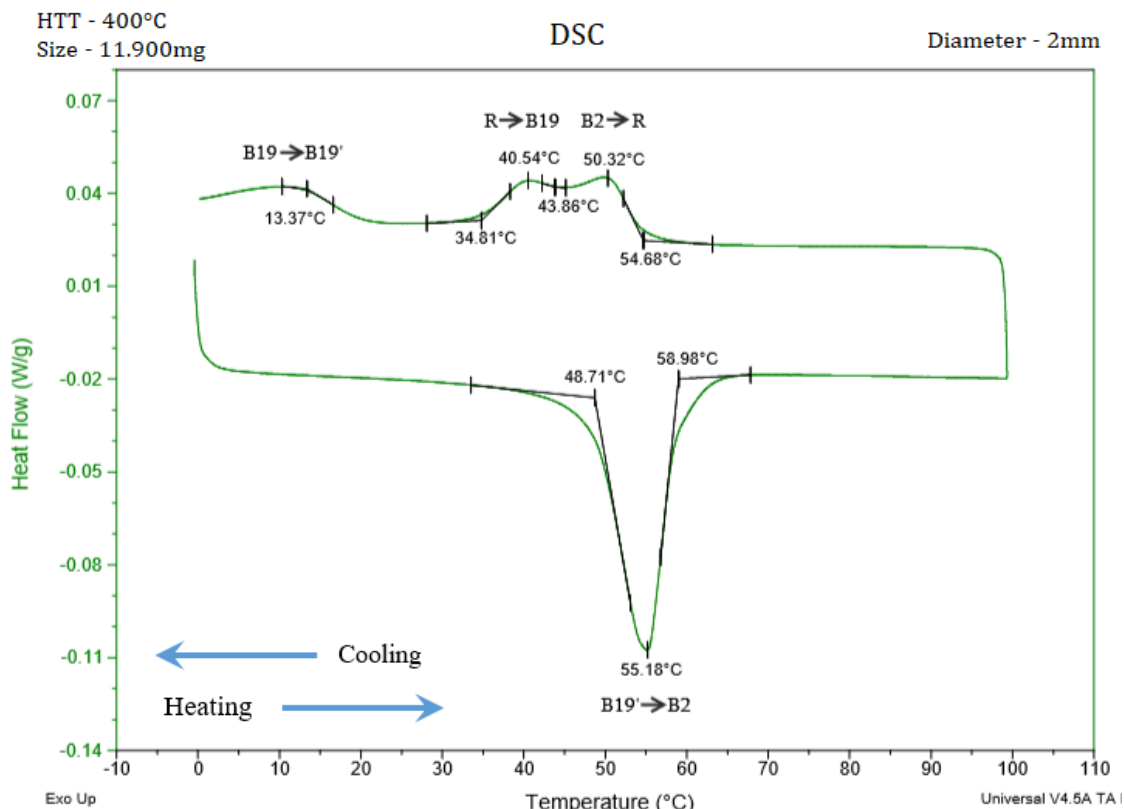
Figure 4.2: DSC Thermogram for Specimen 01

However, transition possessing endothermic apexes, is incurred when heated. This scenario leads to successive reactions being taken place unsatisfactorily in thermograms. The duel overlapping apexes are with respect to M to R transformation which leads to a smaller peak & R to A transformation that leads to a much elevated one. A point to highlight is that above has made it harder to determine completion of transformation of M to R & beginning of transformation of R to A.

Figures 4.2 – 4.6 show DSC thermogram for heat treated NiTiNOL alloy specimens at different temperatures (400, 450, 500, 550 and 600°C) under half and hours (30min). The transformation behavior profiles for the specimen heat treated at 400°C seemed different curve in upper side (positive) than other DSC thermograms (Figure 4.2). It was difficult to identify R phase and matensite phase.

Two phase transformations incurred at R stage while being cooled, but along temperature increase, two exothermic peaks appear in the R phase (Figure 4.3). Also one single endothermic peak is established, which is the austenite phase. The heat treatment of the NiTiNOL between the 400 - 450°C affected a small modification in transformation temperatures of heating.
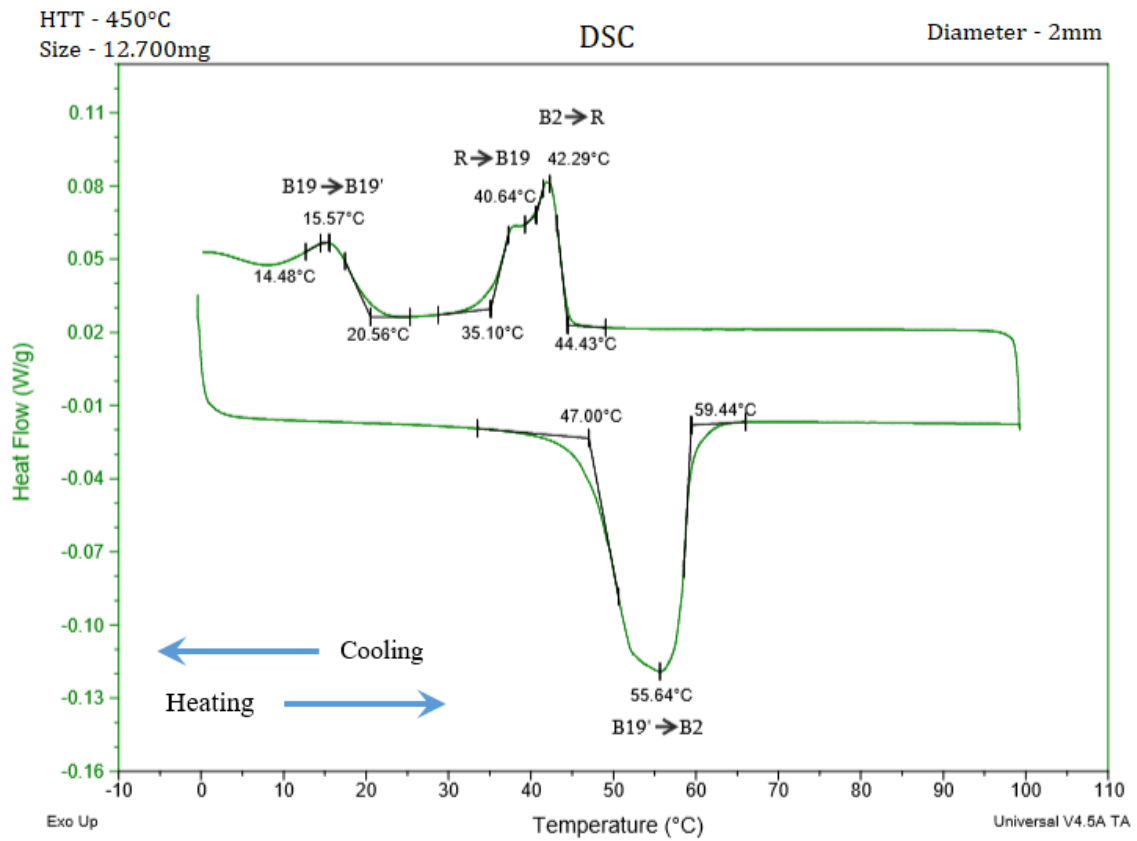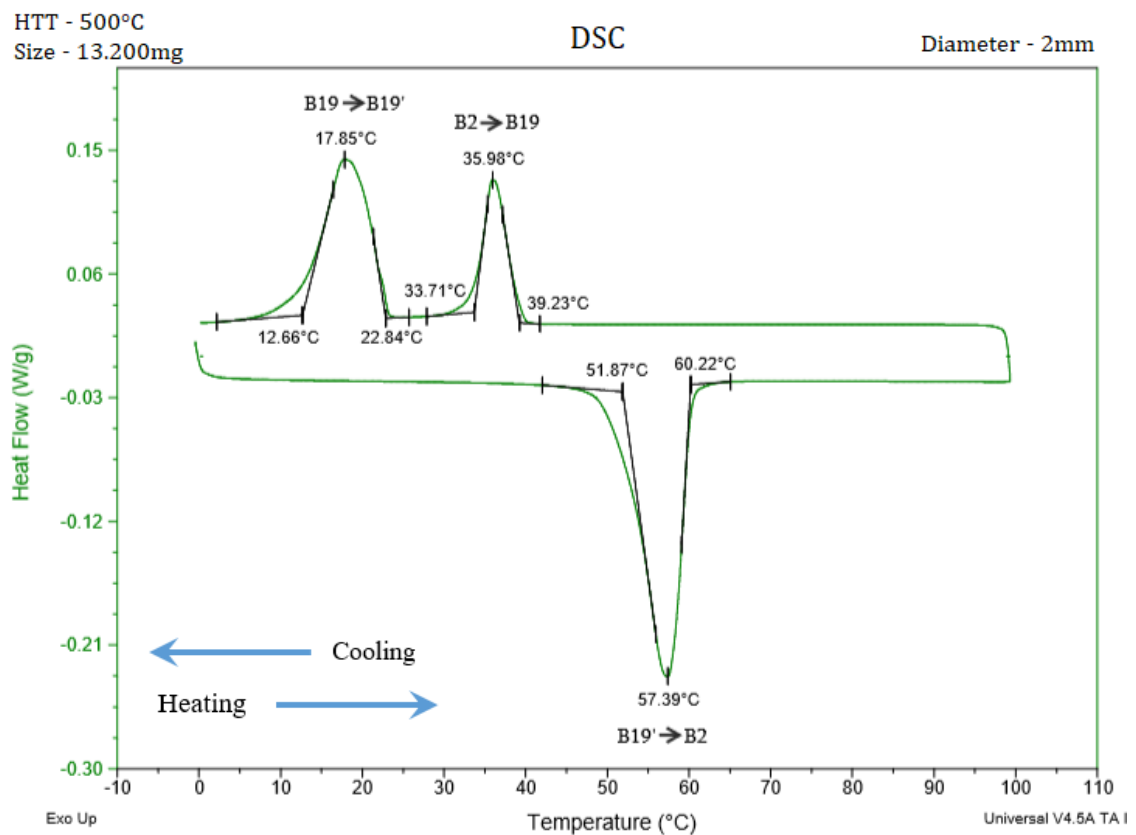
Figure 4.3: DSC Thermogram for Specimen 02

Figure 4.4: DSC Thermogram for Specimen 03
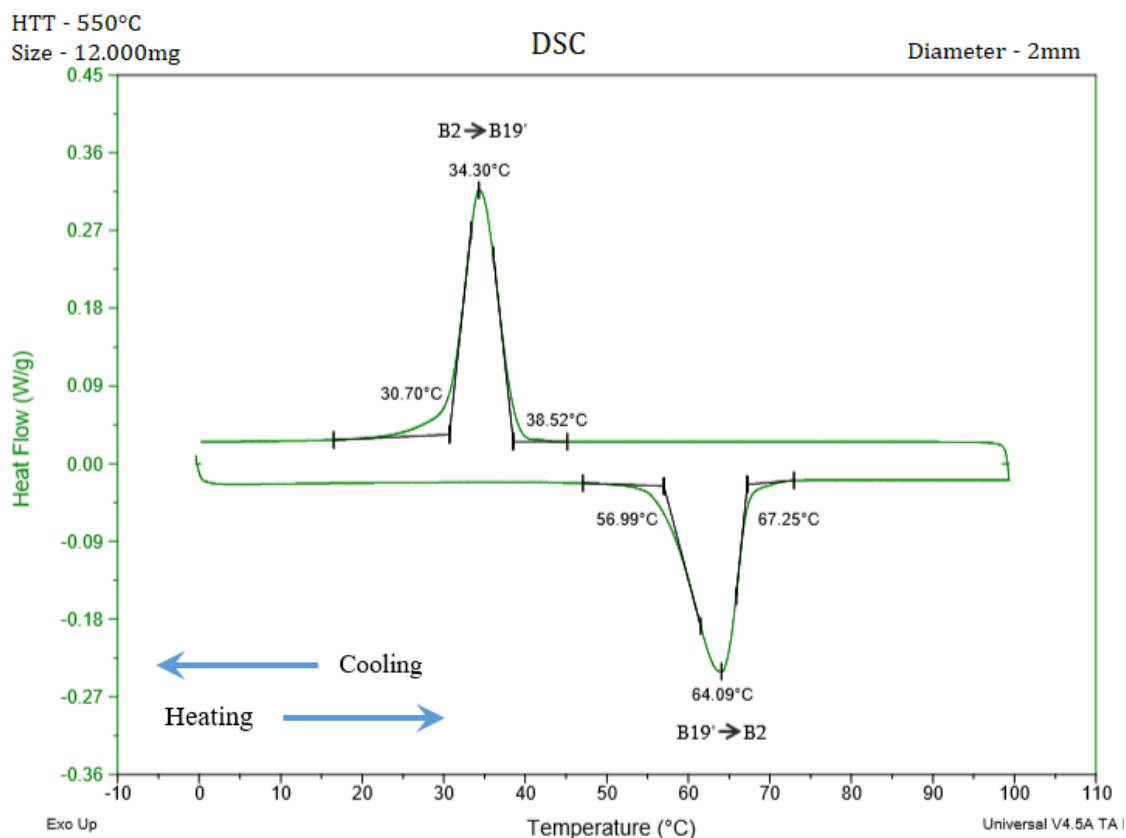
Figure 4.5: DSC Thermogram for Specimen 04

The results of the DSC experiments after heat treatment at temperatures of 450 and 500°C are presented in Figures 4.3 - 4.4. From these curves, the cooling temperatures of transformation had been observed to be consisted of two phases between austenite and R-phase, martensite. The fascinating cases of these curves the R to M apexes inclined rather wide certainly much deep along increase in the heat-treated temperature. It's of significance to note that similar curves related to DSC have exhibited single distinctive endothermic peak.

Again it is difficult to identify both matensite and R-phase correctly. But we can distinctive identify matensite and R-phase very clearly in Figure 4.3. However, in the lower temperature region exothermic apexes are possible to be identified clearly.

The Figures 4.5 and 4.6 shows the DSC thermogram of the specimen heat treated at 550°C and 600°C. There was a qualitative difference in phase transformation behavior between Figure 4.2 - 4.4 and Figure 4.4 - 4.5. These two DSC thermograms, the R-phase transformation was not presented. The Figure 4.5 - 4.6, both heating and cooling transformation temperate took place in one stage from martensite to austenite (M to A) and from austenite to martensite (A to M), respectively. Such behavior (direct phase

transformation of A to M) attests to the happening of only one exothermic and endothermic peak in the DSC thermogram.
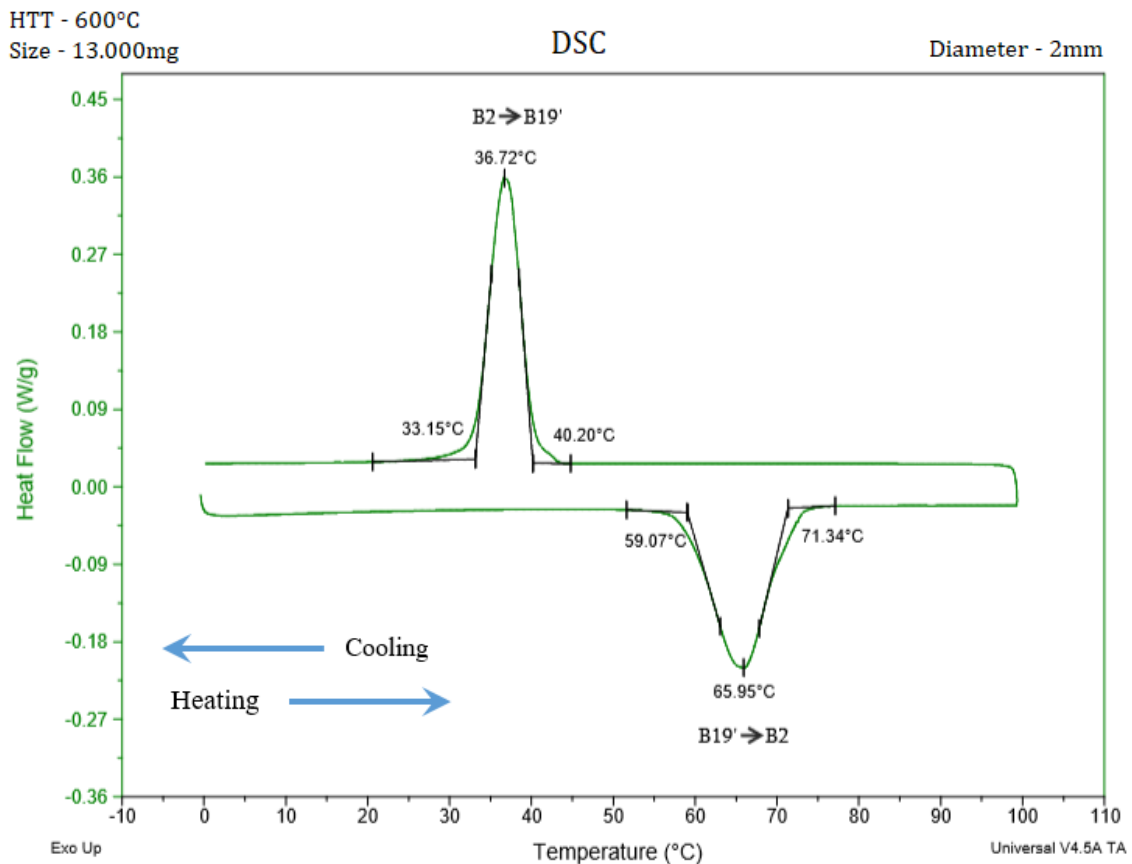
Figure 4.6: DSC Thermogram for Specimen 05

Considering results derived in heat treatment temperatures of range of four hundred Celsius to six hundred an important effect on phase transition characteristics of raw material is observed. In specifically, some heat treatment temperatures in the vicinity of 550°C and 600°C suggests the critical temperature as it shows the distinctive phase transformation behavior than other specimens. Along the rise of heat treatment temperature increased to higher amounts, R-phase becomes unstable eventually disappearing altogether. Once, it reaches 550 °C – 600 °C, the direct martensitic transformation takes place. Further details of these DSC thermograms are given in Appendix C.

4.2.   Topological analysis of NiTiNOL material

Scanning electron microscopy is primarily concerned with analyzing the topology of NiTiNOL specimens at very high magnifications using a part of equipment called the scanning electron microscope. SEM magnification is more than 300,000X, but most of the topological testing applications used in shape memory alloy only in less than 10,000X magnifications. The electron beam is swept across the area being inspected to produce the SEM image, producing many such signals. Then these signals are amplified, analyzed and translated into images of the topography being inspected. The image is finally displayed on a monitor. SEM also gave other very important results in the analysis of NiTiNOL elements (composition) using energy - dispersive X - ray (EDX or EDS) techniques. The data produced by the EDX experiment consists of spectra with peaks consistent to all the different elements present in the NiTiNOL specimen. Following EDS figures are given in the more details of the analysis of the elements. In addition, EDX spectra is used for both qualitative (Ni, Ti and other elements) and quantitative (% of concentration of each element) investigation. Another very important advantage of the EDX method is that it is a non - destructive material characteristic method and less or no sample preparation.

Figure 4.7, Figure 4.9, Figure 4.11 and Figure 4.13 showed the SEM images for various NiTiNOL specimens. Also Figure 4.8, Figure 4.11 and 4.13 and Figure 4.14 given the NiTiNOL specimens EDX analysis at different heat treatment temperatures.
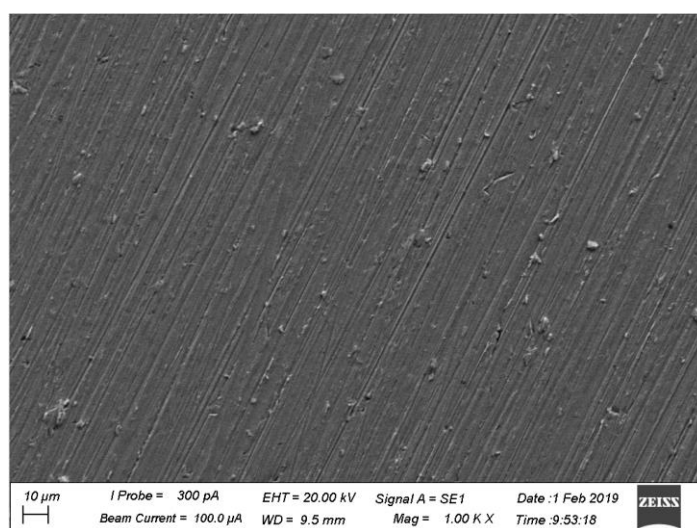

Figure 4.7: SEM image of NiTiNOL raw material
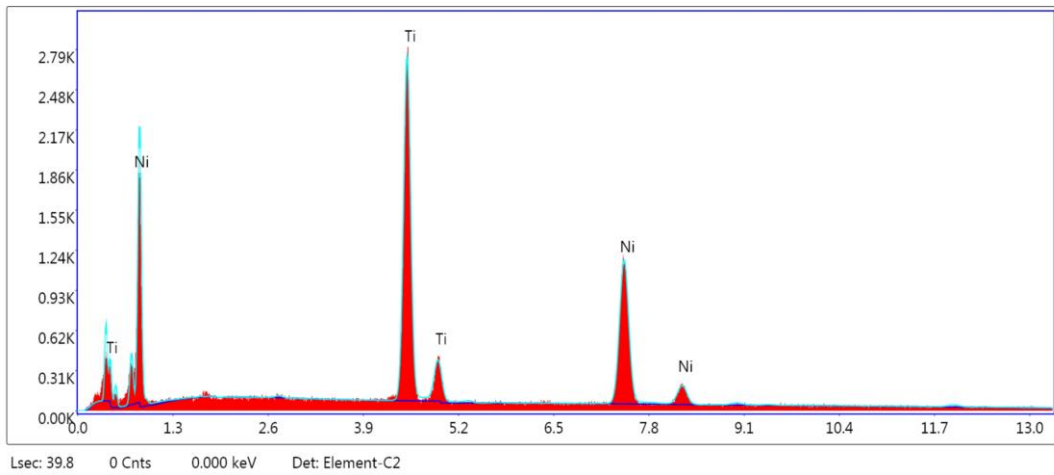
Figure 4.8: EDS diagram of NiTiNOL raw material
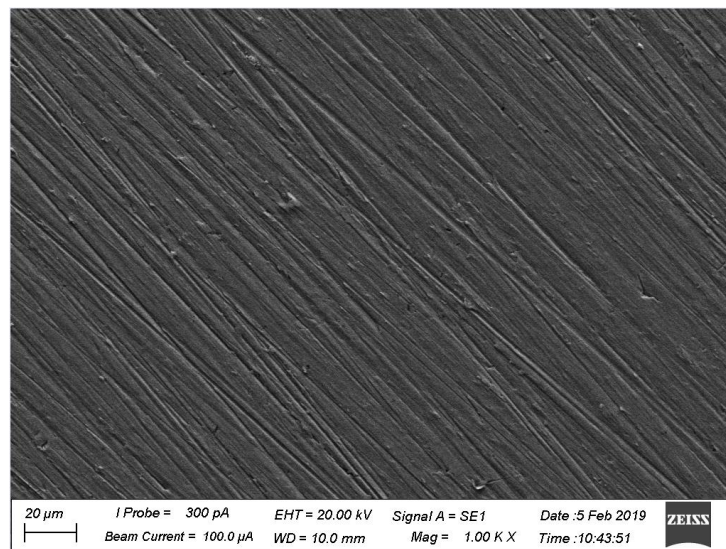
Figure 4.9: SEM image of NiTiNOL at 400°C
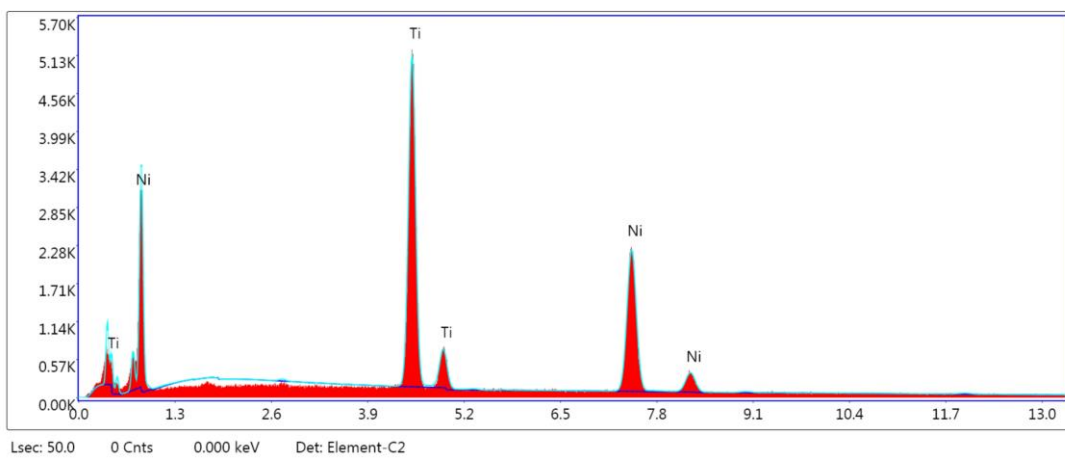
Figure 4.10: EDS diagram of NiTiNOL at 400°C
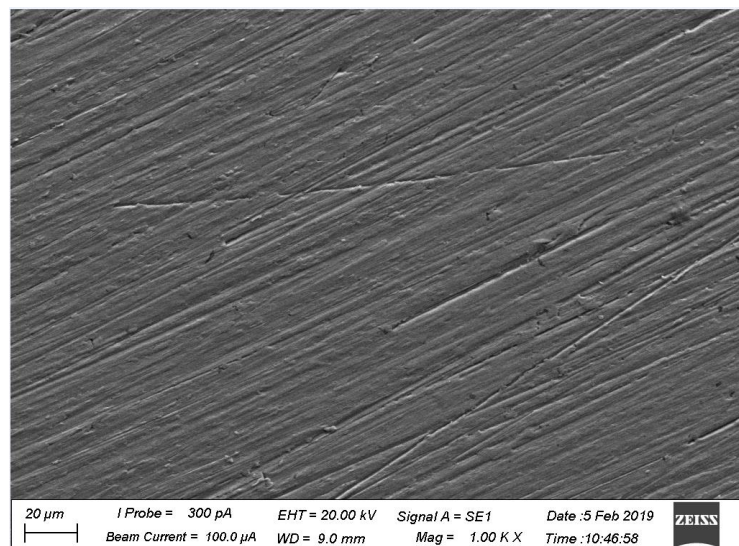
Figure 4.11: SEM image of NiTiNOL at 500°C
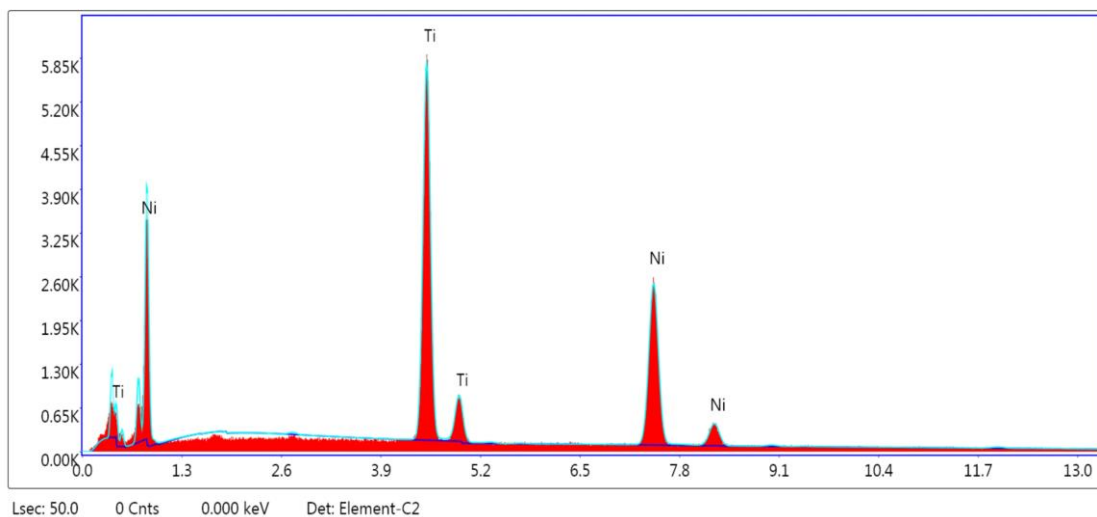
Figure 4.12: EDS diagram of NiTiNOL at 500°C
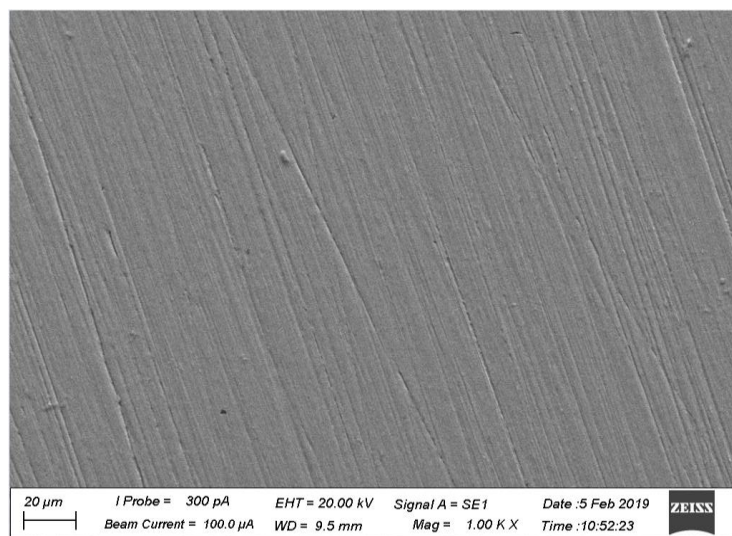
Figure 4.13: SEM image of NiTiNOL at 550°C
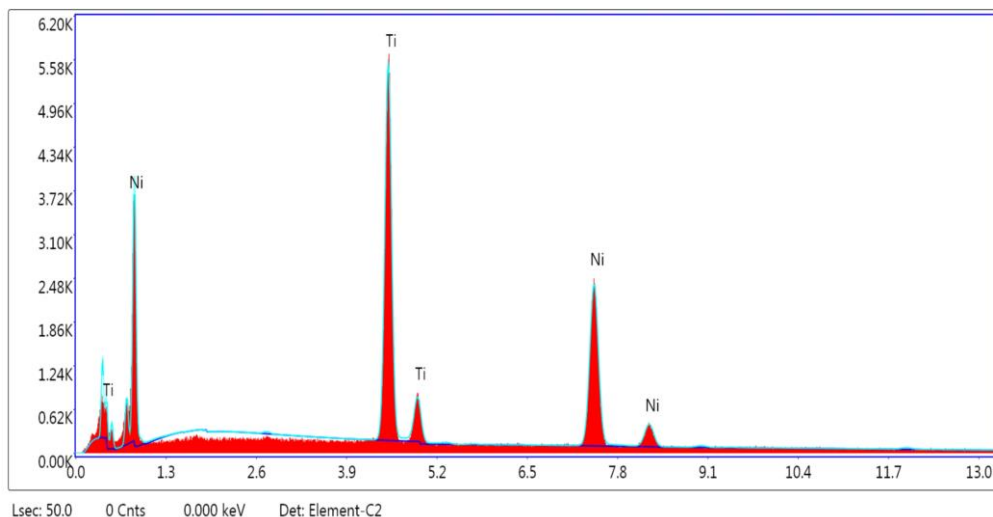
Figure 4.14: EDS diagram of NiTiNOL at 550°C

According to the EDS (energy dispersive spectrometer) diagram, the NiTiNOL alloy chemical composition is nearly close.

Table 4:1: Variation of chemical composition of NiTiNOL alloy

HTT °C	Element	Weight %	Atomic %	Error %
400	Ti	46.38	51.46	2.14
	Ni	53.62	48.54	2.79
500	Ti	46.33	51.41	2.13
	Ni	53.67	48.59	2.66
550	Ti	46.29	51.37	2.15
	Ni	53.71	48.63	2.80
Raw Material	Ti	46.92	52.01	2.35
	Ni	53.08	47.99	3.19

The results of the EDS given in Table 4.1 clearly show that variation in the composition of Ni and Ti alloys in both atomic, weight and total error percentages. The chemical composition of each element changes very slightly with heat treatment temperatures. The raw material indicates that the values of Ni (53.08 + /- 3.19) and Ti (46.92 + /- 3.19) are very close to the other specimens.

Chapter 05

5 NiTiNOL actuating element for Biomedical Applications

5.1. Working principle of SMA helical spring based actuator

This chapter will discuss the manufacture of actuating element to develop the following gripper. The developed gripper included of several individual components and functionality of each component are given below. Figure 5.1 shows a linear actuated gripper that was developed by Uditha et al. as a piston/cylinder assembly.[32]
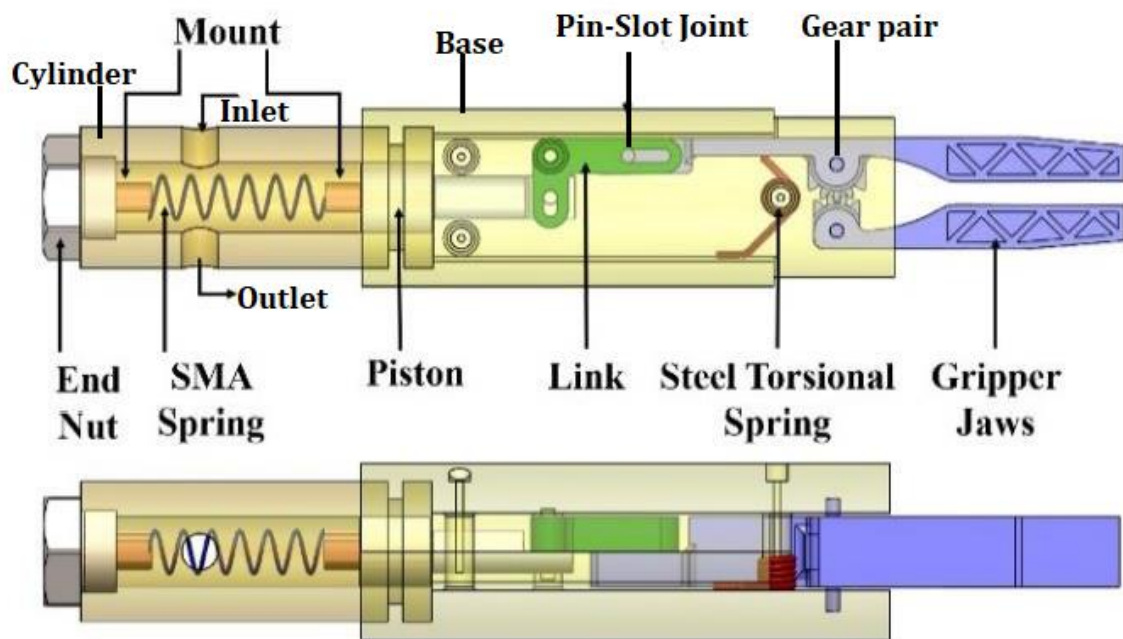
Figure 5.1: Top view of developed gripper assembly [32]

The function, materials and manufacturing processes of each component in developed gripper has given below.

Table 5:1: Detail description of gripper components

Component	Function	Material	Manufacturing Process
End Nut	To easy assemble of the spring	Steel	Machining
Helical Spring	To operate the jaws and it is the actuator element	NiTiNOL	Manual Making by using fixture
Mounts	To connect the spring inside the cylinder	Brass	Machining

Base	Mount the linkage mechanism	ABS+	3D Printing
Piston	To move link linearly	Aluminum	Machining
Cylinder	To pass water for heating and cooling of helical spring through inlet and outlet	Brass	Machining
Link with Pin-Slot joint	To operate the jaw mechanism Two slots and pins limit the motion of the piston and driver jaw	ABS+	3D Printing
Gripper Jaws	To grip the object	ABS+	3D Printing
Torsional Spring	To provides the closing action of the Gripper Jaws	Steel	Manual Making
Gear Pair	To achieve compactness the Gripper pair and move gripper close and open positions	ABS+	3D Printing

5.2. Design of SMA based Helical Spring

5.2.1. Parameters of SMA based Helical Spring

The composition of NiTiNOL (54% Ni and 46% Ti wt. %) spring wire material would find by using Scanning Electron Microscopy. Specifications of helical spring given in Table 5.2 and Figure 5.2 given the dimensions of helical spring in millimeters. Spring wire material would find the composition of NiTiNOL (54 % Ni and 46 %Ti − wt. %) using Scanning Electron Microscopy. The specifications for helical spring given in Table 5.2 and Figure 5.2, and developed by Uditha et al. [32]

Table 5:2: Parameters of Helical Spring [32]

Parameter	1mm Spring	2mm Spring
Wire Diameter - d	1mm	2mm
Outer Diameter – D	7.5mm	7.5mm
Pitch – p	2.5mm	2.5mm
Length of Spring – L	10mm	15mm
No of (terns) coils – N	04	04
Vertical Attachment Length - L_{VAL}	10mm	10mm
Horizontal Attachment Length - L_{HAL}	6.5mm	6.5mm
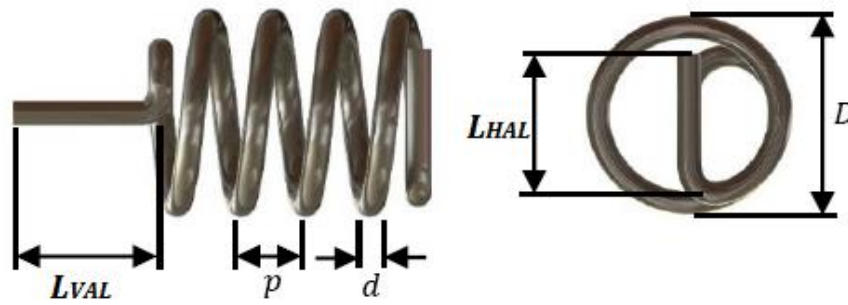
Figure 5.2: NiTiNOL Helical Spring Parameters [32]

5.2.2. Design and Development of Spring Forming Fixture

The actuator helical spring formed by using specially developed fixture. The fixture dimensions and parts are given in Figure 5.3 and Figure 5.4. The shape of fixture was selected by after doing number of surveys about the fixtures for setting the shape of helical springs. The dimensions of spring forming fixture depend on the parameters of helical spring given in Table 5.2.
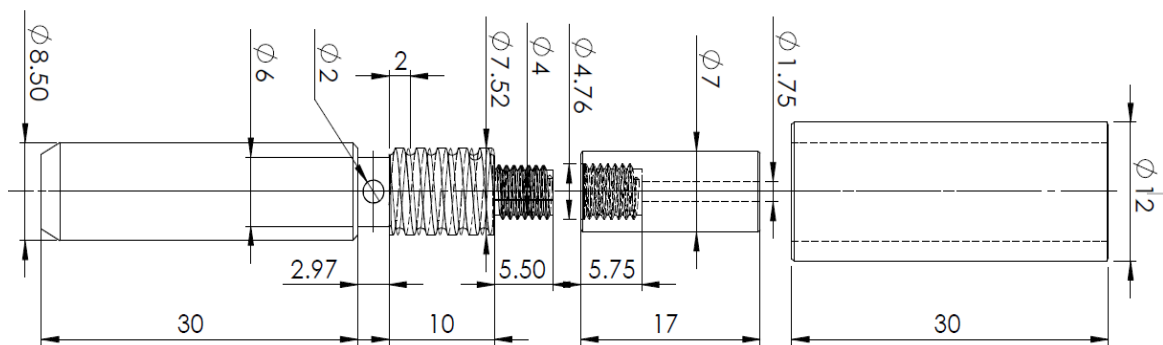
Figure 5.3: Shape setting fixture dimensions [32]

This developed fixture is used to achieve two important requirements of the helical spring.

    i.   Develop the correct shape of helical spring

    ii.   Hold the spring shape and dimensions during heat treatment processes
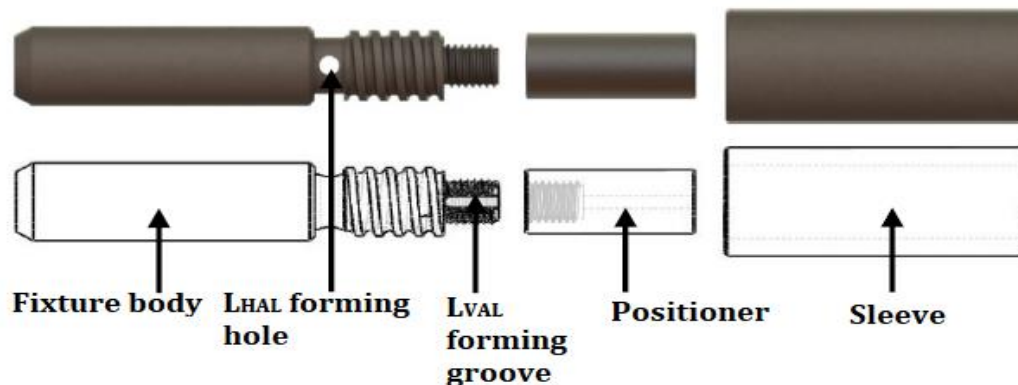
Figure 5.4: Important parts of spring forming fixture [32]

The process of forming the initial spring shape would require a rigid holding method for the fixture and a rotational motion at the same time. A rotatable chuck was used to hold the fixture during the winding process. The fixing part was tightly held in the chuck jaws, and the L_{VAL} was placed in the centering groove. The positioner was then screwed to the fixture. The NiTiNOL wire's free end was pulled and rotated through the helical groove. As the wire winds along the helical grove, the sleeve was used to restrict the shape of the spring to avoid unwinding due to bending resistance. The free end was guided through the hole perpendicular to the axis of the fixture to form the L_{HAL} at the final turn of the winding. The sleeve was finally tightened to the attachment.

This NiTiNOL helical spring would have two different attachment lengths at the both ends. A positioner aligns the vertical attachment length (L_{VAL}) with the axis of the spring. A sleeve then restricts the spring to maintain its shape during the heat treatment process. The horizontal attachment length (L_{HAL}) is formed by a hole perpendicular to the fixture axis. The material for the fixture is AISI1010 Carbon Steel and conventional lathe machine was used for machining (Figure 5.3). AISI1010 carbon steel should therefore have a low coefficient of thermal expansion and, due to the number of thermal cycles, should withstand the original position.

5.2.3. Forming of NiTiNOL Helical Spring
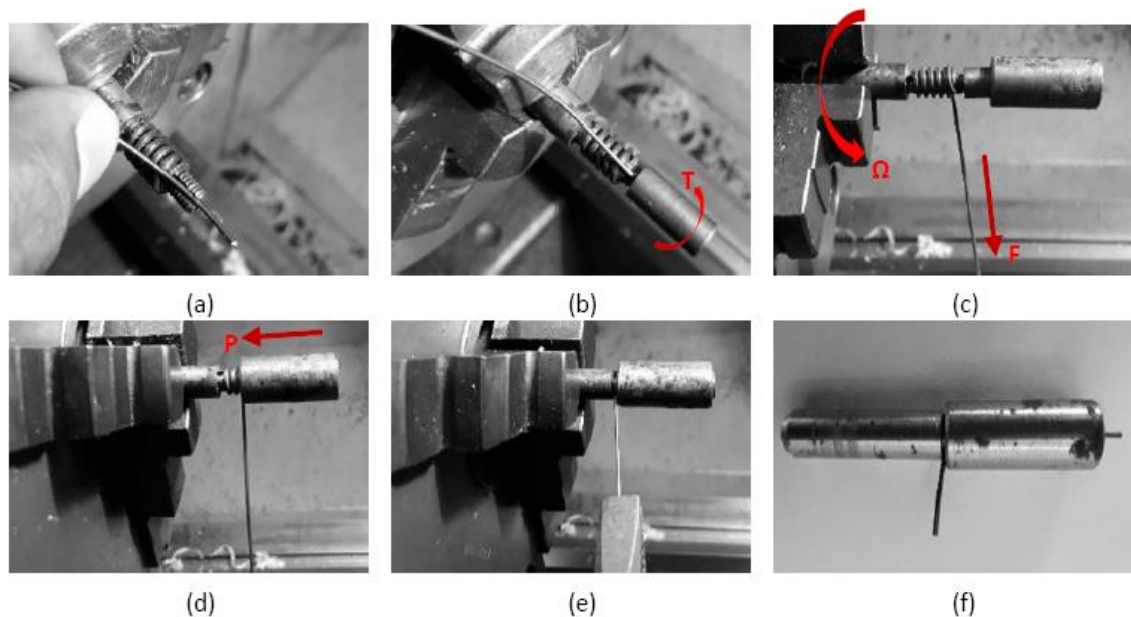
(a) Positioning the L_{VAL} (b) Tightening L_{VAL} by the Positioner (c) Winding the Wire
(d) Constraining by the Sleeve (e) Tightening the Sleeve (f) Wire and the Fixture before Shape Set-ting

Figure 5.5: Forming of NiTiNOL based helical spring [34]

In this project work, used special technique to wind the NiTiNOL wire into a spring shape. The gauges of NiTiNOL wires are 1mm and 2mm. Forming of NiTiNOL spring can be divided into several tasks.

5.3. Heat Treatment Process (Shape Setting) of NiTiNOL Spring

In the shape setting of cold worked material (after preparation of the spring), great care must be taken to limit the strain of deformation to avoid damage to the helical spring. I should be aware that in an unprotected furnace environment, NiTiNOL will be oxidized. The type of heat treatment furnace very carefully selected. To overcome these problems, we selected seal type electric muffle furnace.

The properly constructed NiTINOL helical spring was heat treated with proper condition. The following steps were taken to complete the heat treatment process.

   i.   Increase the temperature of the furnace to the required temperature.

   ii. Hold the furnace temperature at required level to ensure that the furnace temperature is stable. (400, 450, 500, 550 and 600°C separately)

   iii. Place the fixture with helical spring inside furnace (Figure 5.6).

Figure 5.6: Complete unit for heat treatment [32]

   iv. Close the furnace door correctly.

   v.   Heat treat the specimen for 30min at the required temperature.

   vi. Cool the specimen with water after time 30min.

Figure 5.6 shown in the NiTiNOL helical spring after heat heated and oxidization of fixture.
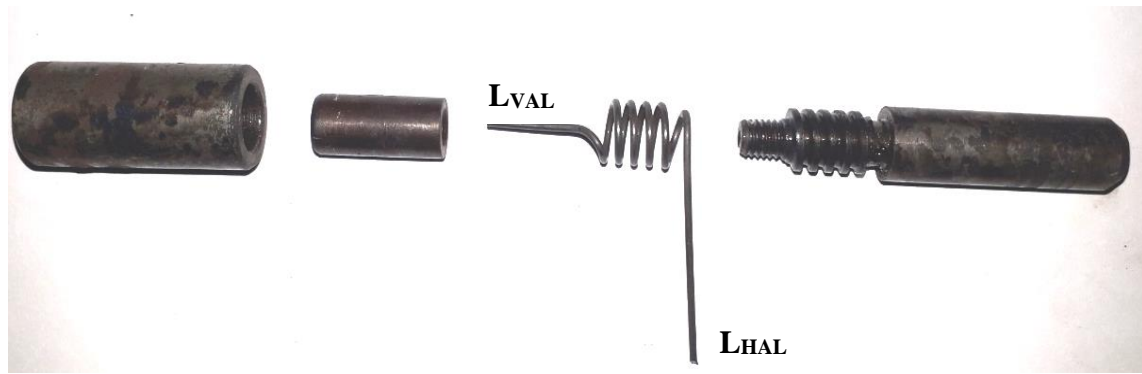
Figure 5.7: Heat treated NiTiNOL based helical spring [32]

It is remarkable that the geometries of the helical springs of NiTiNOL have a strong relationship between the temperature of heat treatment and the fixture rigidity. In this work, the spring does not set the shape at lower heat treatment temperatures.

Table 3.1 shows temperatures for heat transfer and aging with different NiTiNOL helical spring temperatures for heat treatment.

Chapter 06

6 Results and Discussion

6.1.   Representation of DSC thermograms

The Figure 6.1 shows in all the DSC thermograms of specimen heat treated by various HTT's at 3°C min^{-1} heating and cooling rates. A_f is the very important temperature that given by manufacturer. However, DSC experiment used to find the exact value of A_f temperature and we can change it permitting to various heat treatment temperatures. According to the Table 6.1, austenite finish temperature (A_f) varied from 56°C to 74°C at various heat treatment temperatures.
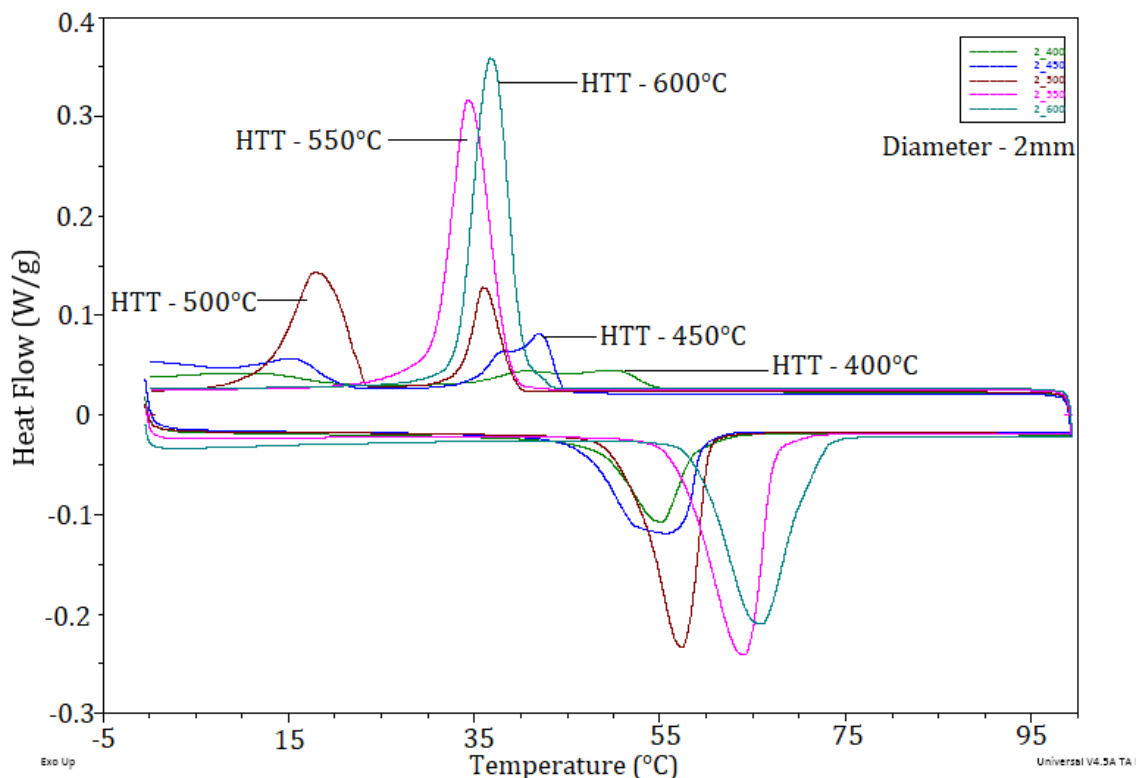
Figure 6.1: DSC Thermogram of all specimens for 30 minutes

The Table 6.1 – 6.3 shown in summarization of transformation temperatures, exothermic and endothermic peaks and enthalpy values.   The determined area under peak temperatures represented latent heat of each and every DSC curves. The description of terms given in abbreviations. The collected results from Table 6.1 - 6.3 show that the heat treatment ranges from 400 to 600 ° C. Values are included in the start and finish phase transformation temperatures of the R-phase to lower values, whereas a small

improvement at 400 ° C was apparent with reference to the raw material. The temperature of the martensite start (Ms) is not clearly identified at 400 ° C and the phase temperature of Ms decreased after a small growth for the heat treatment temperature at 450 ° C. However, Ms clearly increased at 500 ° C from specimen no. 03. The temperature of the martensite finish (M_f) is between 400 ° C and 600 ° C.

Due to the very wide and flattened DSC thermogram peaks, the Ms and M_f transformation temperatures in Table 6.1 are not very accurate for specimens at 400 - 450 ° C. They are defined by increasing heat treatment temperatures.

Table 6:1: Transformation temperatures of specimens

Specimen No	Heat Treatment Temperature (HTT) °C	Transformation Temperatures (TTs) °C					
		M_s	M_f	A_s	A_f	R_s	R_f
Specimen – 01	400	-	13.37	48.71	58.98	34.81	54.68
Specimen – 02	450	20.56	14.48	47.00	59.44	44.43	35.10
Specimen – 03	500	22.84	12.66	51.87	60.22	39.23	33.71
Specimen – 04	550	38.52	30.70	56.99	67.25	-	-
Specimen – 05	600	40.20	33.15	59.07	71.34	-	-

Phase transformation measurements show that the temperatures of Ms and M_f were below the room temperature due to the R - phase in heat specimens treated between 400 - 500°C. This reduced the possibility of forming as the temperature of Ms moved to higher temperatures. Some transformation behavior, without revealing an R-phase (rhombohedral), occurred at higher heat treatment temperatures.

As in Figure 6.2 of heat treatments, the austenite starting temperature (As) and the austenite finishing temperature (A_f) gradually increased significantly in the range of 400-600 ° C with the heat treatment temperature. The starting temperature of the R - phase (Rs) was increased and decreased at 400 - 500 ° C and temperatures of the Rs were not observed. Again, the R - phase finishing temperature (R_f) decreased significantly at 400 - 500 ° C and R_f temperatures did not appear.
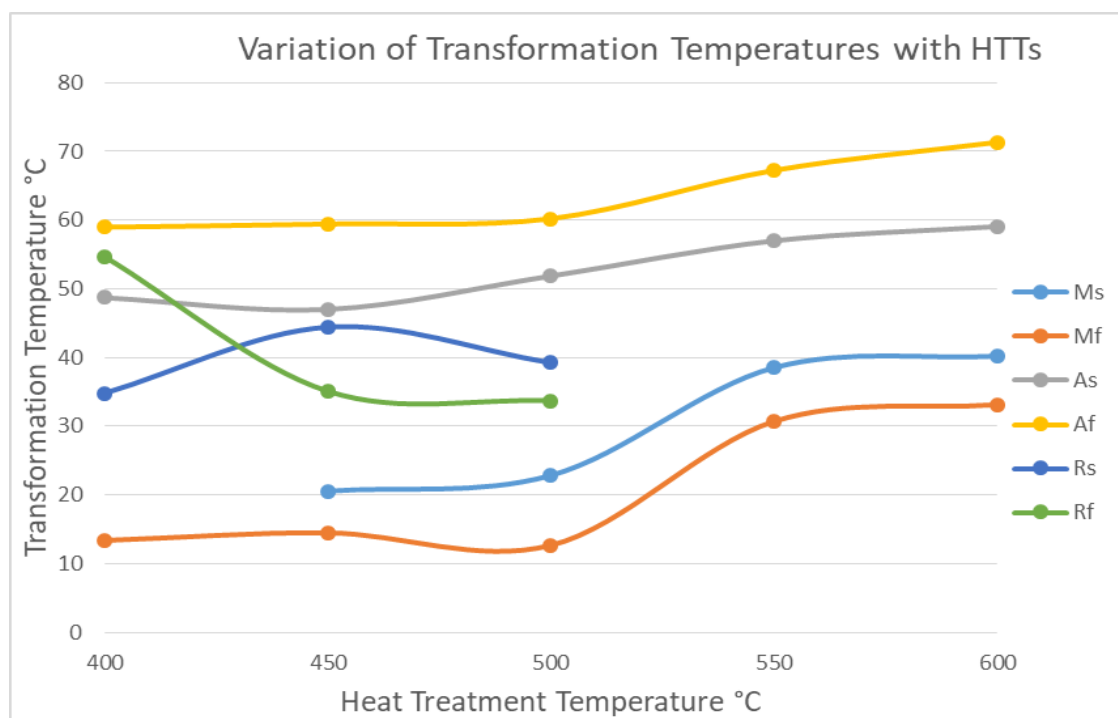
Figure 6.2: Variation of phase transformation temperatures

Table 6:2: Peak temperatures of specimens

Specimen No	Heat Treatment Temperature (HTT) °C	Peak Temperatures °C		
		Ap	**Mp**	**Rp**
Specimen – 01	400	55.16	40.12	50.37
Specimen – 02	450	55.65	15.59	42.27
Specimen – 03	500	57.40	17.86	35.97
Specimen – 04	550	64.10	34.34	-
Specimen – 05	600	65.94	36.70	-

The determined peak temperatures are shown in Table 6.2 and the variation in peak temperature as shown in Figure 6.3. The peak austenite temperature (Ap) gradually increased between 400 and 600 ° C. But martensite peak temperature degrease from 400 ° C to 500 ° C and again increase from 550 ° C to 600 ° C. But, the peak temperature value of the R-phase decreased to 500 ° C and did not appear at 550–600 ° C, corresponding to the peak temperature of the R-phase transformation into the austenite phase.
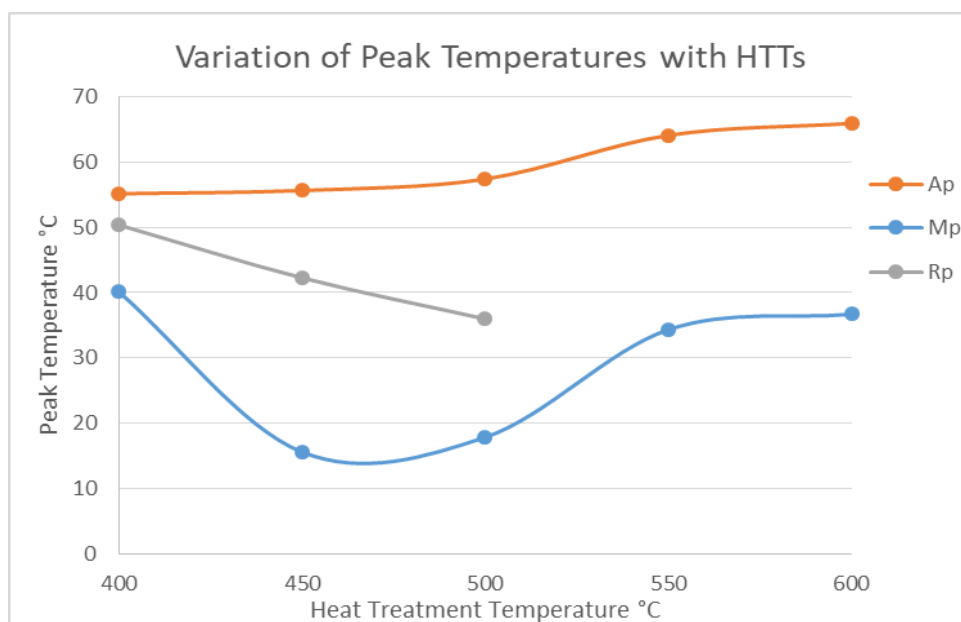
Figure 6.3: Variation of Peak temperature values

Figure 6.3 and Table 6.2 shown in the R - phase peak temperature reduced from 400 ° C to 500 ° C with heat treatment temperature and did not appear from 550 ° C to 600 ° C. For the R - phase, the raw martial was not given peak temperatures. The temperature of the Mp moved significantly to higher temperature with respect to an increasing temperature of heat treatment. As a result, the peak temperature differences between Mp and Rp dropped dramatically after 500 ° C heat treatment temperature and only Mp peaks are approximately stable after the same heat treatment temperature. There was a unique transformation of peak temperature from A to M when cooling.

The Ap value increased slightly up to 500 ° C and increased rapidly after heat treatment at 500 ° C. The transformation hysteresis is given by the deference between peak temperatures of Ap and Mp at the heat treatment temperature at 600 ° C. It was only about 29.24 ° C.

Exothermic heat (release energy) from austenite to martensite increased with temperature of heat treatment. The enthalpy values of austenite slightly decreased and it became stable as negative enthalpy values after 550 ° C heat treatment temperature (Figure 6.4 and Table 6.3). But martensite enthalpy values are up to 450 ° C more stable. After that, it increased drastically from 450 ° C to 550 ° C and became a stable after 550 ° C. Even though the values of R - phase enthalpy increased slightly up to 500 ° C heat treatment temperature. Then R - phase enthalpy values do not exhibit after 500 ° C temperature.
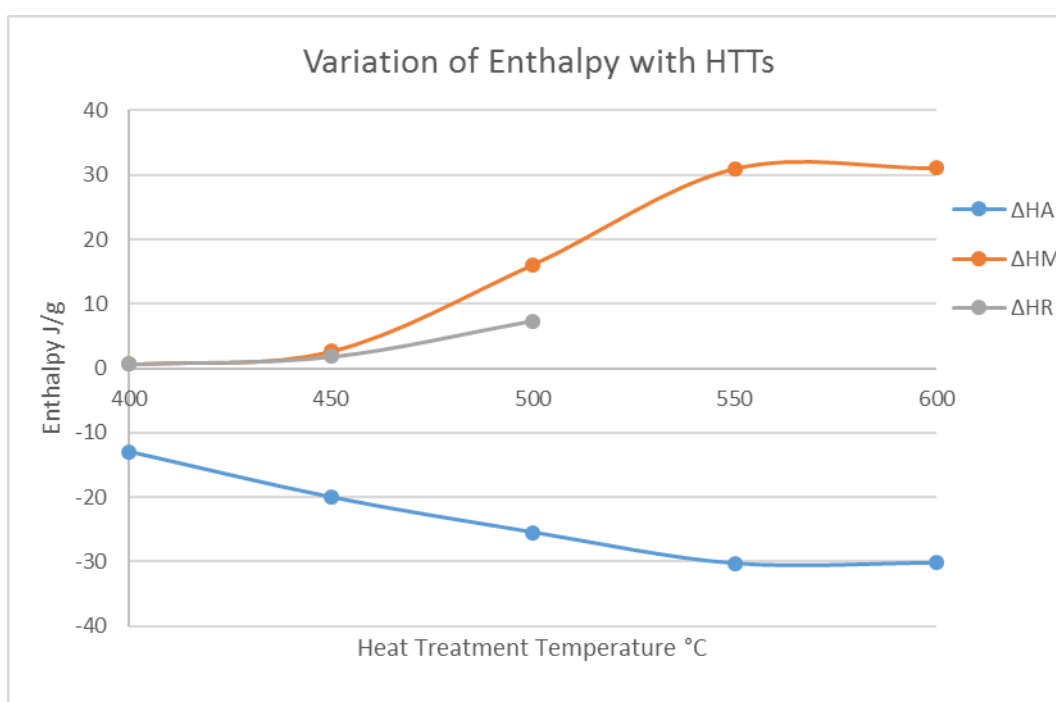
Table 6:3: Enthalpy values of specimens

Specimen No	Heat Treatment Temperature (HTT) °C	Enthalpy J/g		
		ΔH_A	ΔH_M	ΔH_R
Specimen – 01	400	-12.965	0.649	0.671
Specimen – 02	450	-19.997	2.668	1.814
Specimen – 03	500	-25.446	16.106	7.328
Specimen – 04	550	-30.255	30.985	-
Specimen – 05	600	-30.212	31.086	-

Figure 6.4: Variations of Enthalpy values

However, average values are given in Table 6.4, showing austenite, martensite and R - phase approximately -23.775, 16.298 and 3.271 J/g respectively. The average absorption of endothermic heat was 16,298 J / g. The minimum and maximum endothermic heat absorption values given in 0.649 J / g and 31.086 J / g respectively. The austenite phase given the average exothermic heat was -23.775 J/g. The minimum and maximum exothermic heat release values given in -30.212 J / g and -12.965 J / g respectively. Therefore, at 600 ° C heat treatment temperature, NiTiNOL alloy absorbs and releases the highest energy.

Table 6:4: Average enthalpy values of each phases

	ΔH_A	ΔH_M	ΔH_R
Average Enthalpy Values (J/g)	-23.775	16.299	3.271

Table 6.5 shows the variation of the elements with respect to the temperature of the heat treatment and it almost closes each other. The average composition of the selected NiTiNOL material was Ni - 54 percent wt. And Ti, 46 percent wt.

Table 6:5: Variation of composition with HTT

	Raw material	HTT					Average Values
		400 °C	450 °C	500 °C	550 °C	600 °C	
Elements	Weight %						
Ti	46.92	46.38	46.36	46.33	46.29	46.21	**46**
Ni	53.08	53.62	53.64	53.67	53.71	53.79	**54**

6.2. Validation of the SMA spring actuator element

This actuator element was used to develop a spring actuated gripper to facilitate minimally invasive surgery (MIS). The gripper used a novel mechanism to transfer the actuator force to the gripper jaws (Figure 5.1). The spring actuated gripper was developed by the same research team to investigate shape memory alloy actuators for biomedical applications in the Department of Mechanical Engineering at the University of Moratuwa. [32]

7 Conclusions

After completing experimental activates at the University of Moratuwa, the results of the research work on this thesis are presented. The main objective of these experimental activities is to study the fascinating area of smart materials that is the functional behavior of NiTiNOL Shape Memory Alloys (SMAs). This research studies the thermal behavior of Nickel Titanium shape memory alloy (NiTiNOL) with different heat treatment temperatures. This selected NiTiNOL with two sizes such as 1 mm and 2 mm diameter.

Previous researches have focused on developing integration between thermal stability and SMA microstructure. However they do not have enough thermal behavior data with different heat treatment temperatures. Although phase transformation temperatures and microstructure patterns with different heat treatment temperatues are unique characteristics of NiTiNOL. The aim of this study is to investigate NiTiNOL characteristics and thermal behavior of SMA based actuating elements for minimally invasive surgical technologies.

According to the literature, the most functional SMA based actuator is a gripper which could be a microgripper or a macrogripper depending on the application. In this particular study, macro level gripper was selected based on the availability of tools and experimental setups. Most significant part of any actuator is the actuating element. Helical spring was selected as an actuator element made of shape memory alloy (NiTiNOL) in this study, after studying research work carried out previously.

The developed gripper which is a linear actuated one designed as a piston/ cylinder assembly includes several individual components and functionality of each component is given in Figure 5.1. This helical spring actuator based on SMA was made from commercially available NiTiNOL alloy wire with two diameters of 1 mm and 2 mm. The composition of NiTiNOL (54% Ni and 46% Ti wt. %) spring wire material was found by using a Scanning Electron Microscopy. Specifications and dimensions of helical spring are given in Table 5.2 and Figure 5.2 respectively.

The actuator helical spring was formed by using a specially developed fixture. The shape of fixture was selected after doing number of surveys about the fixtures. The dimensions

of said fixture depend on the parameters of helical spring as given in Table 5.2. Helical spring was prepared by 30-minute heat treatment inside the Muffle furnace with different heat treatment temperatures.

Then DSC experiment was performed for each specimen no. 01 to 05 and raw specimen. The DSC thermogram features represented on the NiTiNOL raw specimen without heat treatment and on the other specimens (no. 01 to 05) that were heat treated at selected temperatures (400, 450, 500, 550 and 600°C) for 30 minutes are reported. The DSC thermogram was used to determine the characteristics temperature and distinguish the transition phases. The Martensite to austenite phase transformation is taken place on the reverse transformation of this curve while subjected to heating. Endothermic phase transitions from austenite to R - phase and R - phase to martensite are taken place when being cooled at relatively lower heat treatment temperatures of 400°C – 500 °C. The DSC thermogram showed only specimen No. 01 to 03 for the R - phase transition.

However, along with increase in heat treatment temperature, the transition temperature of each phase was correctly established in specimens at 550 °C. In this study, the heat treatment process used equal time period for each specimen.

The variations of grain sizes due to heat treatment temperatures were observed in SEM images (20μm resolution) of the specimens which revealed distinctive grain structure changes along with the increase in temperature. Enthalpy values had not been not shown after 500 ° C in the R - phase and did not represent energy release or absorption of the material however, at 600 °C heat treatment temperature, absorption and release of energy are taken place in NiTiNOL alloys.

Considering factors above, specimen 05 and 06 were found as possible for the manufacture of the actuator element however due to proper phase transformation temperatures at 600 ° C, specimen No. 06 is found to be the most suitable for manufacturing the helical spring-based actuator element for MIS-based macro-scale gripper.

Further work using X - ray diffraction to critically evaluate the crystallographic structures in different planes by changing strain rate or stresses would lead to determining the shape memory alloy's superelastic (psudoelastic effect) behavior.

References

[1]. A. Kumar, Comprehensive modeling of shape memory alloys for actuation of large-scale structures, PhD dissertation, Civil Engineering, The University of Akron, 2010.

[2]. J. Mohd Jani, M. Leary, A. Subic, M.A. Gibson, A review of shape memory alloy research, applications and opportunities, Mater. Des. (1980–2015), 56, 2014, 1078–1113.

[3]. C. Song, "History and Current Situation of Shape Memory Alloys Devices for Minimally Invasive Surgery", *Open Medical Devices Journal 2*, pp 24-31, 2010.

[4]. A. Ölander, "An electrochemical investigation of solid cadmium-gold alloys", *Am Chem Soc*; 54, 1932, pp 3819–33.

[5]. W. J. Buehler, J. V. Gilfrich, R. C. Wiley, "Effect of low-temperature phase changes on the mechanical properties of alloys near composition TiNi", *Appl Phys*; 34, 1963, pp1475–7.

[6]. K. Otsuka, C. M. Wayman, *Shape Memory Alloys*, Cambridge University Press, United Kingdom, 1998.

[7]. M. Kohl, *Shape memory microactuators (microtechnology and MEMS)* 1st ed. Heidelberg: Springer-Verlag Berlin, 2010.

[8]. O. M. Akselsen, "Joining of shape memory alloys", *Published by Sciyo Janeza Trdine 9*, 51000 Rijeka, Croatia, ch. 9, pp. 183-209, 2010.

[9]. Y. Li, "Design and analysis of energy harvesting with shape memory alloy", MSc Thesis, Electrical Engineering, The University of Akron, 2012.

[10]. M. István, "Fundamental characteristics and design method for nickel-titanium shape memory alloy". *Journal of Ser. Mech. Eng.*, 45(1), pp. 75-86, 2001.

[11]. J. Ryhanen, Biocompatibility Evaluation of Nickel-Titanium Shape Memory Metal Alloy", Ph.D. Thesis, Oulu University, Finland, 1999.

[12]. Y. H. The, Fast, Accurate Force and Position Control of Shape Memory Alloy Actuators, Ph.D. Thesis, The Australian National University, 2008.

[13]. E. Zanaboni, One Way and Two Way-Shape Memory Effect: Thermo-Mechanical Characterization of Ni-Ti Wires, MSc Thesis, The University of Pavia, Italy, 2008.

[14]. J. M. Jani et al, "Designing shape memory alloy linear actuators: A review", *Journal of Intelligent Material Systems and Structures*, Vol. 28(13) pp. 1699–1718, 2016.

[15]. J. A. Shaw, "A Thermomechanical Model for a 1-D Shape Memory Alloy Wire with Propagating Instabilities", *International Journal of Solids and Structures*, Vol. 39, pp. 1275-1305, 2002.

[16]. C. U. Pons, "Improvement of the one-way and two-way shape memory effects in Ti-Ni shape memory alloys by thermomechanical treatments", Ph.D. dissertation, Department of Mechanical Engineering, Rovira i Virgili University, Spain, 2011.

[17]. W. Huang, "On the Selection of Shape Memory Alloys for Actuators", *Materials and Design*, Vol. 23, pp. 11-19, 2002.

[18]. B. Söylemez B., "Design and analysis of a linear shape memory alloy actuator", Ph.D. dissertation, Mechanical Engineering Department, Middle East Technical University, Turkey, 2008.

[19]. K. Ikuta, M. Tsukamoto and S. Hirose, "Mathematical model and experimental verification of shape memory alloy for designing micro actuator". *In Micro Electro Mechanical Systems, MEMS '91, Proceedings of IEEE: An Investigation of Micro Structures, Sensors, Actuators, Machines and Robots*, 1991, pp 103-108.

[20]. M. E. Brown, *Handbook of thermal analysis and calorimetry – volume - I principles and practice*, Elsevier science B.V. Sara Burgerhartstraat 25 P.O. Box 211, 1000 AE Amsterdam, The Netherlands, pp 1-28, 1998.

[21]. A. Arghavani, "Thermo-mechanical behavior of shape memory alloys under multiaxial loadings: constitutive modeling and numerical implementation at small and finite strains", Ph.D. dissertation, Sharif University of Technology, Tehran, Iran, 2010.

[22]. R. Abeyaratne, J. K. Knowles, "On the driving traction acting on a surface of strain discontinuity in a continuum". *Journal of the Mechanics and Physics of Solids 38 (3)*, pp 345-360, 1990.

[23]. J. M. Ball, R. D. James, "Fine phase mixtures as minimizers of energy". *Archive for Rational Mechanics and Analysis*, pp 13-52, 1987

[24]. F. Falk, 1980. "Model free-energy, mechanics and thermodynamics of shape memory alloys". *Acta Metallurgica* 28, pp 1773-1780, 1980.

[25]. F. Falk, "One-dimensional model of shape memory alloys". *Archives of Mechanics*, 35, pp 63-84, 1983.

[26]. Q. P. Sun, K. C. Hwang, "Micromechanics modelling for the constitutive behavior of polycrystalline shape memory alloys: I - Derivation of general relations, II - Study of the individual phenomena", *Journal of the Mechanics and Physics of Solids* 41 (1), pp 1-17 and pp 19-33, 1993a, 1993b.

[27]. M. Mehrpouya, and H. C. Bidsorkhi, "MEMS Applications of NiTi Based Shape Memory Alloys: A Review", *Micro and Nanosystems,* 8, pp 79-91, 2016.

[28]. Y. Fua et al., "TiNi-based thin films in MEMS applications: a review", *Sensors and Actuators A: Physical*, 112, pp. 395–408, 2004.

[29]. H. Adldoost, "Design of SMA Micro-Gripper for Minimally Invasive Surgery", Department of Mechatronics, International campus, Sharif University of Technology, 2012.

[30]. J. H. Kyung, B. G. Ko, Y. H. Chunga, "Design of a microgripper for micromanipulation of microcomponents", *Sensors and Actuators A: Physical*, Volume 141, Issue 01, pp144-150, 2005.

[31]. K. P. Rathnayake and H. S. Lakmal Perera, "Design and Simulation of a Shape Memory Alloy Based Microgripper for Minimally Invasive Surgery", *Annual sessions of IESL*, The Institution of Engineers, Sri Lanka, pp. 507-513, 2018.

[32]. T. A. U. Roshan, Y. W. R. Amarasinghe, N. W. N Dayananda, "Design and Development of a Shape Memory Alloy Spring Actuated Gripper for Minimally Invasive Surgeries", *International Conference on Artificial Life and Robotics (ICAROB2018)*, Feb. 1-4, B-Con Plaza, Beppu, Oita, Japan, pp. 566-569, 2018.

[33]. D. C. Lagoudas, *Shape Memory Alloys - Modeling and Engineering Applications*, Springer Science, 2008.

[34]. T. A. U. Roshan, Y. W. R. Amarasinghe, N. W. N Dayananda, "Design and Fabrication of a Minimally Invasive Surgical Device with Customized Shape Memory Alloy Spring Actuator", Volume 5, Issue 3, pp194 – 198, Dec 2018.

[35]. T. W. Duerig, K. Bhattacharya, The Influence of the R-Phase on the Superelastic Behavior of NiTi, Springer, Shape Memory and Superelasticity volume 1, pp153–161, May 2015.

[36]. L. A. Santos et al., "Effects of R-Phase on Mechanical Responses of a Nickel-Titanium Endodontic Instrument: Structural Characterization and Finite Element Analysis", *Hindawi Publishing Corporation*, [Online], vol. 2016, Available: http:// https://www.hindawi.com/journals/tswj/2016/7617493/

[37]. Y. Zheng, Y. Dong, Y. Li, Resilience and life-cycle performance of smart bridges with shape memory alloy (SMA)-cable-based bearings, Constr Build Mater 158: pp389–400, Jan 2018.

[38]. W. Wang, C. Fang, A. Zhang, and X. Liu, (2019, Feb). "Manufacturing and performance of a novel self-centring damper with shape memory alloy ring springs for seismic resilience", *Structural Control and Health Monitoring*, [Online], vol. 26, issue 6, Available: https://onlinelibrary.wiley.com/doi/abs/10.1002/stc.2337.

Appendix A

Shape Memory Alloy material manufacturer

SHAANXI YUNZHONG INDUSTRY DEVELOPMENT CO.,LTD

Address: NO.128 ,Gaoxin Road ,Baoji, 721013 , Shaanxi , China
Tel:0086 917 3373378   Fax:0086 917 3372200

YUNCH

PROFORMA INVOCIE

To	H Suranja Lakmal Perera			Invoice No.	YZ3629-20180829
Address	No: 170/A Thanthirimulla Panadura Sri Lanka ,Panadura ,No: 170/A Thanthirimulla Panadura Sri Lanka ,Sri Lanka,Post Code : 12500 + 94777290079			Date	29th-08-2018
Mark & No.	Description of Goods		QTY	Unit Price (USD/PC)	Total (USD)
20180829	Nitinol wire	1.0mm shape memory wire	2 meters	10.0USD/meter	USD20.0
20180829	Nitinol wire	2.0mm shape memory wire	1 meter	10.0USD/meter	USD10.0
20180829	Nitinol plate	1.0*10*610 dimensions	1 piece	8.9USD/piece	USD8.9
EXW Price	38.9USD				
Lead Time	About 3 DAYS				
Delivery cost by express with insurance	31.9USD				
Total amount	USD70.8				
Payment term	100% prepayment by trade assurance				
Material report	MTC supplied base on EN10204.3.1				
Offer validity	3DAYS				

BANK DETAILS

https://biz.alibaba.com/ta/detail.htm?orderId=93983721217446 payment link

Signature:

Figure A.1: Manufacturer Invoice

Appendix B

SMA helical spring setting fixture design
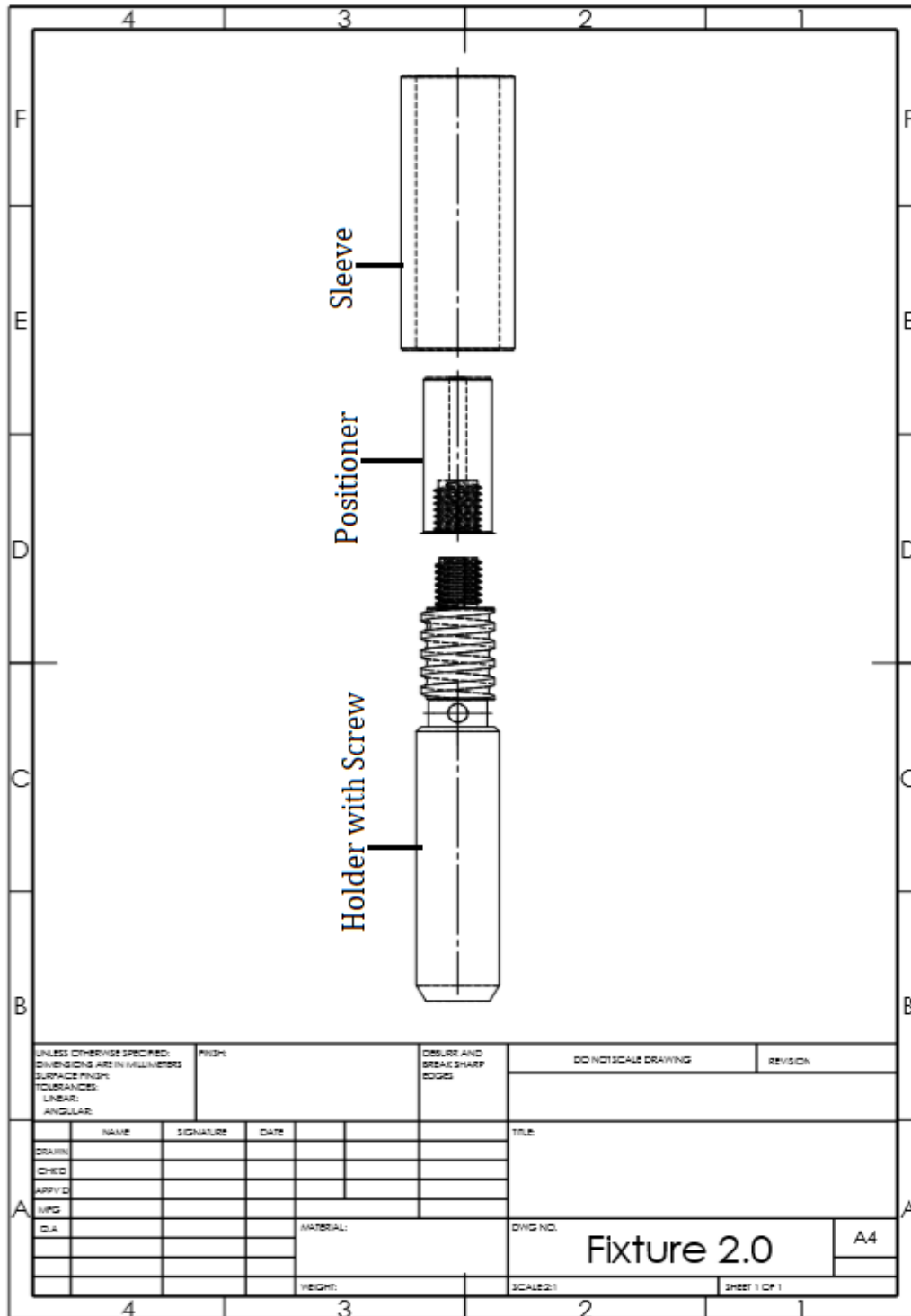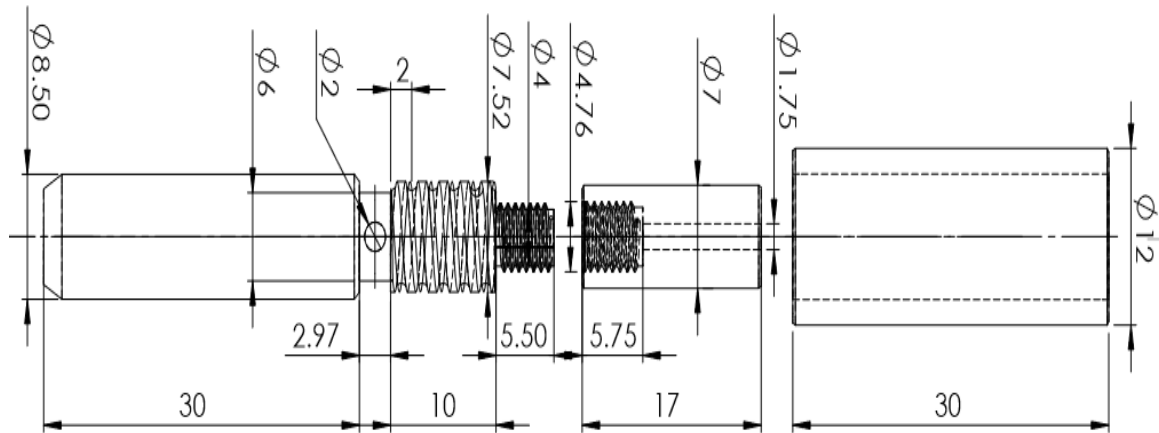

Figure B.1: Complete assembly of fixture
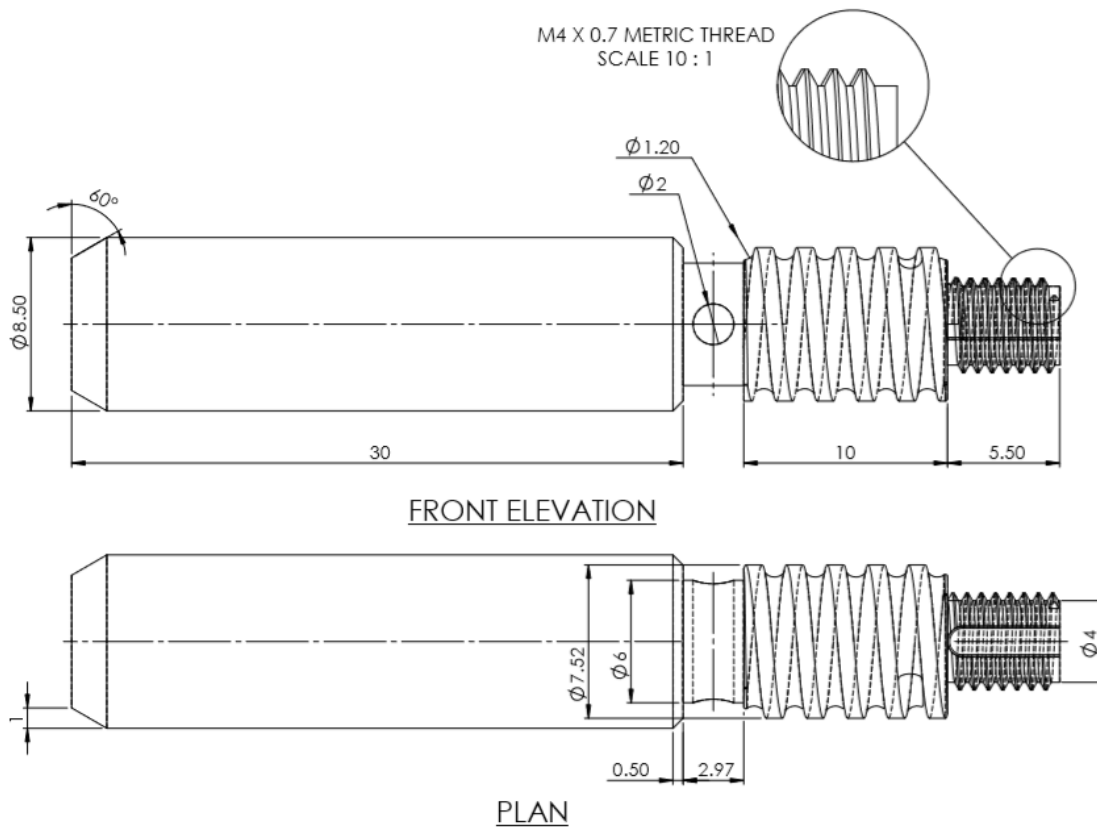
Figure B.2: Dimensions of fixture

Figure B.3: Detail dimensions of holder and screw

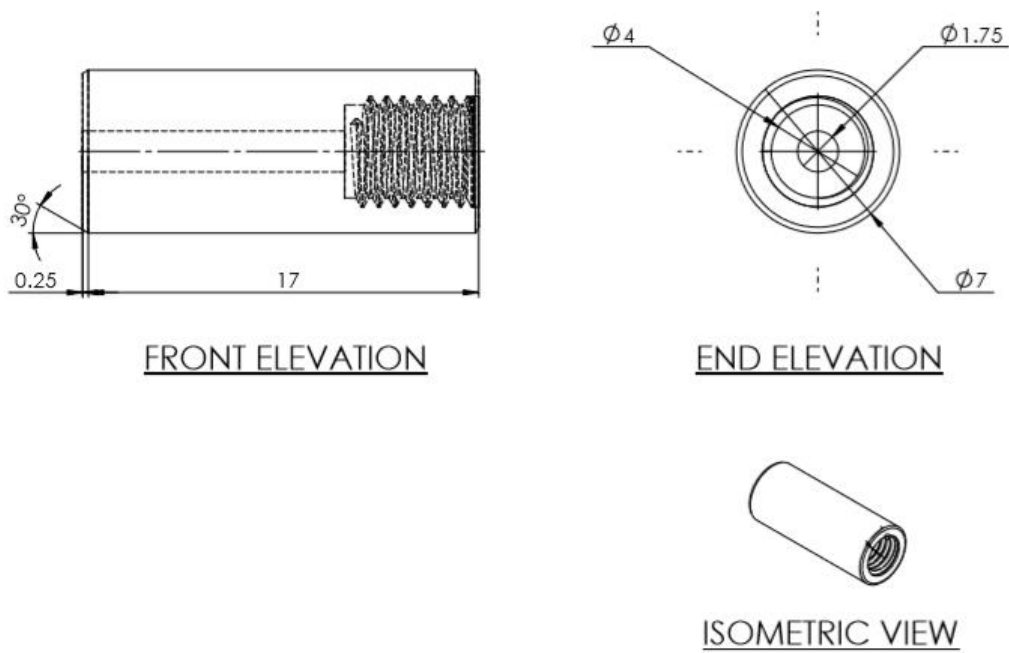FRONT ELEVATION

END ELEVATION

ISOMETRIC VIEW

Figure B.4: Detail dimensions of positioner
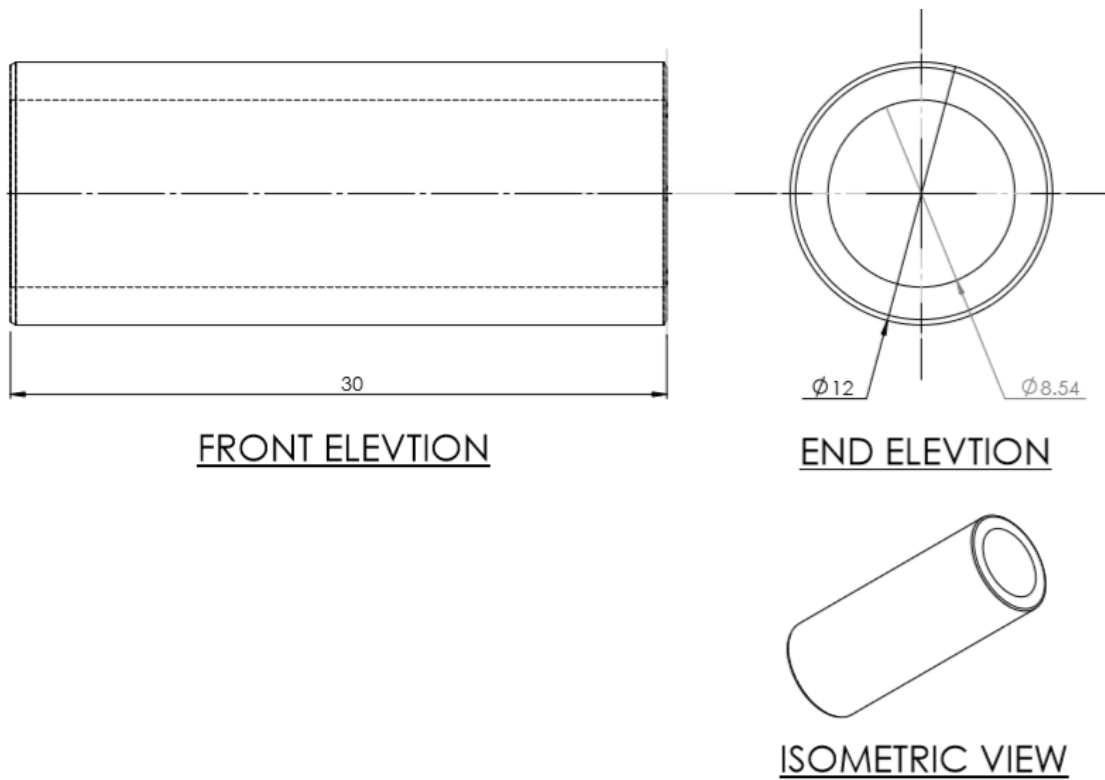
FRONT ELEVTION

END ELEVTION

ISOMETRIC VIEW

Figure B.5: Detail dimensions of sleeve

Appendix C

DSC Thermograms with more details
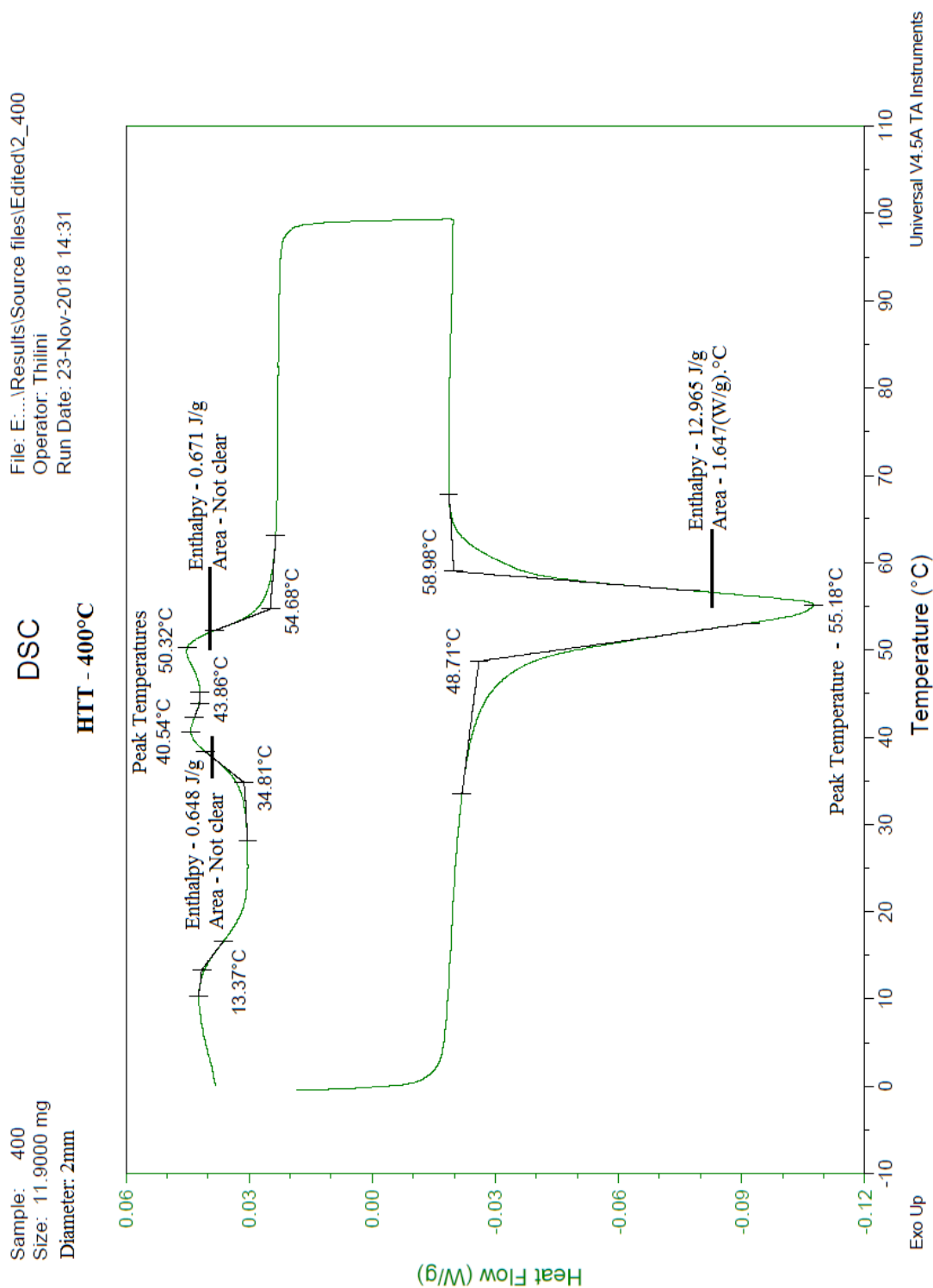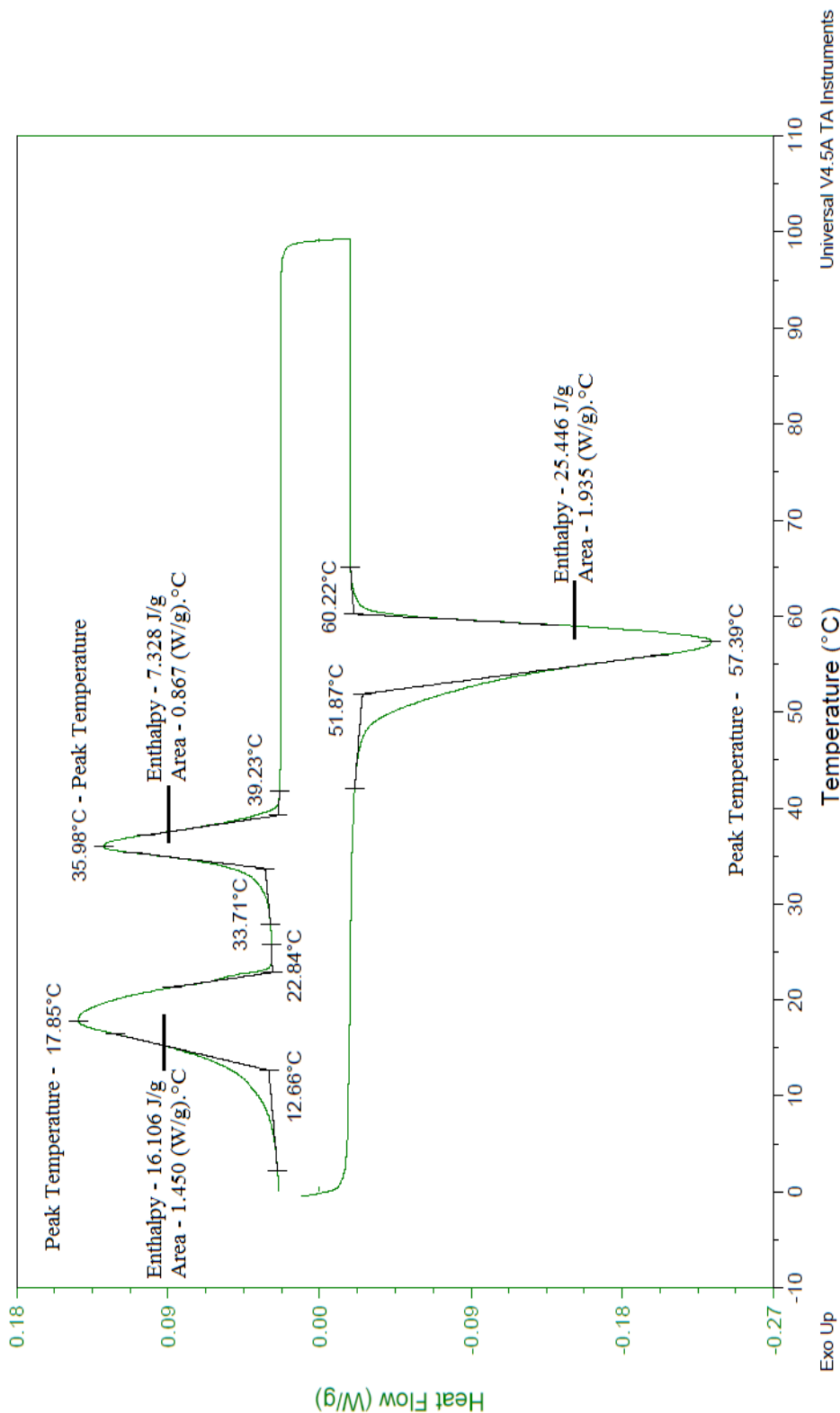

Figure C.1: DSC heat-treated Thermogram at 400 ° C for 30min.
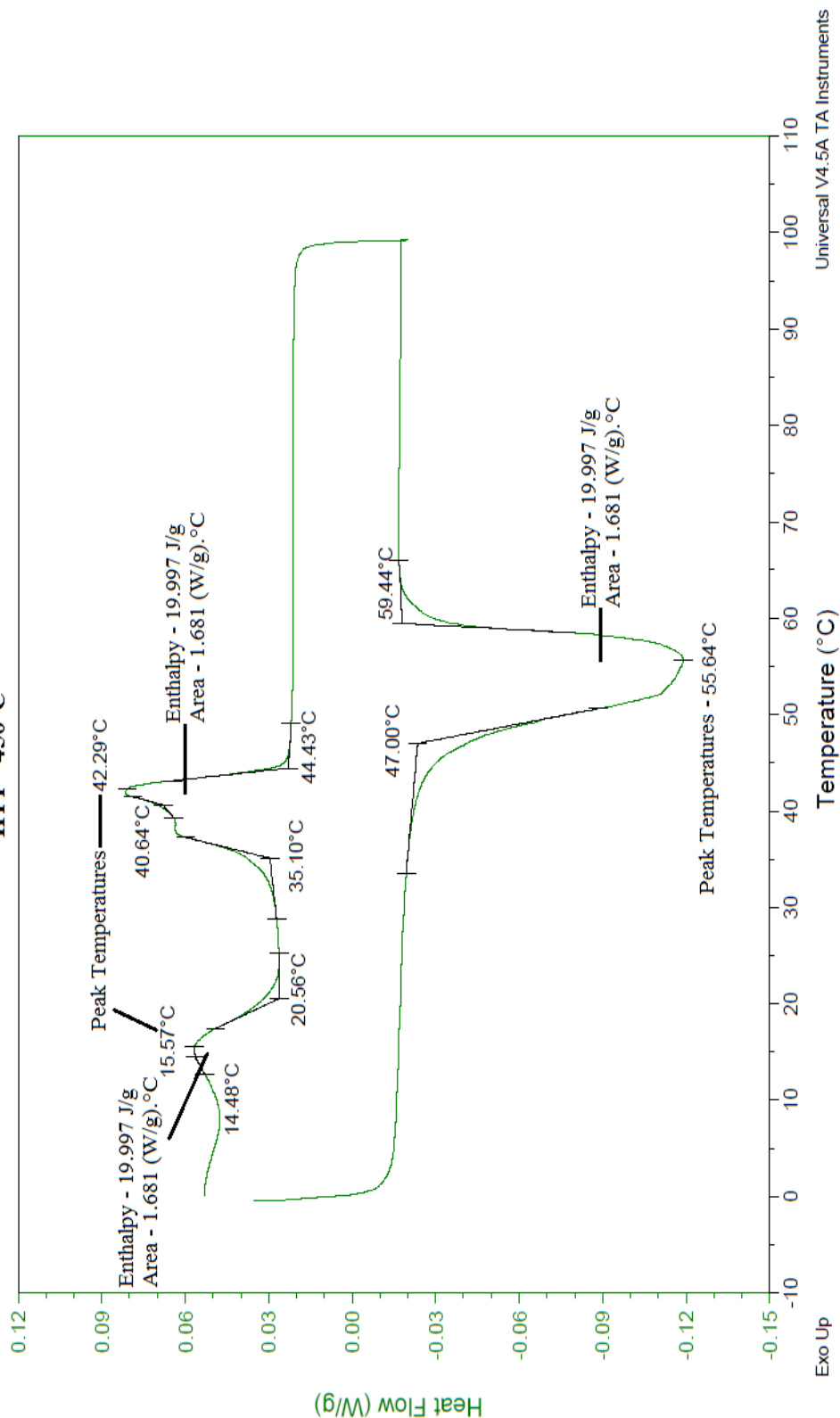
Figure C.2: DSC heat-treated Thermogram at 450 ° C for 30min.

Figure C.3: DSC heat-treated Thermogram at 500 ° C for 30min.
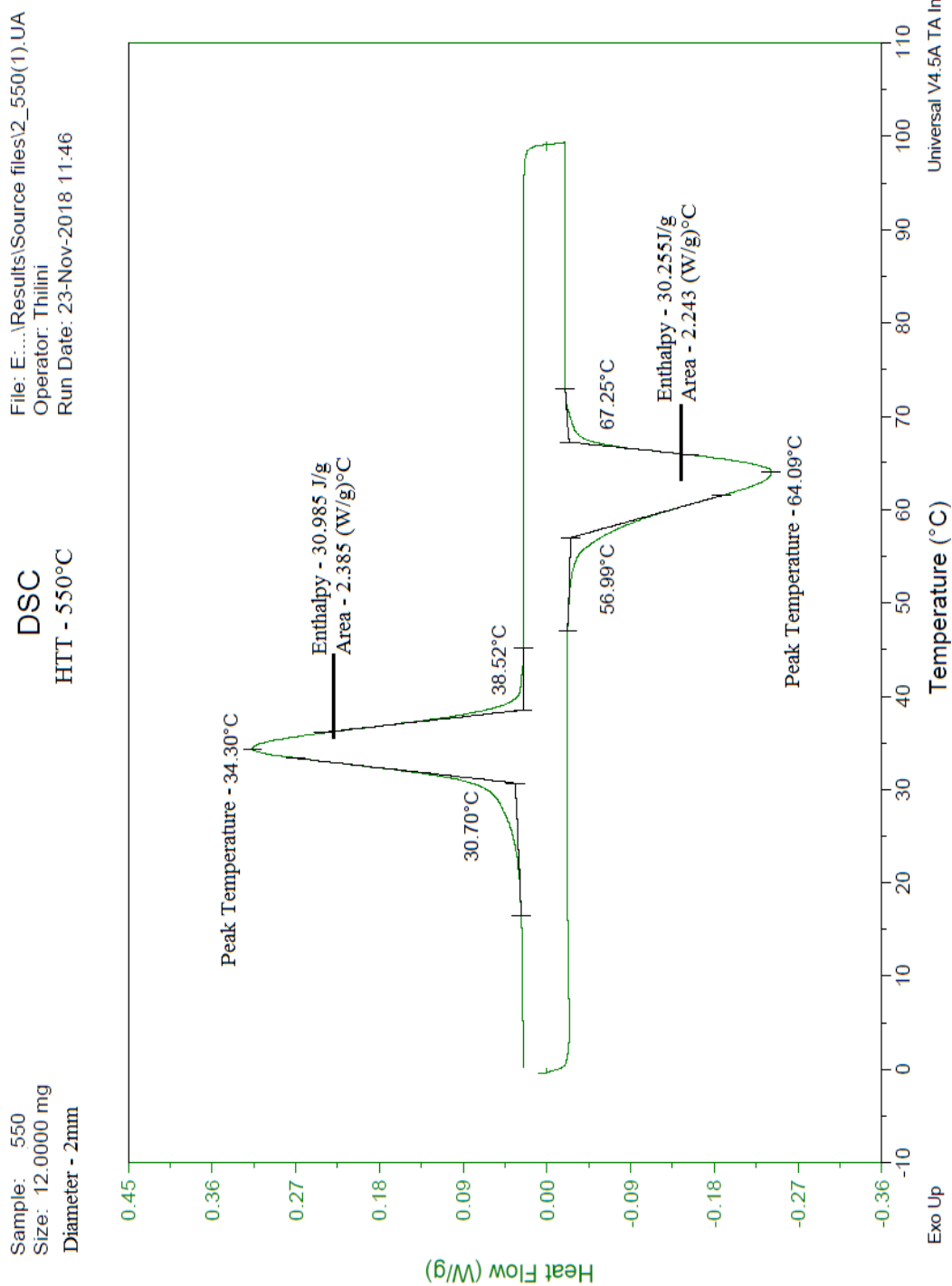
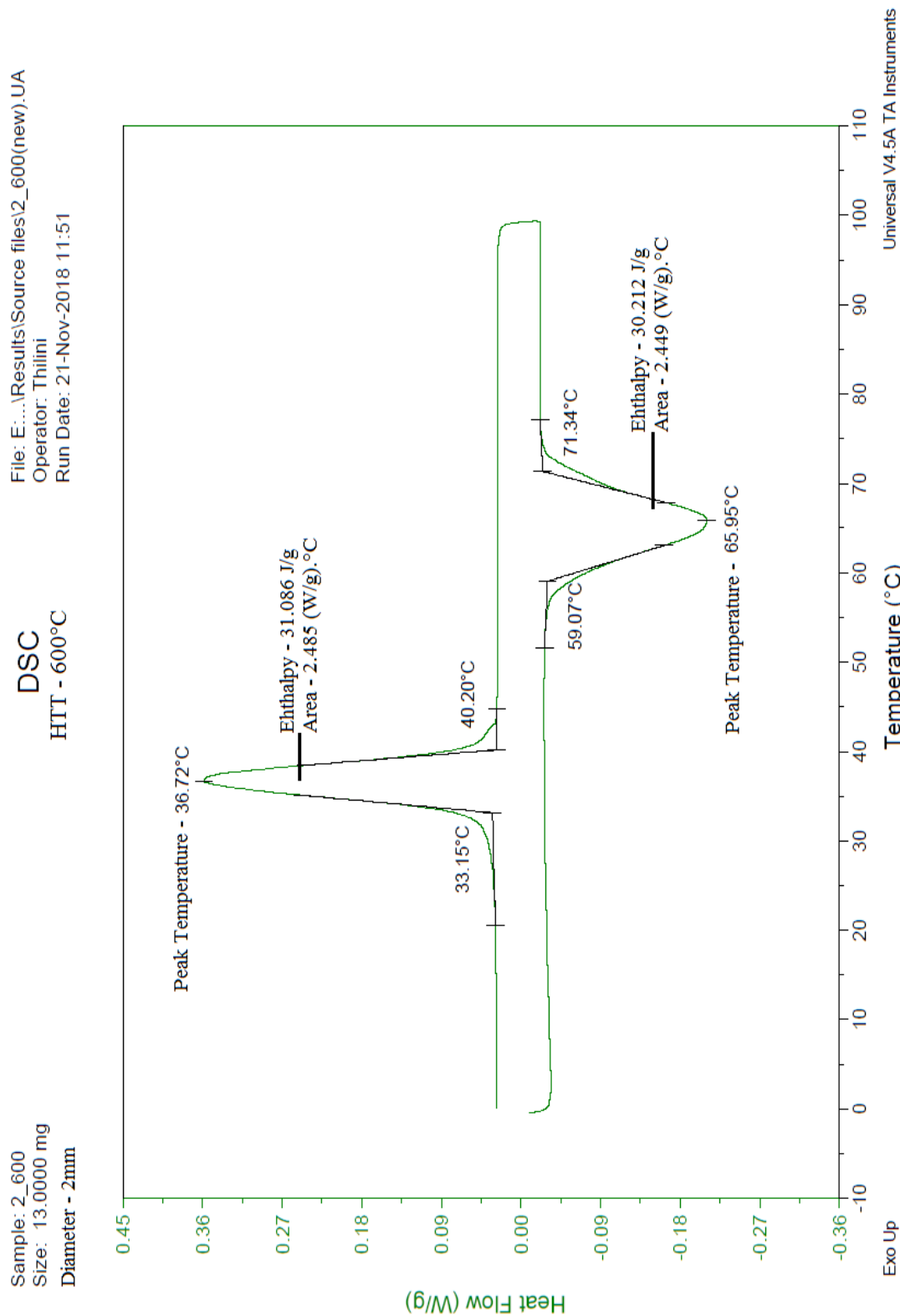**Figure C.4: DSC heat-treated Thermogram at 550 ° C for 30min.**

Figure C.5: DSC heat-treated Thermogram at 600 ° C for 30min.